DEVELOPMENTAL BIOLOGY AND NEUROGENESIS IN THE PRENATAL AFRICAN GREATER CANE RAT (*Thryonomys swinderianus,* Temminck 1827)

BY

OLUWASEUN AHMED MUSTAPHA
D.V.M. (Ibadan), M.Sc. (Ibadan)
Matric No. 106999

A Thesis in the Department of VETERINARY ANATOMY

Submitted to the Faculty of Veterinary Medicine

in Partial Fulfilment of the Requirement for the Degree of

DOCTOR OF PHILOSHOPHY

of the

UNIVERSITY OF IBADAN

FEBRUARY,2021

ABSTRACT

The African Greater Cane Rat (AGCR) is a precocial hystricomorph rodent largely restricted to the African ecosystem. The drive for home-grown animal research models within the African context has increased studies on the biology and development of this rodent. However, information on prenatal development of this rodent is currently scarce. This study was designed to describe the sequence of morphogenetic developmental milestones in the developing AGCR embryos/foetuses, and to elucidate the prenatal corticogenesis of the developing AGCR brain.

Nineteen timed primi-gravid AGCR does from Gestation Day (GD) 10 to 140 (every 10 days) were used. Sonographic examinations were conducted to determine time-based prenatal parameters. The AGCR were subsequently anaesthetised, dissected and their embryos/foetuses (n = 54) explanted. Embryos/foetuses were then staged based on morphogenetic characteristics of prenatal development in mammals with Carnegie and Štěrba systems. Brains were harvested for gross morphological description and evaluation of morphometric parameters (height, length and width). Brain samples were processed using immunofluorescence biomarkers to determine the pattern, onset, duration and peak of neurogenesis (Pax6, Tbr1, Tbr2, NF, HuCD, MAP2), gliogenesis (GFAP, Olig2) and myelinogenesis (MBP) in the prenatal AGCR. Quantitative analysis of individual neural progenitor cells and Olig2+ cells, as well as radial thickness of the ventricular zones were evaluated. Data were analysed using one-way ANOVA and linear regression at $\alpha_{0.05}$.

The earliest detectable sonographic feature of pregnancy in the AGCR was the gestational sac at GD20, while at GD 50 the first gross indication of an embryo was seen Staging of the AGCR embryos/foetuses revealed a relatively longer period of

embryogenesis in the AGCR compared to humans and other precocial rodents like the guinea pig and agouti. Grossly, gyrencephalization of the neocortex was first noticed by GD90 and continued till GD130. Lobation patterning of the cerebellum was the last distinct gross developmental feature noticed in the prenatal AGCR brain at GD130. Brain height (0.67±0.03 to 1.35±0.07 cm), length (0.88±0.02 to 2.85±0.07 cm) and width (0.56±0.04 to 2.02±0.04 cm) increased significantly from GD60 to GD140. There was a positive correlation between gestational length and each brain parameters measured (height: r = 0.58; length: r = 0.86 and width: r = 0.87). The period of pureneural stem cell proliferation in the developing AGCR was identified at GD50. By GD60, the radial thickness of the ventricular zone had reached its maximum depth, while the peak period of neurogenesis was at GD80. Axonal and dendritic sprouting had begun by GD80 and this progressed until birth. Deep and upper layers of the neocortex were established in an "inside-out" manner by GD120 and GD130, respectively. Active gliogenesis spanned GD110 - 130. Although, oligodendrocyte progenitor cell proliferation had started by GD80, myelinogenesis did not begin earlier than GD120.

The sequences of morphogenetic developmental milestones and prenatal corticogenesis in the African Greater Cane Rat were consistent with the precocity of central nervous system development in the guinea pig. The African Greater Cane Rat is therefore suitable as a research model for neurodevelopmental studies.

Keywords: African Greater Cane Rat, Developmental milestones, Foetus, Corticogenesis, Brain morphogenesis

Word count: 496

ACKNOWLEDGMENTS

Special thanks and praise to God Almighty, my strength, help and eternal counsel all through this journey. Which of your mercies can I deny, Lord? I am eternally grateful, Father!

To my Supervisor, father, mentor and teacher, Prof. J. O. Olopade, I say a big thank you sir. I am immensely grateful for the enormous support, sacrifice, love and push I received throughout the course of the journey. I have no single regret being your student. On the contrary, I am eternally grateful for all you have done for me. Being your student has become a career defining moment for me. I will submit to your tutelage over and over again, sir.

How do I appreciate Prof. Simone Fietz, my international host/boss, whose intelligence, tenacity, analytical probing, drills, fervour for perfection and warmth contributed in no small measure to the success of my Ph.D. *Danke Schon!*

I am also grateful for the funds received from the International Society of Neurochemistry (ISN) and NEEDS Assessment Intervention Fund. The overseas travel grants received were indeed timely for the completion of this work.

I appreciate the entire members of staff of the Department of Veterinary Anatomy, College of Veterinary Medicine, Federal University of Agriculture, Abeokuta. Special thanks to Prof. A.K. Akinloye (The Dean of the College) and Dr. A.O. Adebayo (H.O.D., Vet. Anatomy), the support I have received has been humbling. God bless you sirs.

I am deeply grateful to my pastor, mentor, teacher and father, Dr. M.A. Olude. Indeed, every man needs a shepherd! Thanks for being the correcting and guiding voice in the course of this voyage. Thanks for the numerous encouragements, counsels and prayers. Sir, I love you dearly and would not take your labours over me for granted.

To the amazing, scholastic and loyal research assistants I had in the course of this work - Drs. Awala-Ajakaiye Michael, Ezekiel Samuel, Eniola Popoola and Ebunoluwa Teriba. You guys are simply wonderful! I have no doubts you will surely make great researchers. Men will rise up for you when you need them!

I remain grateful to the entire members of staff of the Department of Veterinary Anatomy, Faculty of Veterinary Medicine, University of Ibadan.

I would like to specially acknowledge, Prof. B.O. Oke for making room for me to fly and also Prof. P.C. Ozegbe (H.O.D., Vet. Anatomy) for the constant encouragement. God bless you sirs. My deep gratitude is extended to Dr S. G. Olukole (Sub-Dean, Postgraduate of the Faculty) and Dr O. O. Aina (Departmental Postgraduate Co-ordinator). Thank you sirs for all you do and have done for me. I am grateful sirs.

To the entire members of University of Ibadan Neuroscience Team, thanks for the positive criticism and support. This is one of the best thing that has happened to me. I would love to single out Dr. Francis Olaolorun who has been a huge personality for me. Thanks for making all the long journeys and visits to the farm with me. I drew a lot of motivation with you around. Dr (Mrs) Oluwabusayo R. Folarin was always there for me even at the shortest notice. I truly appreciate you for coming through for me when I needed you most ma. To my darling sister, Amany Ladagu, words fail me to appreciate your pleasantness and selflessness. You know I love you and appreciate you!

Profound appreciation goes to the entire members of staff and post graduate students of Veterinär-Anatomisches Institut, Faculty of Veterinary Medicine, University of Leipzig, Germany, for the tremendous assistance I received during my visits most especially from the Head of Histology and Embryology Unit, Prof. Johannes Seeger. To Thomas, Britta, Megan, Hannah, Thawart, Kevin, Christine and Frau Gabi, you all made work seamless for me. Nicola Koenig (The Placenta Lady!) – you were simply an angel sent ahead of me to Leipzig. A toast to the wonderful moments we shared together; encouraging and urging ourselves on during our bench work. “We are finishing this year!!!” we always chorused. Thanks, you are simply amazing! *Vielen Dank!*

I call her *Mummy*, because indeed she is one. Prof. Morenike A. Dipeolu has been phenomenal. I am indebted to your resolute commitment to finishing my Ph.D. Thank you mummy for the constant and consistent calls, encouragement and love. Despite your busy schedule, you always watched out for me. God bless you ma!

My profound gratitude goes to Dr (Mrs) Funmilayo E. Olopade. Thanks for your motherly love and support ma. Thanks for showing up for me at a time when I needed help. Your humility and intervention will forever linger in my heart. God bless you richly ma.

To my boss and teacher, Dr. R.A. Ajadi, your type is rare. Thank you for the technical assistance with my work. Thank you, a hundred thousand times over. I also want to specially recognize and appreciate Dr(Mrs) Temitope A. Ajadi, your contribution to the success of this work is huge ma. You are the answer to my numerous prayers on this work. Our paths crossed when I needed a miracle! You soon proved to be the miracle. I still ponder and wonder why you did all you did for me. God bless you, ma.

I am eternally grateful to be blessed with wonderful parents, Pastor and Pastor (Mrs.) Raphael Idowu Mustapha. I have lost counts of the calls, prayers, encouragements and supports all through this journey. I won't trade you for anything in this world, sir and ma. I am also grateful to my second mummy (Mother-in-law), Deaconess Deborah Sanni. Thanks for being there for my family those times I had to travel out of the country. I am blessed to be your son-in-law; more appropriately your adopted son!

I appreciate specially the team of budding potential neuroscientists in my house (my lovely children) – Boluwatife Bunmi, AsepeIseOluwa Deborah, David OroOluwaseyi and IreOluwatomiwa Rehoboth Mustapha. I thank God for blessing me with these intelligent, thoughtful, wonderful and inspiring kids. Thanks for your kind understanding and your awesomeness!

To a super duper woman, I am lost for words on how to say thank you for bearing up for the family and making the sacrifice to watch me fly. Indeed, a virtuous woman who can find?! Adunni, your price is worth far more than rubies. You are the singular reason for the completion of this work. If I ever got another chance to choose a wife, I would choose you over and over again without thinking. Marrying you is one of the best decisions in my life. I love you, Olamide Mustapha. I cherish you, Love. "AOMM, ULSC, MSW".

CERTIFICATION

I certify that this work was done by Oluwaseun Ahmed MUSTAPHA under my supervision in the Department of Veterinary Anatomy, Faculty of Veterinary Medicine, University of Ibadan.

……

Supervisor

J. O. Olopade

DVM (Ibadan), Ph.D. (Ibadan), FCVSN

Professor, Department of Veterinary Anatomy

Facultyof Veterinary Medicine

University of Ibadan

Ibadan, Nigeria.

TABLE OF CONTENTS

LIST OF FIGURES

Figure

LIST OF TABLES

Table

LIST OF ABBREVIATIONS

AGCR	African Greater Cane Rat
AGD	Ano-genital Distance
ANOVA	Analysis of Variance
BPD	Bi-Parietal Diameter
CNS	Central Nervous System
CP	Cortical plate
CRL	Crown Rump Length
DAPI	4', 6-diamidino-2-phenylindole
FL	Foetal Length
FW	Foetal Width
GD	Gestation Day
GFAP	Glial Fibrillary Acid Protein
IZ	Intermediate Zone
MAP2	Microtubule-associated protein 2
MBP	Myelin Basic Protein
NCC	Neural Crest Cells
NEC	Neuroepithelial Cells
NF	Neurofilament
NPC	Neural Progenitor Cells
NSC	Neural Stem Cell
Olig2	Oligodendrocyte transcription factor
Pax6	Paired box gene 6
PBS	Phosphate-Buffered Saline
PNS	Peripheral Nervous System

PP	Preplate
SEM	Standard error of the mean
SVZ	Sub-ventricular Zone
Tbr 1	T-box Brain-1
Tbr2	T-box Brain-2
VZ	Ventricular Zone

CHAPTER ONE

1.0 INTRODUCTION

1.1 Background

The mammalian neocortex is the major characteristic and extremely divergent portion of the brain (Watakabe, 2009). It is composed of radially oriented neurons, organized into six strata; the most superficial being layer I and layer VI being the deepest abutting the white mater (Gilmore and Herrup, 1997).A greater proportion of the cortical neurons are produced during the prenatal period and are derived from distinct neural stem cell (NSC) types located in the proliferative zones near the lateral ventricle. These neurons then travel radially immediately after they are generated (Fietz and Huttner, 2011). Hitherto, the serial events in corticogenesis have been elucidated in laboratory rodents and other mammals, most of them being born in an altricial state (Sauerland *et al.,* 2016). Developmental modes along the 'altricial-precocial' spectrum influences the social life of vertebrates ranging from behavioural, physiological and cognitive perspectives (Scheiber *et al.,* 2017). Also there exists a relationship between these ontogenic modes and development of different organs, including the brain (Sanchez-Villagra and Sultan, 2002).

The African Greater Cane Rat, AGCR (*Thyronomys swinderianus*) is a native African rodent commonly calledGrasscutter, (Akpan *et al.,* 2018). With a mean body weight of 4kg, this rodent is ranked as the second and fourth largest African and world rodent respectively (Adu and Yeboah 2003; Eben, 2004; Jori *et al.,* 2005; Skinner and Chimimba, 2005; Ibe, 2016; Mustapha *et al.,* 2017). This precocial hystricomorph has an unusually long period of gestation (150 days), giving birth to an average litter size

of four pups (Opara, 2010). Neonates are born with two incisorson their upper jaw and two incisors on their lower jaw, which keeps growing all through the course of their entire life (van der Merwe, 2000; Jori *et al.,* 2005). AGCRs are monogastric herbivores with a dental formula 2(I 1/1, C 0/0, P 1/1, M3/3) and their favourite diet contains guinea grass and elephant grass augmented with mineral salt, maize and wheat.

Adult AGCRs are well built with sturdy bodies, chunky neck, diminutive legs, and are sexually dimorphic (Skinner and Chimimba, 2005; Adu *et al.,* 2017). The deep-brown coloured tail, overlaid with small spinous hair, thins out caudally.

Adult bucks possess penises with baculum (*os penis*) while their females have six mammary glands; three on either side of the ventrolateral sides of the abdomen (Okorafor *et al.,* 2013). Sex identification in the postnatal AGCR is best done by either using the sex apparati: scrotal sac and penis (males) and,mammary glands and vulva (females) or ano-genital distance, measured as the metric interval between the external genital tubercle and anus, or by using a combination of both parameters (Adu and Yeboah, 2003).

Pregnancy is indicated in AGCR as a result of progressive changes in body weight gain usually after four weeks post-coital and occasional vaginal bleeding (Addo *et al.,* 2007). Vaginal mucus plug is first seen on gestation day 59, and is useful in the diagnosis of pregnancy (Adu and Yeboah, 2000). Unplugged vaginas 105 days' post mating are judged non-pregnant. The traditional method of detecting pregnancy in AGCR is by usually digital abdominal palpation. This is usually combined with the presence of vaginal mucus plug (Addo *et al.,* 2007). Precise forecast of parturition date

is useful clinically in order to avoid or reduce production losses by well-timed intervention (Kim *et al.,* 2007).

In the African continent, the AGCR is considered a choicest meat, most especially in the Western sub-region where there is ongoing intensive farming of this rodent, commanding huge price per kilogram with plum monetary returns (Jori *et al.,* 2005; Ibe, 2016). Additionally, this rodent, which is largely restricted within the African ecosystem, has enjoined heightened interest in a currenteffort to probe, establish and embrace indigenous species as experimental models for research in Africa, especially for eco-toxicological investigations (Asibey and Addo, 2000; Ibe, 2016). These scientific curiosities and commercial explorations have resulted in a number of research efforts tailored in the direction of domesticating and improving our knowledge of the biology and behaviours of this rodent (Adebayo *et al.,* 2011; Olukole *et al.,* 2014; Mustapha *et al.,* 2015; Adu *et al.,* 2017; Mustapha *et al.,* 2017; Akpan *et al.,* 2018). Other research efforts include reproductive anatomy (Olukole *et al.,* 2014), digestive anatomy (Van Zyl *et al.,* 2005), musculoskeletal system (Onwuama *et al.,* 2014 and 2018), dental eruption (van der Merwe, 2000) and neuroanatomy (Spruston, 2008; Mustapha *et al.,* 2017).

1.2 Justification

Despite several research efforts in understanding the biology of the AGCR, information on the prenatal development, more particularly on specific information on corticogenesis including the availability and quantity of the subtypes of neural progenitor cells in the developing cortex of this rodent is currently lacking. With less than 10% success rate in translational research with mouse models, there is a heightened effort to survey, establish and appropriate indigenous species as

spontaneous experimental models for research in Africa (Asibey and Addo, 2000; Perrin, 2014; Ibe, 2016; Kramer and Greek, 2018). AGCR is being proposed as an indigenous laboratory model for home-grown neuroscience based research (Asibey and Addo, 2000; Mustapha *et al.,* 2017). Their foetuses and their translational potential portend great advantages in scientific research within the African context, most remarkably in neural stem culture and eco-toxicological investigations (Asibey and Addo, 2000; Ibe, 2016; Mustapha *et al.,* 2017).

1.3 Aim and Objectives of the Study

This study was aimed at describing the sequence of morphogenetic developmental milestones in the developing AGCR embryos/foetuses, and to elucidate in details the prenatal neocortical development of the developing AGCR brain.

The specific objectives include:

1. To determine the sonographic features and measurements at different stages of gestation in the AGCR.
2. Characterize definitive developmental occurrencesin the prenatal AGCRthroughout its entire length of gestation and to generate baseline ontogenetic attributes for AGCR embryos and foetuses.
3. To identify and describe distinctive external developmental features in prenatal brain across the entire gestational length in the AGCR
4. To determine the period of pure neural stem cell production in the developing AGCR.
5. To elucidate the developmental pattern and timing (most especially the onset and peak periods) of neurogenesis, gliogenesis and myelinogenesis in the developing AGCR neocortex.

1.4Significance of Study

- The chronological sequence of developmental milestones in the prenatal AGCR will be investigated and documented. This may help to shed more light on the biodiversity and evolution of hystricomorph rodents and strengthen the drive towards adopting the AGCR as a spontaneous indigenous research model
- This study is also significant as it will provide baseline timelines that would be useful for further studies within the African context, most especially for neural stem culture and ecotoxicological studies.

CHAPTER TWO

2.0 REVIEW OF LITERATURE

2.1 The African Greater Cane Rat

The AGCRis a mammal categorized under the order *Rodentia*based on the presence of a pair of incisors (chisel-like) on both the upper and low jaws. They are considered to be the fourth largest currently existing rodent (Eben, 2004; Ibe *et al.,* 2017) and the second largest African rodent; considered as one of the wild rodents presently being reared and domesticated in several regions in Africa. They are also reputed as Africa's leading "micro-livestock" (Mustapha*et al.,* 2015; Ibe *et al.,* 2016).

2.1.1 Taxonomic Classification of the African Greater Cane Rat

Kingdom: Animalia

Phylum: Chordata

Class: Mammalia

Order: *Rodentia*

Sub-order: Hystricomorpha

Family: Thryonomyidae

Genus: *Thryonomys*

Species: *Thryonomys swinderianus,* (Temminck, 1827)

Figure 2.1: Adult African Greater Cane Rat. (Source: AU-IBAR, 2016)

2.1.2 Features and Peculiarities of the African Greater Cane Rat

The AGCR is a wild hystricomorphic rodent found predominantly in sub-Saharan Africa and serves an alternate source of organic protein (NRC 1991, Addo*et al.,*2002). They possess thick bodies but with pale and very soft integuments, especially those of the limbs, making them more susceptible to injury which may be as a result of poor restraint or exposure to injurious objects (Adu *et al.,* 2017). The entire body measures up to 40-60cm body length while the tail can measure up 20-25cm (Opara, 2010). AGCR has rounded ears almost hidden in its coat and shorter forelimbscompared to the hindlimb (Igado *et al.,*2016). Notwithstanding their sheer body size and small limbs, they are swift runners and are also, known to be expert swimmers (Mustapha*et al.,* 2015). Their visual powersare quite poor hence, making it a compensatory communication solely dependent on auditory and olfactory cues. (Jori and Chardonnet, 2001).

The AGCR are easy to breed, and concerned an alternative to the pouched meat (African giant rat). It is a fast growing animal, mainly in high intensive system, which values very many agricultural by-products unfit for human consumption. The carcass yield is nutritionally very important. They usually do not dig holes or tunnels even though they take cover in holes nonetheless scratch a small crater within the vegetation (Opara, 2010).

2.1.3 Distribution and Habitat of the African Greater Cane Rat

The AGCR is located geographically exclusively within Africa with distribution ranging from far north to as far south (Opara, 2010) (Fig. 2.2a). They are found in wooded savannah and grasslands (NRC, 1991). The AGCRare also seen in places with dense flora, particularly especially fast growing long grasses in humid or swampy

places. Hence, they do not dwell in the rainforest or hot regions (Ajayi, 1971; NRC, 1991).The AGCR is not reported as athreatened species of wildlife in West Africa (Ibe, 2016).

Intriguingly, all research efforts (with the exception of three publications) on the AGCR were done by African scientists in countries found within the natural geographical distribution of this rodent (Fig. 2.2b).

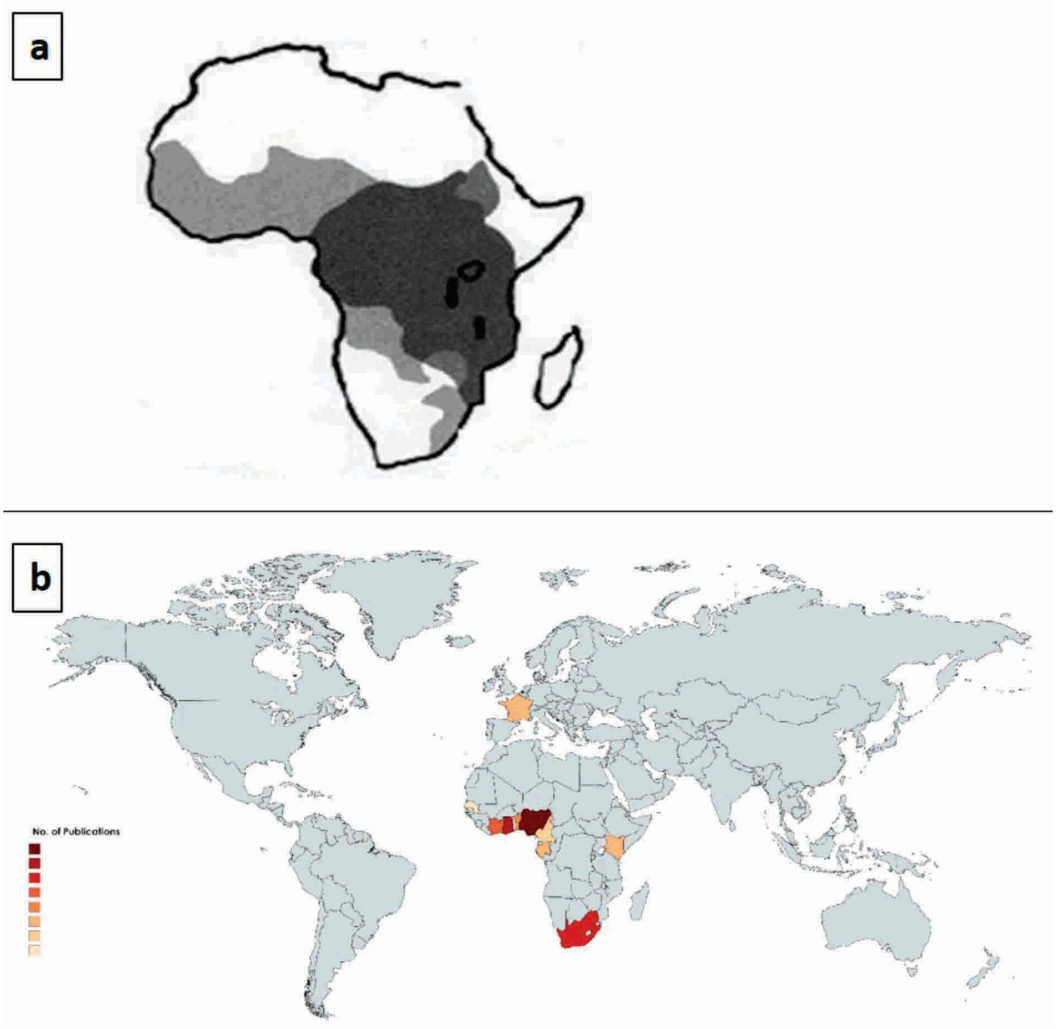

Figure 2.2: The geographical spread of (a) the AGCR, *Thryonomys swinderianus,* (light gray) and *Thryonomys gregorianus* (Dark grey) [Source: National Research Council 1991]; (b) scientific publications on the AGCR [Map was generated using choropleth with the software application mapchart.net®].

2.1.4 Social Behaviour of the African Greater Cane Rat

The AGCR live mainly above the ground level and they are known to be nocturnal i.e. they are more active at dusk and night. Nonetheless, with the abundance of flora and shade for them during the wet season, they may be seen very active during the day. (Ajayi and Tewe, 1980; Opara, 2010). AGCR live mainly in colonies (a ratio of 1 buck : 4 does with their pups). They usually search for food and engage in mating activities between evening and midnight, and at the early hours of the day. They spend the rest of the hours to rest, groom and search for nests (Opara, 2010).

2.1.5 Management System of the African Greater Cane Rat

The AGCR are easy to breed but its rearing and handling requires skills. The breeding of AGCR have been reportedly done in both rural and urban environment, using boxes, pipes and enclosed areas (Addo, 2002). Based on these rearing sites, AGCR management can be done under three systems: Enclosure, Cage and Floor (Opara, 2010).

2.1.6 Mini-Livestock Production in Nigeria

The current estimate of the global human population is 7 billion, and expected to be 9.3 billion by the year 2050, with Africa recording the highest growth rate (Bloom, 2011). This demographic upheaval exerts pressure on food supply, including animal protein. According to Auzel and Wilkie (2000), at least 20% of the animal protein source in Africa is obtained through hunting and fishing, such that wildlife represents a substantial source of animal protein and income for a large part of the rural populations. Mini-livestock encompasses small indigenous vertebrate and invertebrate wildlife which can be produced on a sustainable basis for food, animal feed and as a

source of income for local populations living in peri-urban areas (Hardouin *et al.,* 2003).

The current decline in protein in Nigeria, and the rapidly increasing demand for livestock products, is addressed through mini-livestock production such as the production of African grasscutter meat (Adekola and Ogunsola, 2009). Different rodent species are sources of food in Nigeria, especially among the rural populace. They represent a high proportion of bush meat on sale in city markets (Fa *et al.,* 2002). Some of these rodents include African grasscutter (*Thryonomysswinderianus*), African giant pouched rat (*Cricetomysgambianus*), Teddy guinea pig (*Caviaporcellus*), Syrian hamster (*Mesocricetusauratus*), grass rat (*Rhabdomysdilectus*) and the brush-tailed porcupine (*Atherurusafricanus*). Rodent farming is mostly inter-changed with mini-livestock production, as the mini-livestock industry almost exclusively involves the production of rodent species. However, some of the other small-sized wild animal species that make up the mini-livestock industry include rabbits, snails, pangolin, edible frogs, manure worms and insects. Reptiles like snakes are also considered as eligible for mini-livestock status (Hardouin *et al.,* 2003).

In a study that examined the consumption of rodents as a food source in the south of Benin, Edo state, Nigeria by Assogbadjo *et al.,* (2005), the AGCR and the grass rat were the most and the least consumed rodents, respectively, from a list of 10 different rodents. Similarly, Sacramento *et al.,* (2013) reported that the number of AGCR farmers in the Republic of Benin has increased a tenfold between 1996 and 2004. The increased demand for the meat of the AGCR has been attributed to the low cholesterol and fat content as well as its sweet taste (Attakumah, 2013).

The sequel of growing human populations is a continuous increased demand for wild meat. Facilitated access to remote areas stimulate trade for the mini-livestock industry. In consequence, wild meat harvest is now the primary illegal activity in many protected areas. The devastating effects of wildlife hunting are numerous. The ecological implications and depletion of wildlife population in Africa have been reported by Auzel and Wilkie (2000). The public health implication of the unwholesome slaughter and sale of bush meat have also been reported by Pointing and Teinaz (2004). Furthermore, there is no veterinary control of the bush meat since it is an informal trade. The need for the preservation of these wildlife and improved method of processing them led to the domestication and commercial production of small-sized wild animals such as the AGCR. Such domestication can only be fully achieved, if the biology and behaviour of the animal is well understood; thus, the need to study the brain of the AGCR.

2.1.7 Reproduction and Pregnancy Diagnosis in the African Greater Cane Rat

Sexual maturity in male AGCR is determined by evidence of ano-genital region stain (Adu, 1999), while in the sexually matured female AGCR, oestrous cycle ranges between 30-40 days (Addo *et al.,* 2002). AGCR sexually matures from 5-6 months to about twelve months. These rodents are induced ovulators (Adu *et al.,* 2017) therefore, capable of breeding all through the year and have no specific time or period considered unsuitable for mating. Although their sexual activities vary (Opara, 2010), the shape of reproductive organ and size of the head of AGCR is the most common method of sex identification and distinguishing criteria between sexes (Adu, 1999). The ano-genital distance has been described as the benchmark for sex characterization in AGCR (Opara, 2010). At birth, the ano-genital distance of the male is about 10mm

while in female its less than 5mm while in adult, the distant measures up to about 37mm in male and 12mm in female (Opara, 2010).

Embryonic resorption has been reported in the AGCR, hence the need and recommendation for all year pregnancy diagnosis (Asibey, 1974; Adu and Yeboah, 2000; Owusu *et al.,* 2010). The parameter evaluated for in pregnancy diagnosis is subject to the frequency of examination. Diagnostic parameters checked out for daily include the status of vaginal membrane, and evidence and character of vaginal secretion. For weekly diagnosis of pregnancy: body weight changes and the palpable foetuses *in utero*coupled with evidence of vaginal bleeding at about 5weeks post-coital are considered (Addo, 2002). Accuracy of positive diagnosis with digital abdominal palpation is usually between 87–88% around the second trimester (Kim *et al.,* 2007). The gestational length of the AGCR is about 148- 170 days making farrowing two times a year possible (Adu, 1999; Onadeko and Amubode, 2002).

2.2 Ultrasonography in Pregnancy Diagnosis

Ultrasonography is regarded as a safe and reliable method for the diagnosis of pregnancy. Its use present no danger or hazard to both the patient and operator (Blanco *et al.,*2008; Kustritz, 2005). Three types of ultrasound for diagnostic purposes have been reportedin companion animals, more specifically in canine species. Amplitude depth ultrasound (A- mode), identifies presence of fluid in and around the foetus. Its limitation however is it inability to delineate the fluid origin and its inability to assess foetal viability and numbers (England *et al.,* 2003).Similarly, Doppler ultrasound makes aperceptible signal detectingthe heartbeats of foetuses, but provides no clue of the number and viability of foetuses (Di Salvo *et al.,*2006; Blanco *et al.,*2008).

The above two mentioned modalities are seldomly used in the rabbits. Brightness mode (B-mode),on the contrary permits the evaluation of the status of pregnancy, the numbers and viability of foetuses, examination of uterus and extra-reproductive organs. number and viability, and investigation of the uterus and extra-reproductive abdominal structures (Kutzler *et al.,* 2003). An accuracy of between 94-98% has been noted for pregnancy diagnosis using B-mode ultrasonography after 2 weeks of gestation while an accuracy of 99% after 3 weeks from the last breeding in rabbits (Gutierrez and Zamora, 2004). Foetal heartbeats have been noted from 15 days of gestation, while foetal movement was noticeable 12 days after gestation (Gutierrez and Zamora, 2004). Measurement of bi-parietal head diameter of foetuses has been shown to be reliable for gestation age estimation in dogs and rabbits (Beccaglia and Luvoni, 2006).

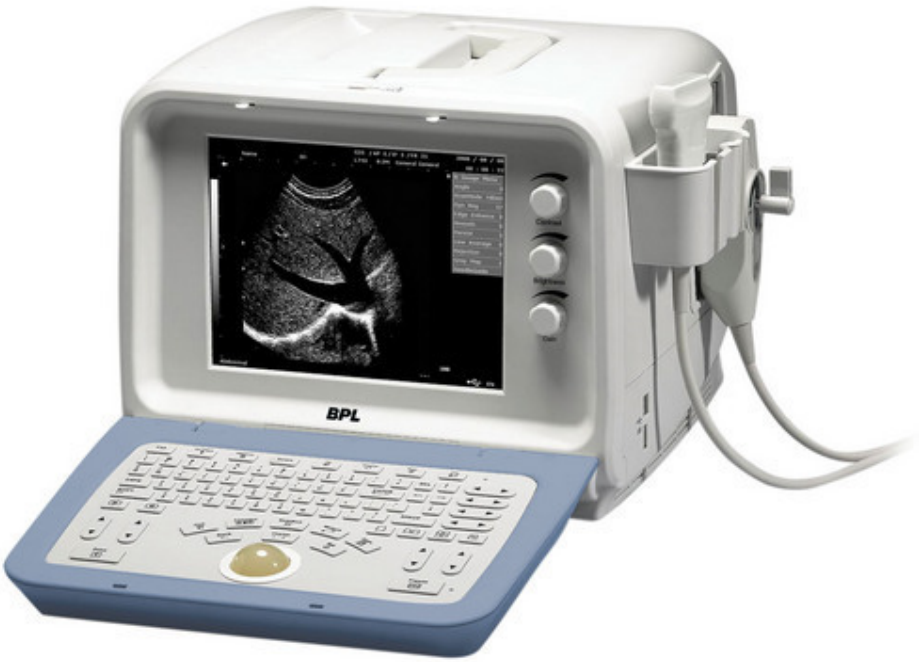

Figure 2.3: Brightness-mode ultrasound machine (Source: www.edanusa.com)

2.3 Developmental Horizons

2.3.1 Definition of Developmental Horizon

Developmental horizons describe the chronologic progression of development of several external morphogenetic structures of the developing embryo or foetus at a given time point in gestation (Laing, 1979). Some of these developmental features include limb buds, eyelids, folliculogenesis, emergence and distribution of hairs on the different body regions, skeletal growth (Jaji*et al.,*2011).

2.3.2 Criteria of Developmental Horizons

The documentation of normal developmental milestones in embryos and foetuses at a given time point in gestation provides valuable data that will be useful for embryonal/foetal age estimation for research purposes. It also allows for evaluation of the effect of environmental factors, drugs and radiation amongst others on development (McGeady *et al.,* 2006). Although foetal parameters such as length and weight at different phases of gestation provide estimated indices for estimating the age of foetuses, they are rather subjective to inherent individual and breed variation within species (Greenwood *et al.,* 2005).

The developmental features evaluated encompass the gradient of skin transparency, and consequent upon that are the blood vessels that are visible and prominent under the skin; calvarium consistency, regional appearance and distribution of hairs and timing and pattern of dental eruption and onset of phenotypic sex differentiation and development (Sivachelvan *et al.,* 1996; Jaji *et al.,* 2011). Several authors have documented the developmental horizons for various animals based on observable external features (Dun, 1955; Evans and Sack, 1973; Osuagwuh and Aire, 1986; Sivachelvan*et al.,* 1996). Shehu *et al.,* (2012) reported foetal developmental landmarks

in the camel at various stages of gestation. Some these features described include the consistency of the calvarium; which was said to be soft, pliable and hard depending on their gestational stage; the skin pigmentation which ranged from thin, transparent, pink, to thick and the presence of some visible blood vessels beneath the skin (the jugular vein and coccygeal vein). The regional appearance of hair in the order of its appearance around the eye, muzzle, neck, head, limbs and tails, then the rest of the body had also been used (Waziri *et al.,* 2012).However, the accuracy of measuring certain developmental parameters, such as crown rump length (CRL), may become unreliable, for example, in animals with long necks (like camels) and a wide variation may be observed in the practice of measuring the CRL along the neuraxis (Waziri *et al.,* 2012).

2.4 The Nervous System

The nervous system is responsible for the transmission of nerve signals to and from different regions of the body. In vertebrates, the nervous system is made up of two main parts namely: central nervous system (CNS) and peripheral nervous system (PNS). The CNS encompasses the brain and spinal cord while the PNS is made up of the peripheral nerves which links the CNS to other body parts (Kandel and Squire, 2000; Tortora and Derrickson, 2016).

2.4.1 Structure and Development of the Brain

The nervous system is a part of the body which commence development early and further lasts to post-birth. Neurulation is the process that leads to neural tube formation, which further and subsequently differentiate into the spinal cord and brain (Sadler, 2005) (Fig. 2.3). The entire neural system develops from the ectoderm. As the

ectodermal tissue thickness increases and subsequently surroundsthe notochord and paraxial mesoderm, theygive rise to the neural plate (Dyce *et al.,* 2002; Shiota, 2008).

The brain is a section of the CNS that is enclosed within the cranium. It is the control hub for almost all significant body functions essential for life. It receives afferent signals from sense organs via cranial nerves and spinal cord; processes these sensory inputs and induces a corresponding motor outputs to effector organs. Thus, the brain is specialized to co-ordinate activities of the animal in relation to visceral and somatic milieu. It is protected by cranial bones along with meninges. In the dogfish, there is only a single meninx, while in the mudpuppies, there is an external dura mater and an internal secondary meninx (Millen, 2003).

The CNS is derived from the dorsal epiblast of the vertebrate embryo, and is initiated by a conflation of signals emanating from the Hensen's node at the caudal end of the embryo (Wurst and Bally-Cuif, 2001). The reviews of the structural development of vertebrate brain by Fletcher and Weber (2003) and by Callebaut *et al.,* (2006) emphasised that the vertebrate brain is ectodermal in origin.

Mitotic division of the fertilized oocyte gives rise to a cluster of daughter cells, the morula which develops an inner cavity, the blastocoele, to become a blastocyst. The blastocyst differentiates into the primitive ectoderm and an underlying parallel layer of endoderm. Subsequently, the primitive mesoderm is formed. Thereafter, the notochord, a rod-shaped aggregate of cells derived from the mesoderm and situated between endoderm and ectoderm, cranial to the embryo's primitive streak, is formed. The notochord initiates the process of cephalic formation, neural and somitedevelopment. It induces the overlying ectoderm to become neuroectoderm. It denotes the position of the prospective vertebral column and the base of the skull. The

notochord is present at some stage in the life cycle of all chordates (Monk *et al.,* 2001). It persists throughout the life cycle of some invertebrate chordates, but is replaced during embryological development in most vertebrates by the vertebral column (Monk *et al.,* 2001).

Through the release of growth factors, the overlying neuroectoderm is induced to develop more rapidly, forming a thick mass of simple columnar epithelium, the neural plate, on the upper, longitudinal axis by a process known as neural induction (Monk *et al.,* 2001). According to Jacobson and Tam (1982), the cephalic neural plate exists, and its thickening commences at the presomite stage of the mouse embryo. The neural groove is formed as a consequence of the neural plate folding. The groove continues to deepen until its sides, the neural folds, arch over and fuses with each other, forming the neural tube, which surrounds a fluid-filled neural canal.

The apposition of the neural tube is called primary neurulation; it occurs at about gestation day 20 in the human foetus (Gilbert, 2000a). Neural tube formation starts in the neck region and extends forward and backward from that point. However, while the apposition of the folds in the rodent embryo occurs on multiple sites, there are only 2 sites of fusion in humans(O'Rahilly and Müller, 2002). Neural crest cells (NCC) develop just prior to the formation for the neural tube and are located dorsolaterally at the junction of the neuroectoderm and ectoderm. TheseNCCs separate from this junction as the tube develops. Columns of NCCs form along the dorsal and lateral parts of the neural tube, while the ectoderm fuses dorsal to the neural tube creating the overlying skin (Thomson and Hann, 2012). The neural tube extends the length of the embryo including into the head region and forms the basis of the spinal cord and the brain. The proliferation of cells into the neural tube is two-staged in mammals:

symmetrical and asymmetrical (Monk *et al.,* 2001). The former is characterized by a progenitor cell giving rise to two progenitor cells, while the latter is characterized by a progenitor cell giving rise to one progenitor cell and one post mitotic neuron that cannot undergo further proliferation.

These series of proliferations lead to the outpocketings of the neural tube within the head into three vesicles. Caudo-rostrally, they includethe rhombencephalon, mesencephalon and prosencephalon(Randall *et al.,* 2002). The sulcus limitans is a groove that forms in the lateral walls of the neural canal, which demarcates the tube into alar and basal plates that are associated with sensory and motor functions, respectively (Thomson and Hann, 2012). During differentiation of the neural tube, three cell layers develop from the original pseudostratified, single cell layer. Innermost, sited around the neural canal, is the germinal layer, in which cellular proliferation occurs producing both neurons and the supporting glia - oligodendrocytes and astrocytes (Kessaris*et al.,* 2008). The post-mitotic cells migrate so that the neurons are located in the middle or mantle layer (Thomson and Hann, 2012). Astrocytes are found in both the mantle and marginal layer. Oligodendrocytes settle in the marginal layer to myelinate the axons. After development, the germinal layer becomes the ependymal layer surrounding the ventricles; mantle layer becomes the grey matter and marginal layer becomes the white matter (Gilbert, 2000b).

Further cellular differentiation and migration produces a series of five vesicles which become the major part of the brain. The prosencephalon differentiates into the telencephalon which grows laterally, and the diencephalon that stays medially (Randall *et al.,* 2002). The mesencephalon (midbrain) remains undifferentiated while the pontine flexure separates the rhombencephalon into the metencephalon (pons and

cerebellum) and myelencephalon (medulla oblongata) (Foley and Stern, 2001). The NCCs arise in the upper mid-line of the embryonic neural tube and move peripherally to contribute to a host of tissues and organs such as peripheral neurons, smooth muscles, and craniofacial bones. Axonal outgrowth and synaptogenesis are paramount to brain function. Formed synaptic connections are regulated by neurotrophic factors which are necessary for survival (Costa *et al.,* 2004). During the process, some brain cells die by the process of apoptosis (programmed cell death). Most of these cells are those with poor synaptic connections. Apoptosis is modulated by neurotrophic factors (Costa *et al.,* 2004).

At early first trimester, the primordia of the three primary brain vesicles are visible as neural plate thickenings (Saitsu *et al.,* 2004) (Fig 2.4) Neural tube division includes the cephalic (head) end of the neural tube which appeared larger compared to the caudal (tail) end. Hence, the head end of the tube differentiates into three distinct dilatations before it closes at the cephalic end (Pansky, 1982; Charles *et al.,*2005) (Fig 2.5).

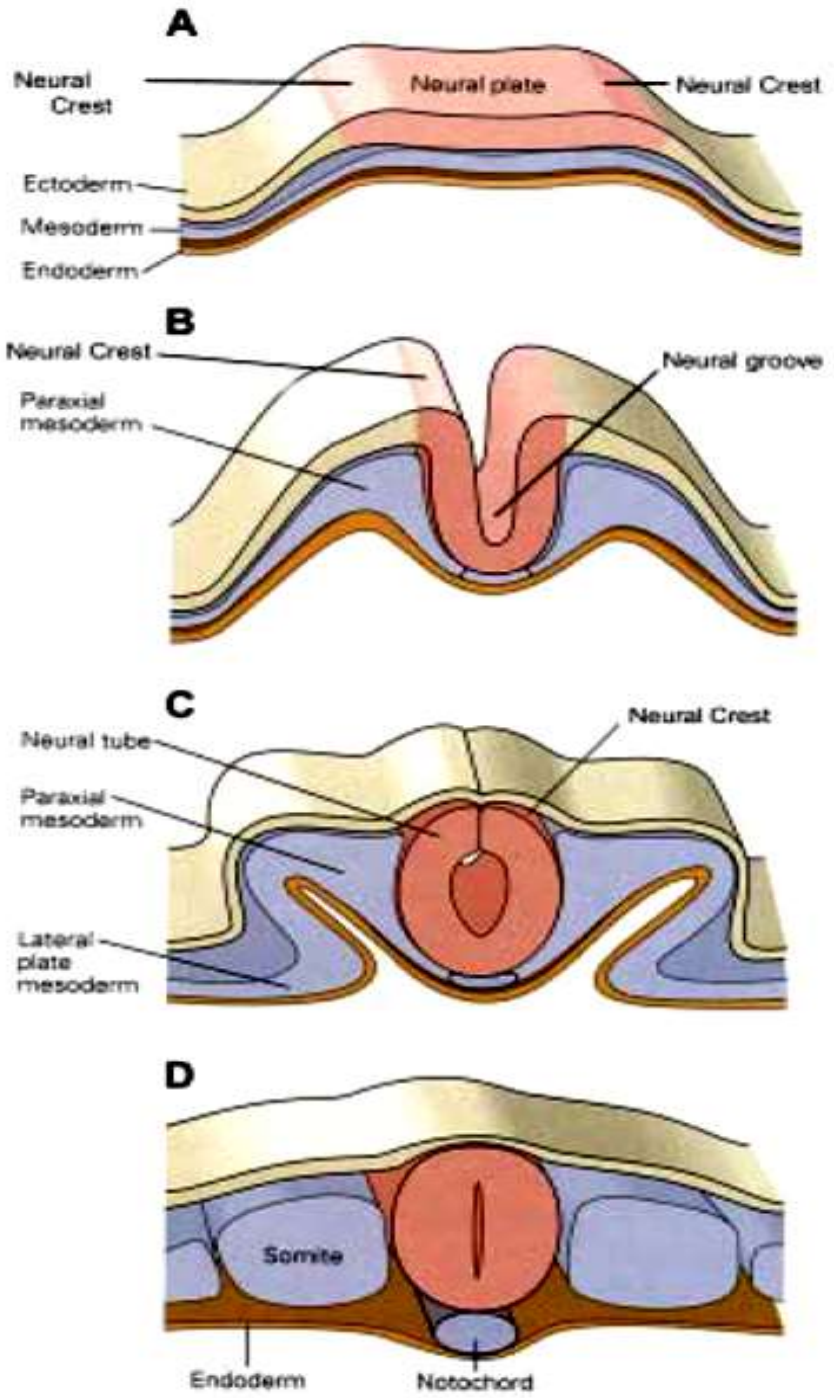

Figure 2.4: Schematic representation showing neural tube folding and the formation of neural tube and neural crest. (Source: Kandel *et al.,* 2012)

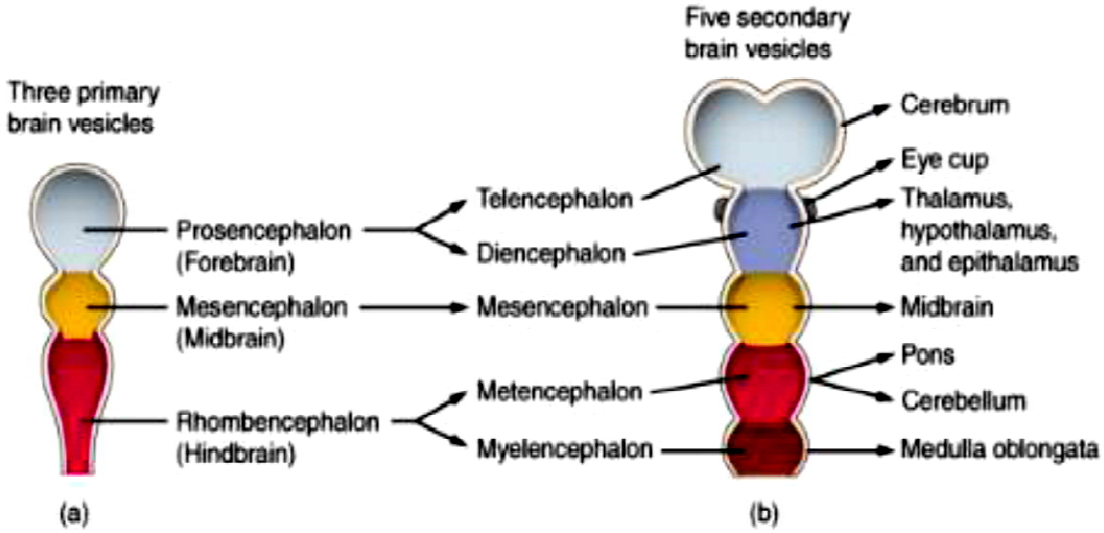

Figure2.5: Brain Vesicles: (a) Primary (b) Secondary [Source: Elshazzly and Caban, 2018].

During brain development, the resulting primary brain vesicles i.e. the prosencephalon, mesencephalon and the rhombencephalon further differentiate into 5 secondary brain vesicles (Thomas and Alvin, 2013; Elshazzly and Caban, 2018) as shown in Fig 2.5. Prosencephalon which is the forebrain forms the largest brain portion subsequently differentiates into the telencephalon (cerebral hemispheres or cerebrum) and diencephalon (epithalamus, thalamus, and hypothalamus) (Pansky, 1982; Elshazzly and Caban, 2018). Mesencephalon, also called the midbrain, undergoes little structural differentiation (compared to other brain vesicles and also, the spinal cord) during further development of the brain, which takes place on its dorsal and ventral part to form the tectum and tegmentum respectively (Bear *et al.,*2001). Rhombencephalon (the hindbrain), further divides into the metencephalon (cerebellum) and myelencephalon (medulla and the pons) (Stiles and Jernigan, 2010) (Fig. 2.5).

2.4.2 Brain Flexures

The brain presents three flexures during development, which generally disappear (straighten out) in vertebrates as the development advances;

1. The ***midbrain or mesencephalic flexure***is found between the prosencephalon and mesencephalon, folding the former ventrally (Fig 2.6c).
2. The ***cervical flexure***bends the neuro axis between the rhombencephalon and spinal cord. This flexure remains postnatally in domestic animals (Fig. 2.6b).
3. The ***pontine flexure***is concave dorsally and it marks the junction between the metencephalon and the myelencephalon. It is found between the cervical and midbrain flexures as an unequal growth in the hindbrain in the

opposite direction (the other flexures are concave ventrally). This flexure is seen as a bend in the axis of the embryological CNS below the neuraxis (Bear *et al.,*2001) (Fig. 2.6d).

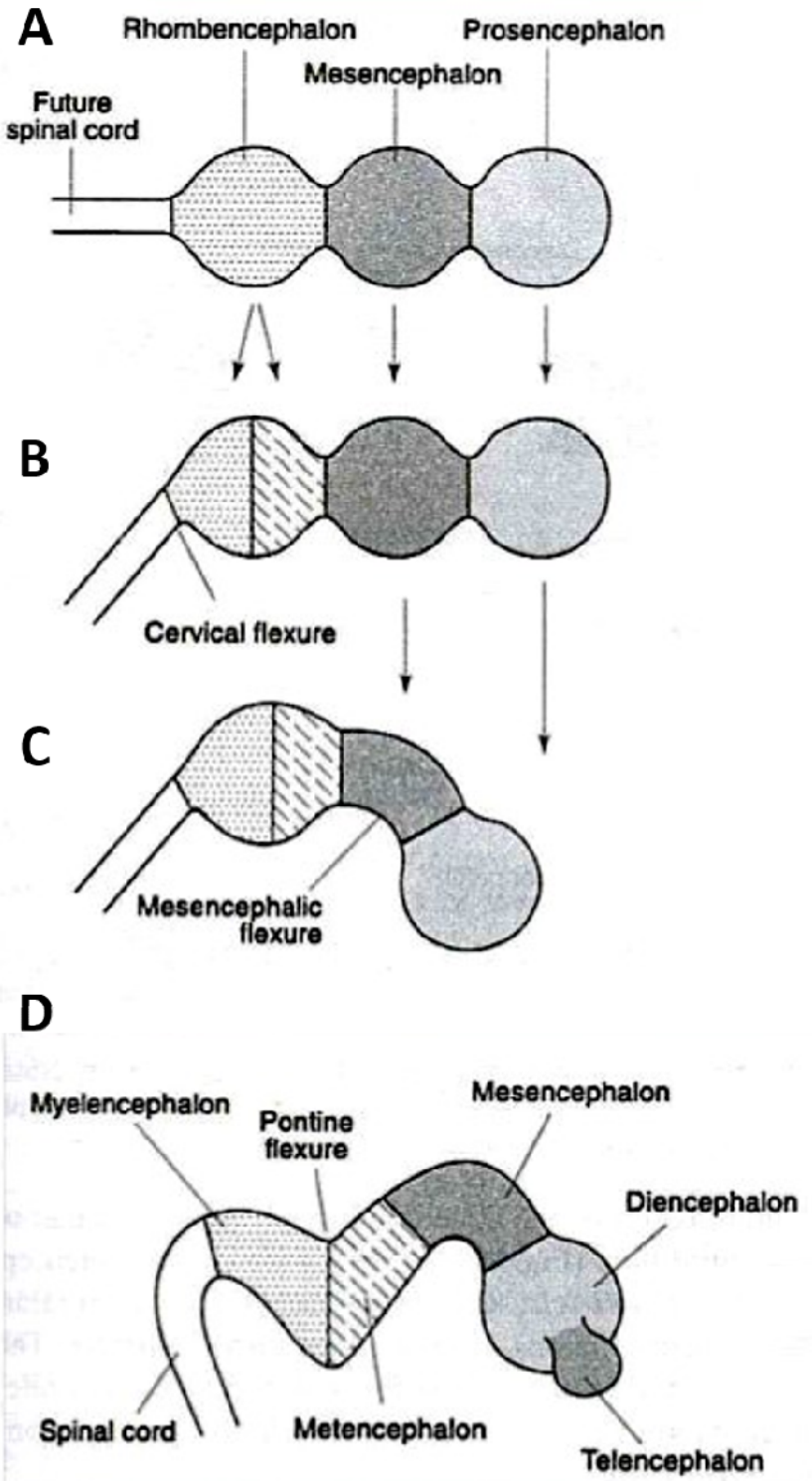

Figure 2.6: Schematic diagram showing sequence of brain flexures formation. (A) primary brain vesicles; (B) Cervical flexure; (C) Midbrain flexure; (D) Secondary brain vesicles and the Pontine flexure. (Source: Eleccion, 2012).

2.4.3 Brain Divisions

2.4.3.1 Forebrain

The forebrain includes a paired cerebral hemispheres (telencephalon) and a median diencephalon. The cerebral hemispheres cover the dorsolateral aspects of the diencephalon (Dyce *et al.,* 2002).

2.4.3.1.1 Telencephalon (Cerebrum)

The telencephalon is of two major components, the paired cerebral hemispheres (cerebrum), and the *lamina terminalis grisea* known as the optic part of the hypothalamus (Dyce *et al*, 2002). The cerebrum or cerebral hemisphere forms the bulk of the brain (Fig. 2.7). It has bilateral hollow outgrowths which are seen as the cerebral hemispheres, comprising of the outer grey matter cortex, inner white matter as well as basal nuclei. The pouch of the telencephalic process becomes the lateral ventricle that continues into the third ventricle by means of the inter-ventricular foramen.Each cerebral hemisphere has four lobes namely: parietal, frontal, temporal and occipital lobes (Jacobson and Marcus, 2008). The mantle layer proximate to the lateral ventricles of the hemispheres becomes the basal nuclei andcerebral cortex.

In higher mammals, the cerebral cortex is convoluted, forming ridges called gyri and troughs called sulci. The convolutions permit more cortical surface areas to be contained in the same volume of cranial vault (Hof *et al.,* 2005). Animals with a convoluted cerebral cortex are said to be gyrencephalic (for example, ruminants),

while those with smooth cerebral cortex are said to be lissencephalic (for example, rodents).

Scarce gross morphometric literature of the adult AGCR brain exists. Nzalak *et al.,* (2008) reported a mean weight of the forebrain of an adult AGCR as 7.22 g, which represented 67.5% of the adult brain; while the forebrain of another rodent, the African giant pouched rat was 3.32 g, represents 66.0% of the adult brain. Thus, from the study, it can be deduced that the adult AGCR has a significantly larger cerebrum than the adult pouched rat. Authors also noted a significantly longer cerebral length in the AGCR, compared to the pouched rat.

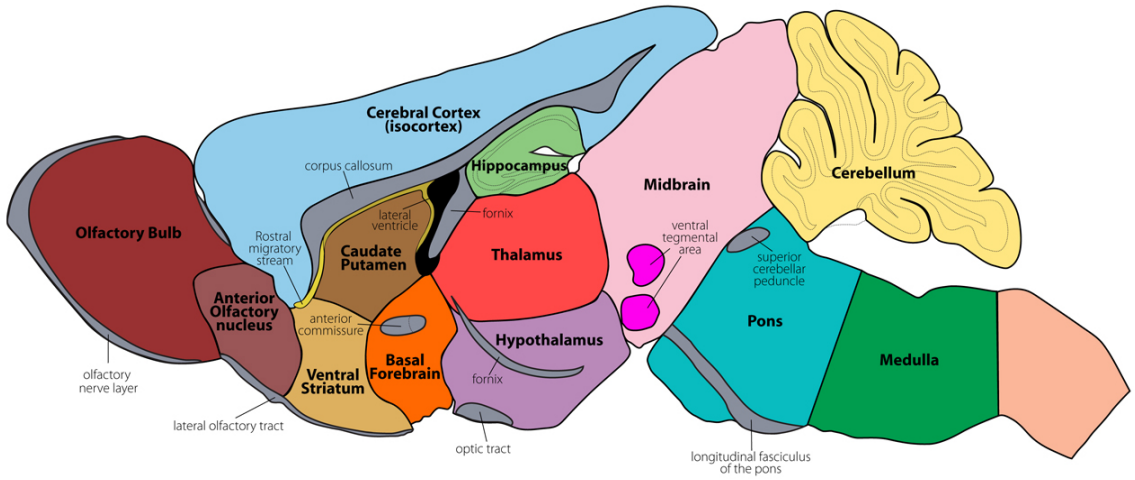

Figure 2.7: Schematic illustration of the mid-sagittal section of the rat brain (Source: GENSAT, 2019).

2.4.3.1.1.1 Layers of the Cerebral Cortex

The neocortical nerve cells are well divided into six distinct layers, with different shape, size, and population at each layers (Fig.2.8). The layers connect and differ in the different cortical region according to the cortical depth and function. These cortical layers include:

i. *Plexiform (molecular) layer*: represents the most external or dorsal layer, which largely contains nerve processes of nerve cells in this region, thereby forming a synapse with one another.
ii. *Outer granular layer*: mainly containsstellate and small pyramidal cells and nerve processes from the deeper layers.
iii. *Pyramidal cell layer*: this layer contains a considerably moderately sized pyramidal and Martinotti cells.
iv. *Inner granular layer*: consists mainly the closely crammed stellate cells.
v. *Ganglionic layer*: This layer is populated largely with the large pyramidal cells, lesser quantities of stellate cells and Martinotti cells and earned its name from the giant pyramidal (ganglion) Betz cells of the motor cortex.
vi. *Multiform cell layer*: This layer contains a large range of different morphological forms of neurons. It contains several minute pyramidal cells, fusiform cells, stellate cells at the surface, and cells of Martinotti.

Synaptic interconnections within the cortex are very complex, with every neuron synapsing with several hundred others (Young *et al.,* 2006).

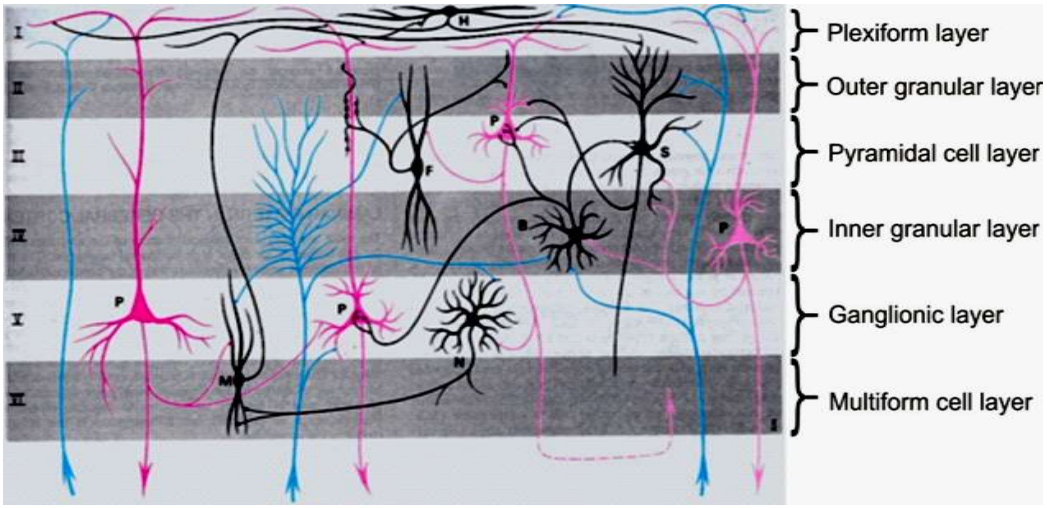

Figure 2.8: Schematic diagram of different cerebral cortical layers. (Source: El-Bab, 2001).

2.4.3.1.1.2 Olfactory Bulb

The development and delineation of the olfactory systems is hinged on epithelial-mesenchymal interactions. These events take place at two locations namely: (1) between the neural crest cells and ectoderm of the frontonasal prominence leading to the formation of the olfactory placodes and, (2) between the neural crest cells and telencephalic floor to differentiate into the olfactory bulbs (Sterling, 2008). The cell populations in the region of the nasal placodes becomes primary afferent neurons of the olfactory mucosa whose axonal processes elongates and form synapses with secondary neurons in the primordial olfactory bulbs (Kim *et al.,* 2004). These synapses become well-established by the seventh week. With the further development of the brain comes the lengthening of the olfactory bulbs and tracts of the secondary neurons, and collectively they make up the olfactory nerve (Gilbert, 2010).

The olfactory bulbs are oval ventro-rostral projections of the rostral end of the telencephalon, that lodges in the *fossa cribriformis*of the ethmoid bone (Nzalak *et al.,* 2005). The rhinal sulcus separates these bulbs from the cerebrum above. Around the temporal region of the cerebrum and somewhat ventral to the mid rhinal sulcus is the pear-shaped piriform area. This piriform area belongs to the phylogenetically older palleopallium or paleocortex (Nzalak *et al.,* 2005).

Microscopically, the olfactory bulb is made up of six layers and it thought to be as a result of the modification of the three-layered allocortical structure, as against the isocortical structure (Nagayama *et al.,* 2014; Ruberte *et al.,*2017) (Fig. 2.9).

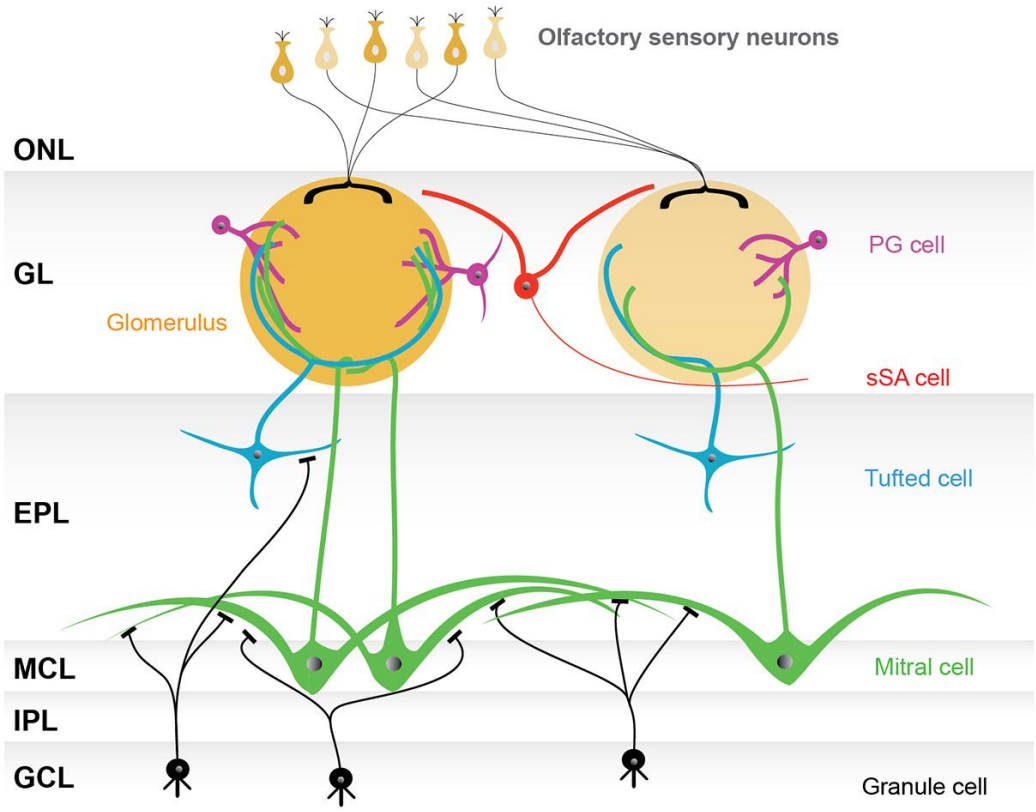

Figure 2.9: Basic cellular architecture of the olfactory bulb network in the rat. ONL: olfactory nerve layer; GL: glomerular layer; sSA: superficial short-axon cell; MCL: mitral cell layer; EPL: external plexiform layer; IPL: internal plexiform layer; GCL: granule cell layer. (Source: Nagayama *et al.,* 2014).

From outward inwards, the layers include:

i. The *olfactory nerve layer*: comprises of the sensory axons of the epithelial olfactory sensory neurons. These neurons are unmyelinated.

ii. The *glomerular layer***:** are globular structures of neuropil, with about 2,000 glomeruli. This layer forms the point where the dendrites and axonals of mitral cells and those of the olfactory sensory neurons terminate and form synapses. Inhibitory juxtaglomerular neurons of different types evidently perform lateral inhibition on neighbouring glomeruli or mitral and tufted cells.

iii. The *external plexiform layer*: is essentiallyconstituted by neuropil. It alsocomprises smaller versions of mitral cells (tufted cells)in addition to various interneuron types.

iv. The *mitral cell layer*: comprises of somata of glutamatergic mitral cells, that make up the chief motor constitution of the olfactory bulb.

v. The thin *internal plexiform layer*: is comprised by collaterals of the mitral cell axons. This layer appears deeper to the mitral cell layer.

vi. The large and cell-dense *granular cell layer*: This layer is filled up by numerous small interneurons called granule cells. This cellular dense layer represents the largest olfactory bulb population and is migrated from the subpallium.

2.4.3.1.2 Diencephalon

The diencephalon is composed of the thalamus, hypothalamus, and epithalamic structures (Fig. 2.7). It is formed as a result of the dorsoventral expansion of the neural cavity which further gives rise to the third ventricle. The neurohypophysis emerges

from the third ventricle while the thalamus, epithalamic structures, subthalamus and hypothalamus are formed from the mantle layer. The optic nerves emanate as extensions from the ventral diencephalic wall (Thomas and Alvin, 2013; Fletcher, 2013).

2.4.3.2 Midbrain (Mesencephalon)

The midbrain is the most rostral portion of the brain stem with its cavity transforming into the mesencephalic aqueduct. The alar plates develop into the corpora quadrigemina (two pairs of rostral and caudal colliculi). In rodents, such as the giant rat, the mesencephalon separates the 3rd ventricle from the 4th ventricle dorsally, while it extends rostrally from the most rostral part of the pons to the caudal part of the mammillary body (Ibe *et al.,* 2014). The mesencephalon gives rise to the third and fourth cranial nerves – the oculomotor and trochlear nerves respectively – which innervates the extrinsic muscles of the eyeball. It consists of a dorsal surface, known as the mesencephalic tectum (roof) of the midbrain bearing bilateral rostral and caudal colliculi (elevations) and a ventral part known as the mesencephalic tegmentum and the pes mesencephalon - the crus cerebri and substantia nigra (Fletcher, 2013; Thomas and Alvin, 2013) (Figs. 2.10and 2.11).

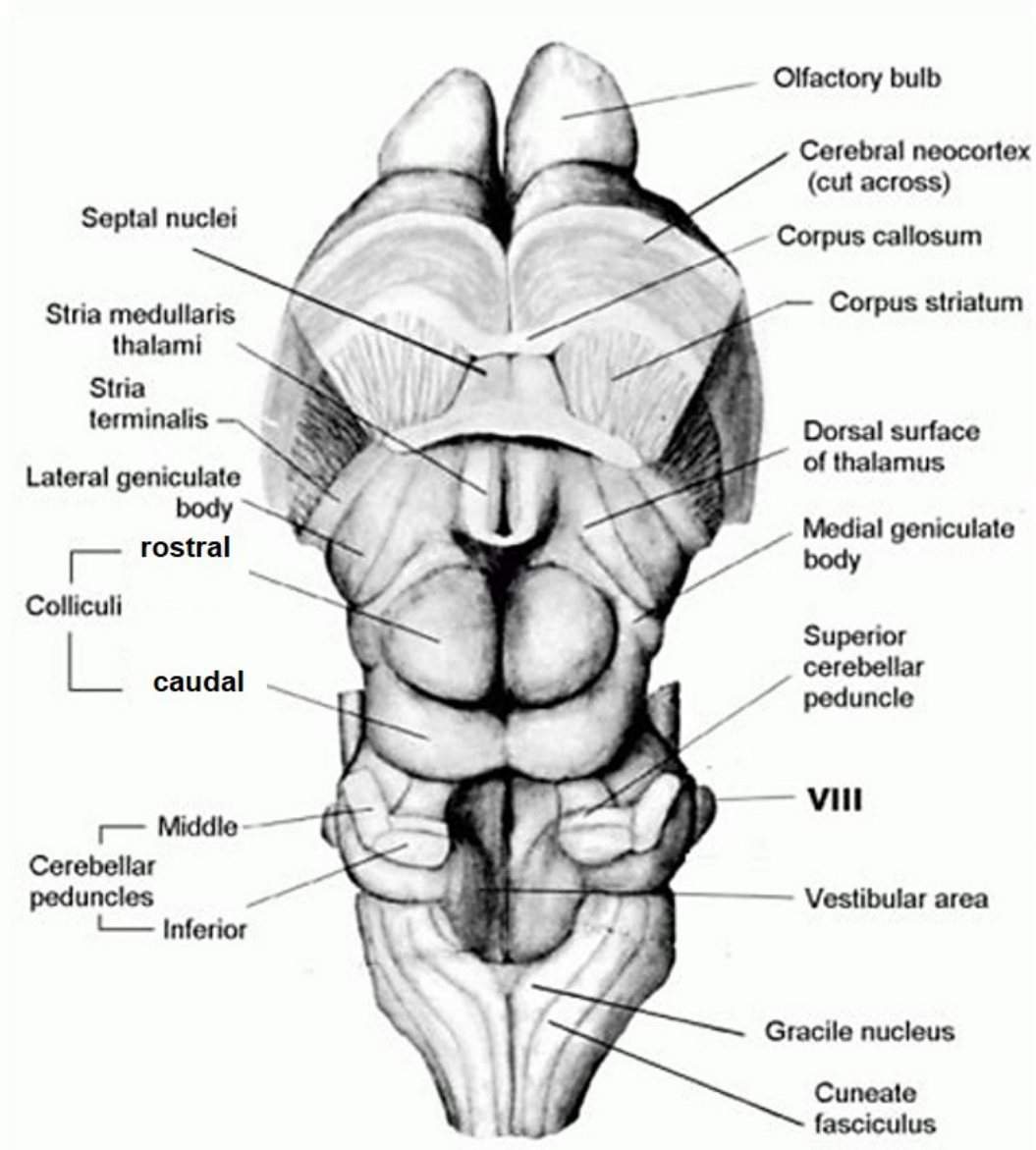

Figure 2.10: Schematic diagram of the rat brain highlighting the diencephalon, brain stem and parts of the prosencephalon (dorsal view) with the cerebellum and caudal two thirds of the telencephalon cut.(Source: Notebaert, 2018).

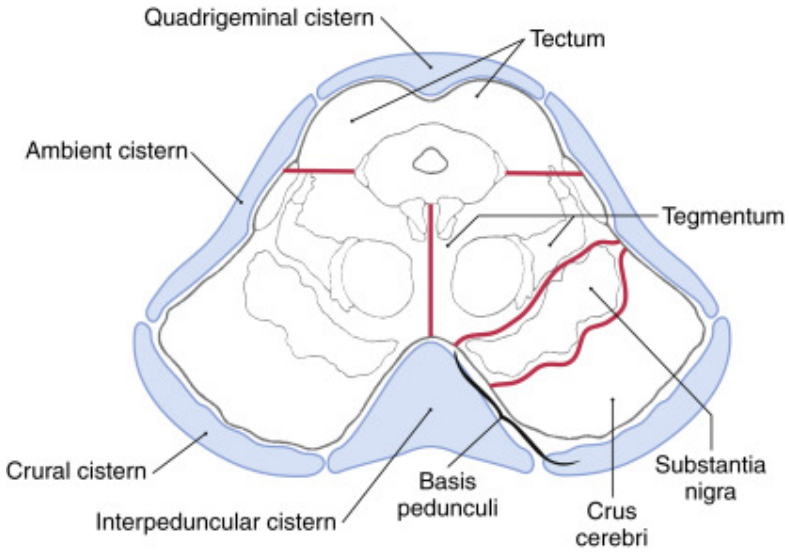

Figure 2.11: Schematic diagram of the coronal view of the mid brain(Source: Haines and Mihailoff, 2018)

2.4.3.2.1 The Mesencephalic Tectum

2.4.3.2.1.1 Gross and Morphometric Organization of Mammalian Mesencephalic Tectum

The mesencephalic tectum constitutes the midbrain roof. It comprises of a pair of rostral and caudal colliculi, together referred to as the corpora quadrigemina. They can either be partially or completely concealed by cerebral and/or cerebellar hemispheres. In larger mammals, it is concealed by the cerebral hemispheres and cerebellum.While in the Wistar rat, the tectum is distinct with the exception of the tips of the caudal colliculi that are covered by the occipital portion of the cerebrum, the pineal body and rostral part of the cerebellum (Suckow *et al.,* 2006). Conversely, Ibe (2010) noticed that the entire rostral colliculus and rostral part of the caudal colliculus of the giant rat are covered by the occipital portion of the cerebrum, while the caudal half of the caudal colliculus can be readily seen dorsally.

All vertebrates are noted to have optic lobes (or rostral colliculi in mammals) except in remarkably large birds with large-sized eyes which depend heavily on visual cues in their environment. In birds, the backward growth of the cerebral hemispheres to meet the cerebellum has pressed the optic lobes outward, thus assuming a lateral instead of dorsal position (Bhatnagar and Bansal, 2008). In the phylogenetic tree, the auditory lobes (or caudal colliculus in mammals) commence from the class Reptilia; fishes have auditory nuclei in this location, but they are not large enough to bulge on the surface (Bhatnagar and Bansal, 2008).

2.4.3.2.1.2 Histological Organization of Mammalian Mesencephalic Tectum

The cytoarchitectural details of the mammalian rostral colliculus has been well elucidated most notably in rabbits (Gonzalez-Soriano *et al.,* 2000), hamsters (Kang *et*

al., 2002), ferrets (Behan *et al.,* 2002), cats (Cirone *et al.,* 2002), Wistar rats (Cooper *et al.,* 2004), monkeys (Krauzlis, 2004), camels (Mensah-Brown and Garey, 2006) and African giant pouched rats (Ibe, 2010). The rostral colliculus consists of several layers, each with distinct neuronal organization. These are the stratum zonale, stratum griseum and stratum medullaria (Nomina Anatomica Veterinaria, 2017). Retinal input to the rostral colliculus is most-dense at superficial griseum layer, which absolutely processes visual inputs (Girman and Lund, 2007). In the Sprague-Dawley rats, the stratum griseum is further divided into superficial griseum layer, optic layer, intermediate griseum layer, intermediate white layer, and deep griseum layer (Telford *et al.,* 1996).

The caudal colliculus is further split into a dorsal cortex, central nucleus, and a lateral cortex (Loftus *et al.,* 2008). The central nucleus is the principal pathway for ascending acoustic information. The greater proportion of neurons found in the central nucleus have roughly spherical basealigned parallel to the several sensory fibres (Gabriele *et al.,* 2000).

2.4.3.2.1.3 Development of Mammalian Mesencephalic Tectum

The mesencephalon is the second vesicle of the three primary vesicles formed from the neural tube. It does not undergo further division, unlike the prosencephalon and rhombencephalon. According to Fletcher and Weber (2003), the dorsal roof transforms into the corpora quadrigermina (rostral and caudal colliculi) of the mesencephalic tectum while the ventral floor generates the oculomotor nerve and trochlear nerve nuclei, and the Edinger-Westphal nuclei. The descending fibres form the cerebral crus, while the space with the mesencephalon becomes the mesencephalic aqueduct.

2.4.3.2.2 Tegmentum

The tegmentum is a phylogenetically old part of the brainstem containing the brainstem nuclei in the adult. It is on the ventral part of the brainstem with coloured markings largely due to the presence of the substantia nigra and the red nucleus which is involved in the involuntary motor control. The remaining cell groups are disseminated in the mid brain and possess axons that project widely throughout the bulk CNS - regulating consciousness, pleasure, pain and moodiness (Bear *et al.,* 2001).

2.4.3.3 Hindbrain (Rhombencephalon)

The hindbrain develops into three chief structures namely; the medulla oblongata, pons and cerebellum (Fig. 2.7). The last two emerges from the rostral-half of the hind brain (metencephalon) while the medulla emerges from the caudal half of the hindbrain (myelencephalon) (Bear*et al.,* 2001).

2.4.3.3.1 Medulla Oblongata and Pons

The dorsal roof of the myelencephalon spreads out laterally while the neural cavity enlarges dorsally giving rise to the fourth ventricle. The dorsal wall of this ventricle becomes extended and thinned out into the ependymal layer surrounded by pia mater.

The medulla oblongata goes into the formation of the bulk of the fourth ventricle and gives off a total of seven cranial nerves (VI to XII). On the other hand, the pons which is a component of the brain stem gives off the fifth cranial nerve (trigeminal nerve). It has a well-defined and conspicuous ventral eminence compared to the dorsal roof (Bear *et al.,*2001; Fletcher, 2013).

2.4.3.3.2 Cerebellum

The emergence of the paired rhombic lips signals the first sign of the development of the cerebellum. These lips later meet medially forming the isthmus at the midline. The rhombic lips eventually differentiate into the two cerebellar hemispheres while the isthmus transforms into the cerebellar vermis. Hence, the cerebellar region is divided into the vermis, and bilateral cerebellar hemispheres while it surface is partitioned into folia (folium = ridge) separated by sulci (sulcus = groove) (Fletcher, 2013).

2.4.3.3.2.1 Gross and Morphometric Organization of Mammalian Cerebellum

The cerebellum is located in the caudal portion of the neurocranium. It is separated from the cerebrum by a transverse fissure and the tentorium cerebelli. The surface of the cerebellum is corrugated by long thin folds, the folia, composed of both cortex and white matter, and demarcated by fissures of varying extents. The collection of white matter that extends into the folia has a tree-like appearance, thus called the *arbor vitae*, a Latin term for 'Tree of Life'. In mammals, folia act as a general base on which the rostro-caudal arrangements of the sensorimotor circuitof the cerebellum is built (Sudarov and Joyner, 2007).

The three cerebellar lobes are found in all vertebrates. The flocculus and paraflocculus on each side of the vermis make up the cerebellar hemispheres demarcated by the falx cerebelli, a meningealextension. The vermis is split, via the dorsal primary fissure, into a rostral and caudal portion. The rostral division of the vermis is made up of the following caudo-rostral lobules: culmen, central lobule and lingula while the caudal division is made up of the following caudo-rostral lobules:nodulus, uvula, pyramis, tuber, folium and declive. Also, the hemispheric lobules include lobulus quadrangularis, lobulus simplex, lobulus ansiformis, lobulus paramedianus (Nomina

Anatomica Veterinaria, 2017). However, there is a vast modification of the above-mentioned vermis and cerebellar hemispheric lobules in various animals, and this has been related to the intricate unique functions of the various lobules in different species. Furthermore, variation in the gross morphology of mammalian cerebellum due to sex is scarce in available literature. Byanet *et al.,* (2014) reported the absence of sexual dimorphic features in the adult AGCR cerebellum.

The cerebellum is linked to the brainstem by 3 bundles of tracts - the cerebellar peduncles. They are named for their site of attachment to the brainstem. The rostral cerebellar peduncle contains mainly cerebellar efferent tracts connecting the cerebellum with the mid-brain, but also has one afferent tract, the ventral spinocerebellar tract. The middle cerebellar peduncle has only afferent tracts that convey impulses from the pons to cerebellum. The caudal cerebellar peduncle possesses both sensory and motor tracts. The cerebellar hemispheres are largest in man (Sultan and Braitenberg, 1993). Similarly, Demaerel (2002), in agreement with early researchers, reported that expansion of individual folia is correlated with behavioural differences among species. The cerebellar vermis and hemispheres in the white rat are broad such that the paraflocculus extends beyond the lateral border of the cerebellar hemispheres (Larsell, 1952).

The gross morphology and morphometry of the cerebellum in some adult rodents, for instance the mice (Inouye and Oda, 1980), white rat (Larsell, 1952), African giant pouched rats (Byanet *et al.,* 2013), and chinchillas (Sultan and Braitenberg, 1993)has been widely investigated. The cerebellum of rodents has a complex folia pattern. The cerebellar weight and length of an adult giant rat are significantly higher compared to the adult AGCR (Nzalak *et al.,* 2008). Sexual dimorphic evaluation of the adult AGCR

cerebellum showed that the cerebellar width and length did not vary significantly between both gender (Byanet *et al.,* 2012).However, the adult male cerebellar circumference was higher compared to the female. It was inferred that the bigger plump head of the male AGCR may have contributed to this difference. Byanet *et al.,* (2012) also reported a positive correlation between the brain length and body parameters in the matured female AGCR.

2.4.3.3.2.2 Histological Organization of Mammalian Cerebellum

Histologically, the mammalian cerebellum is made up of (from inside outwards): the presumptive white matter, granule cell layer, Purkinje layer and molecular layer, (Purves *et al.,* 2001). The neonatal cerebellum howeverhas an additional layer, the external granular layer, which lies the molecular layer (Smeyne and Goldowitz, 1989; Gelpi *et al.,* 2013). The cerebellar Purkinje cell is one of the biggest and most complicated neurons of the nervous system in mammals (Purves *et al.,* 2001). They have very functional dendrites that generate enormous calcium ion stimuli in reaction to synaptic inputs. The queer anatomical arrangement of their dendritesis largely conserved to a noteworthy degree via evolution, signifying that their specific form is fundamental to the Purkinje cell function.Their large dendritic harbours form nearly two-dimensional layers through which parallel fibres from the deeper-layers pass. These so-called parallel fibres are a product of the bifurcation of mossy fibres and granule cells.

Mossy fibres, which originate from the pontine nuclei, ascend from the brainstem and spinal cord to influence Purkinje cells indirectly, by means of the tiny granule cells. Parallel fibres pass through the Purkinje neuron's dendritic arbour forming a granule cell-Purkinje-cell synapse (Landis and Reese, 1977). Unlike the parallel fibres, each

Purkinje cell receives synaptic contribution from only one single climbing fibre from the inferior olivary nucleus. The climbing fibre is literally wrappedabout the soma and dendritic processes of the Purkinje cell, forming numerous synapses (Wadiche and Jahr, 2001).

The white matter layer of the cerebellum contains tracts that serve as impulse channel between the cerebellum and the periphery. These tracts make up the cerebellar peduncles. The caudal cerebellar peduncles include the dorsal spino-cerebellar tract, olivo-cerebellar tract, cuneo-cerebellar tract and vestibulo-cerebellar tract. The middle cerebellar peduncles include the ponto-cerebellar fibres, while the rostral cerebellar peduncle include the ventral spino-cerebellar tract, dentato-thalamic tract and trigemino-cerebellar fibres.

Four pairs of cerebellar nuclei are found within the deep cerebellar white mater, each on either side of the its hemisphere. On a coronal plane of the cerebellum, from the lateral to medial, the nuclei include the dentate, emboliform, globulus and fastigial nucleus. In some animals, including humans, the emboliform and globulus nuclei are fused, thus referred to as interposed nucleus. The dentate nuclei are the largest and located deep within the lateral hemispheres, the interposed nuclei are the smallest and located in the paravermal (intermediate) zone, and the fastigial nuclei are in the vermis (Kurkin *et al.,* 2014).

2.4.3.3.2.3 Development of Mammalian Cerebellum

The cytoarchitecture of the developing and mature rat cerebellum has been documented (Palay and Chan-Palay, 1974). Cells of origin of the climbing fibres, the inferior olivary nucleus, and the point of termination, the Purkinje neurons, all arise from immature cell groups located in the roof of the medulla oblongata. After mitotic

division of neuro-epithelial cells in the mid-embryonic days, one cell type moves in a dorsal direction through the parenchyme of the rhombic lip and the other moves ventrally through the medullary parenchyme, with a small number directed along the subpial region (Bourrat and Sotelo, 1988). Each group of neurons continues to develop at the terminal site of migration. At the perinatal period, each particular group of developing olivary axon terminals finds its own specific group of Purkinje cells as proper targets and makes synaptic contact with the membranes of these cells to establish the basic pattern of organization in the olivocerebellar projection (Kawamura *et al.,* 1990).

Immature Purkinje neurons migrate using non-neuronal processes as possible guides; presumably immature types of astroglial processes (Rahimi-Balaei*et al.,* 2018). In the vestibulo-cerebellum, a group of developing Purkinje cells re-arrange to take up a final position in a single cell layer underneath the immature external granule cells. These cells at later stages also migrate downwards, while extending their axonal processes parallel to the pial surface. Primary and secondary dendrites of Purkinje cells develop during this postnatal period and their spines receive afferent axon terminals (Kaneko *et al.,*2011). All climbing fibres originate from only the ventral olivary nucleus (Llinas *et al.,* 2004).

2.4.4 Neocortical Development

The cerebral cortex is the largest brain part of mammals. It plays important roles for complex sensory and behavioural capacity in various species. Behaviours such as voluntary movement, cognitive prowess, emotion,memory and perception (Van Essen and Glasser,2018).

It is divided into the under listed parts:

1. The Neocortex: the largest of the cerebro-cortical region
2. The Archicortex: includes the retrosplenial, hippocampus, entorhinal cortex and subiculum
3. The Paleocortex include the olfactorycortex (O'Leary *et al.,*2013).

2.4.4.1 The Neocortex

The neocortex is the six-laminated part of the dorsal telencephalon in mammals (Dwyer*et al.,*2016). Furthermore, the neocortex is responsible for much of the expanded cerebral cortex and also, its complexity in more advanced species. It is also probably the most distinctive phylogenetic specializations (Krubitzer and Kaas, 2005).

Neurons of the neocortex originates from the ventricular zone – a zone of neural stem cells known to be of pseudostratified epithelium (Fig. 2.12). These neurons are mainly generated in this VZ and then translocated to their ultimate stationin the laminar cortex (Nadarajah, 2003; Meyer, 2007; Montiel *et al.,*2016).

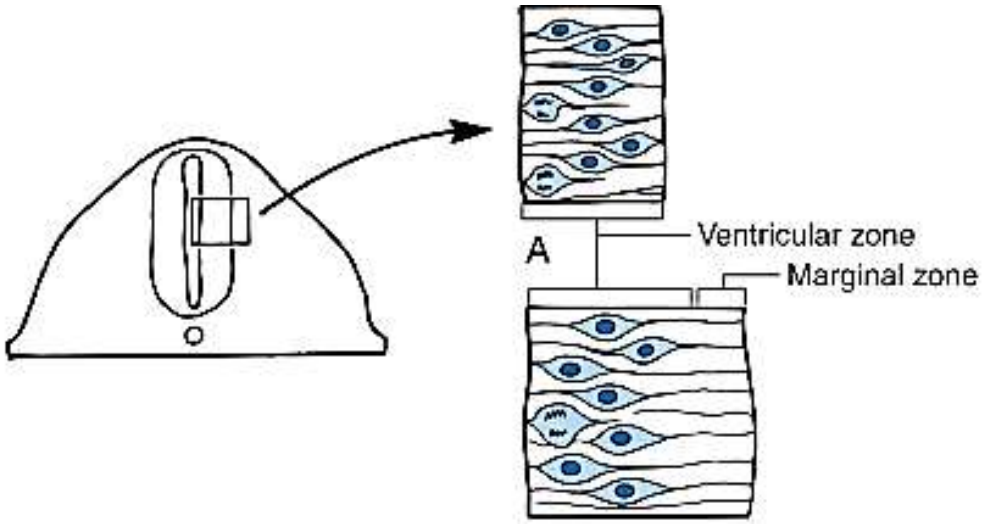

Figure 2.12: Schematic illustration of the pseudostratified layer of the ventricular zone. (Source: Haines, 2015)

Among the main characteristic feature that distinguishes the developing neocortex from other cortical regions is its layered structure which is mainly identified by six chief, radially structuredstrata. These layers are oftentimessubdivided, with each consisting of a mixed population neuronal populations that are structurally and operatively distinct (O'Leary *et al.,*2013). From a tangential perspective, the neocortex is structured into 'areas' that are operatively well-defined and distinguishable by their distinct cyto-architecture and chemo-architecture, afferent and efferent connections, and gene expression patterns (Rash and Grove, 2006; O'Leary *et al.,* 2007).

2.4.4.2 Neurogenesis

Corticogenesis in the mouse takes place between embryonic days 9 and 10 after which there is a subsequent designation of the telencephalon at the cephalic pole of the neural tube (Fig. 2.13). The early cortical NSCs - apical progenitors (APs) - are found in the polarized epithelium with its luminal surface becoming the lining of the future ventricles. The pseudostratified epithelial appearance of the VZ is direct consequence of the inter-kinetic nuclear migration of the APs within the VZ (Dwyer *et al.,*2016) (Fig. 2.14).

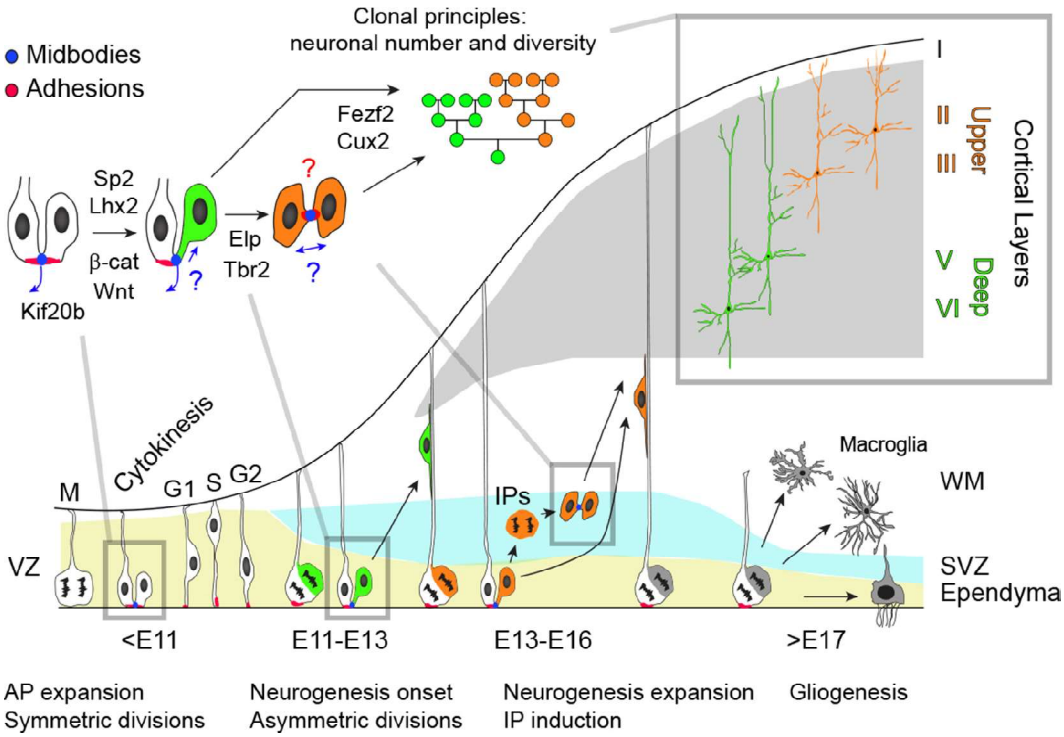

Figure 2.13: Schematic layout of corticogenesis in the mouse brain. (Source: Dwyer *et al.,* 2016)

Prior to the generation of new neurons, the neural tube is seen as a single layer of neuroepithelial cells (NECs) that form the neuroepithelium (Wodarz and Huttner, 2003). The germinal neuroepithelium or VZ is a temporal embryonic layer of tissue consisting of NSCs, predominantly radial glia cells of the CNS and their derivative neural progenitor cells (NPCs) which will divide symmetrically and asymmetrically to differentiate into the mature neural system. This contributes to neurogenesis, gliogenesis and ependymal cell formation (Noctor *et al.,* 2001; Rakic, 2009; Girard *et al.,* 2016).

Adjoining the VZ is a secondary germinal zone – the SVZ comprising of a pool of intermediate neuronal progenitors (NPCs) which are derivatives of the NSCs that ultimately divide and differentiate into postmitotic neurons (Noctor *et al.,* 2004; Hevner and Haydar, 2012) (Fig. 2.14). Peak periods of neurogenesis represent the time point at which the SVZ reaches its maximum thickness with the highest NPCs (Pax6+/Tbr2-) cell populations, more specifically the basal progenitor cells (Florio and Huttner, 2014).

The duration of the neurogenic period has been noted as one of the chief factors that defines the output of neurons and influence interspecies variation. Delayed onset of neurogenesis allows for a greater expansion of NEC pool prior to commencement of neurogenesis. Furthermore, prolonged period of neurogenesis allows for expansion of the NPCs pool, most notably the basal radial glia thus increasing neuronal output. Together, they contribute significantly to the expansion of the neocortex (Florio and Huttner, 2014).

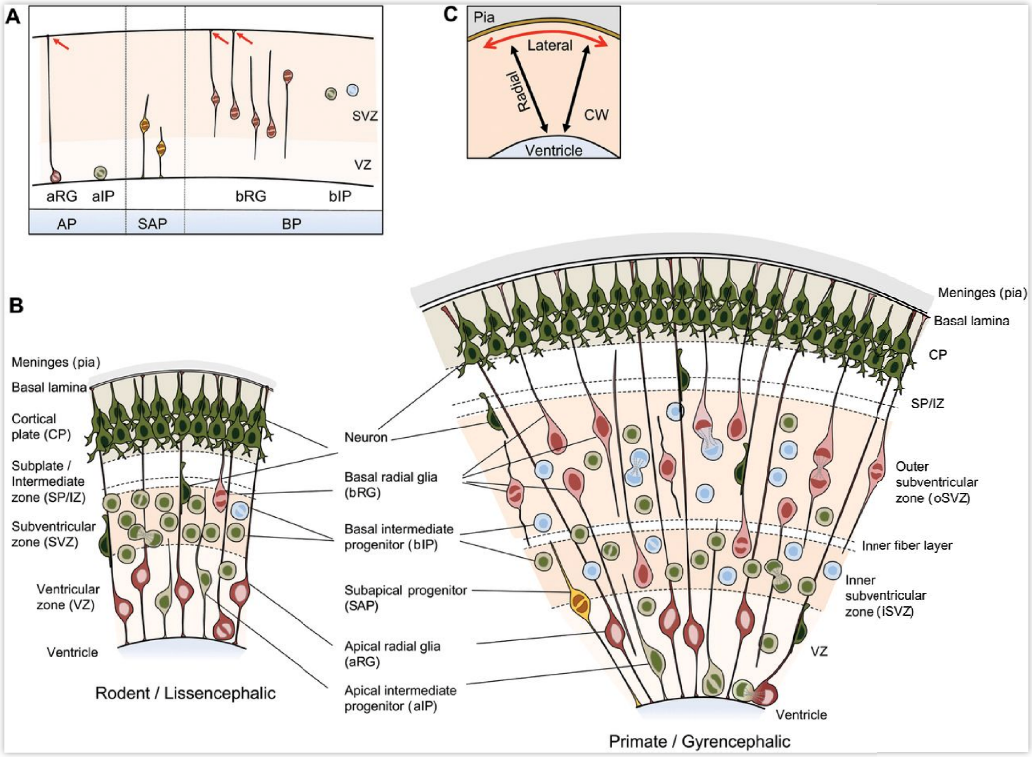

Fig.2.14: Schematic diagram of the different cortical zones and different neural progenitor cell subtypes. (Source: Florio and Huttner, 2014).

2.4.4.3 Neuronal Migration

Generally, in mammals, migration of neurons playsan important part in corticogenesis in the development of the cortex laminae. The migration entails the pattern of movement of neurons from the germinal zone, via the subplate to the variousdestined domains within the cortex (Meyer, 2007) (Fig. 2.15). This migration generally includes radial, tangential and multipolar migration (Meyer, 2007).

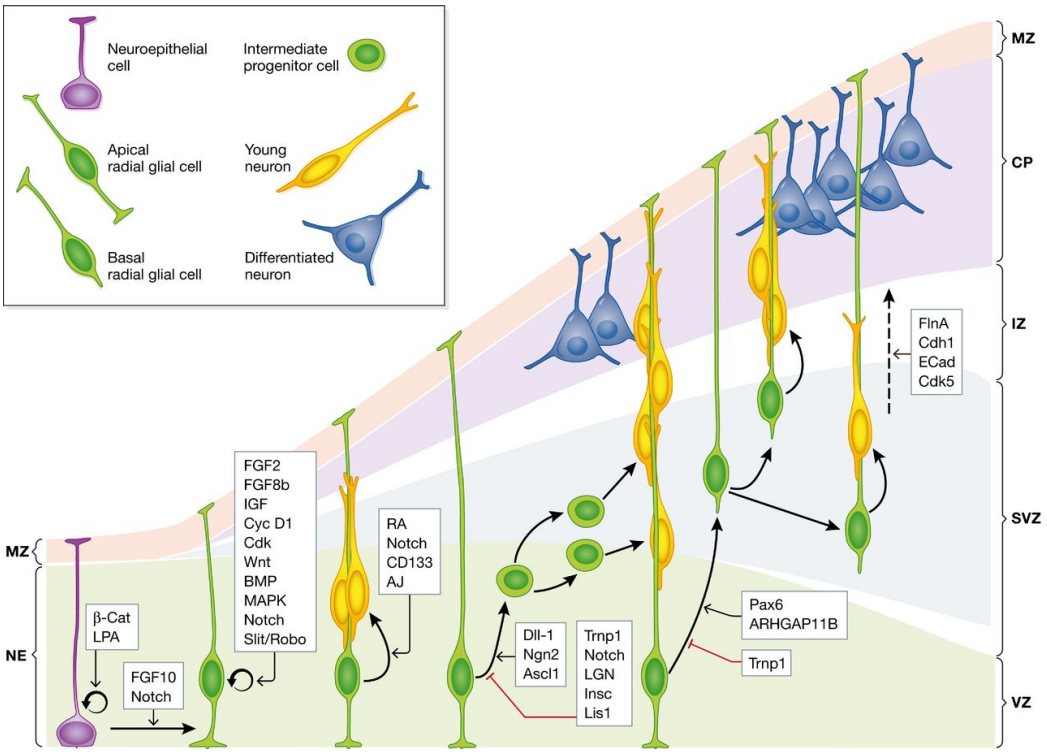

Figure 2.15 Schematic diagram of neuronal migration in the mouse neocortex. (Source: CopperKettle, 2006)

In the cortical plate (CP) and zone, the preplate (*pp*) is the first to be formed during corticogenesis prior to CP development in animal species. The *pp*, found between the pia and VZ, contains the foremost neurons of the marginal zone called Cajal-Retzius cells. They also contain precursors of the subplate (Meyer, 2007).

With the appearance of the CP, the *pp* splits into two portions. The subplate is pushed under the CP; the Cajal-Retzius cells move towards the glia limitans, dorsal to the CP(Meyer, 2007) (Fig. 2.16).

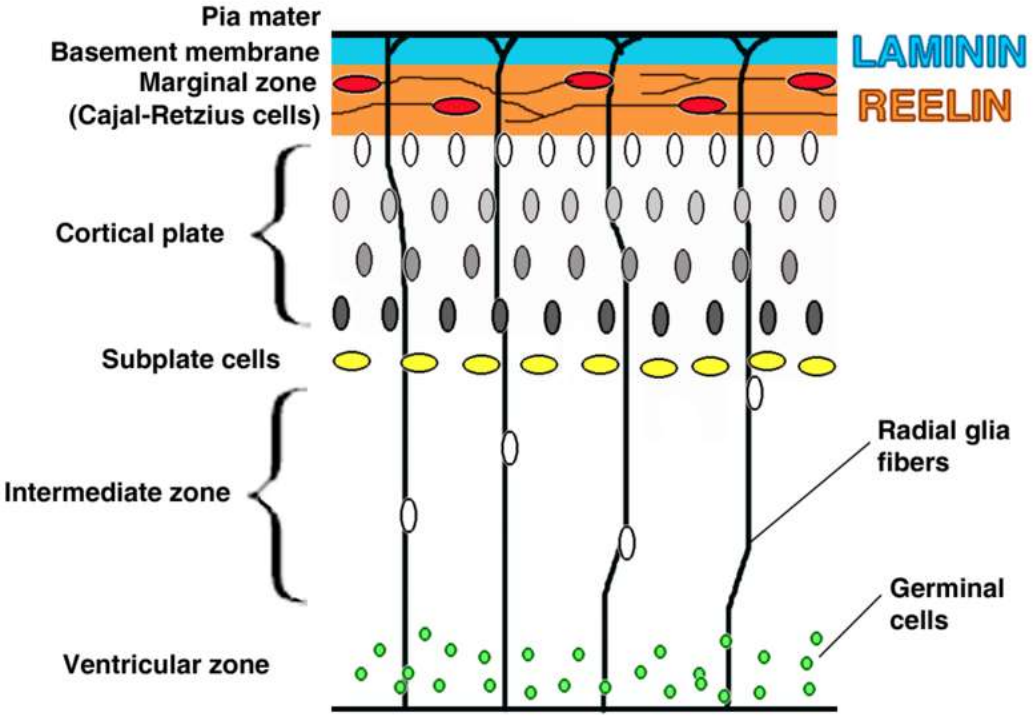

Fig. 2.16: Neuronal migration and neocortical formation in the brain. (Source: CopperKettle, 2006)

The intermediate zone (IZ), between the VZ and CP, creates a pathway for the translocation of neurons from the VZ to the CP, and it thins out in the advance course of development to become the white matter i.e. only present during corticogenesis (Antypa *et al.,*2011).The VZ and SVZ lies ventral to the IZ linking with other regions via cell signalling (Antypa *et al.,*2011) (Figs. 2.17and 2.18).

The CP together with the marginal zone constitutes the six laminae of the neocortex. Pial astrocytes form the limiting glia layer and Cajal-Retzius cells found in this region perform significant roles in the proper migration of neurons during neocortex formation by releasing reelin (Ma *et al.,* 2011).

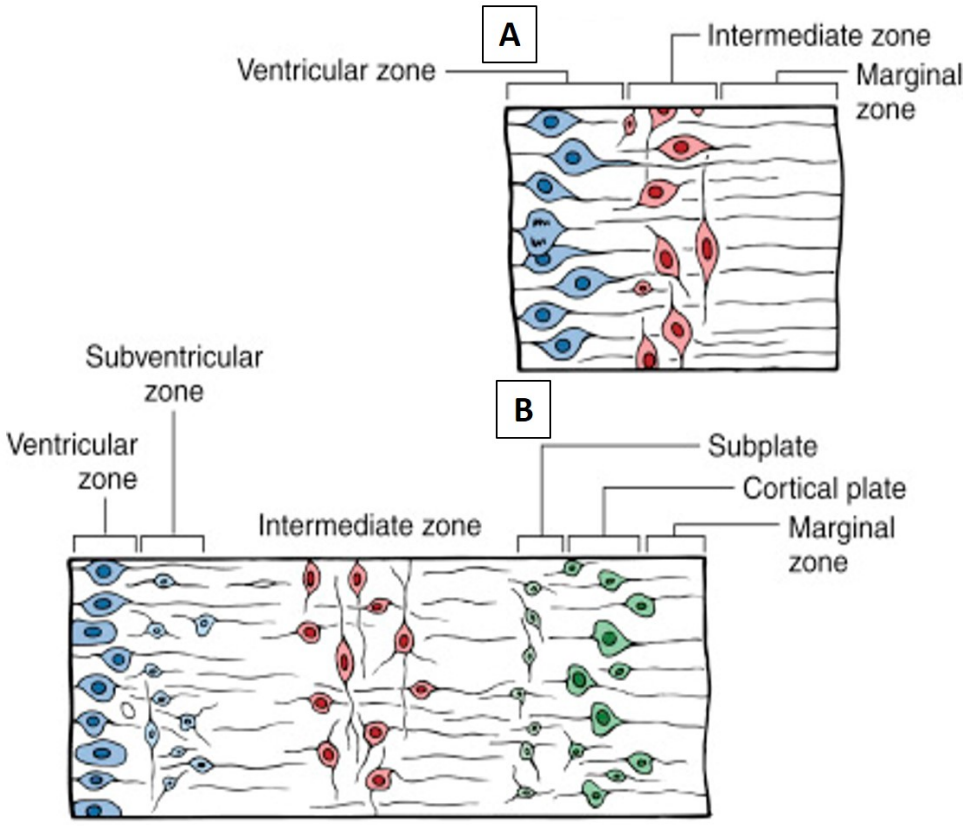

Fig. 2.17: Cortical layers and preplate differentiation of the brain. (Source: Haines, 2015)

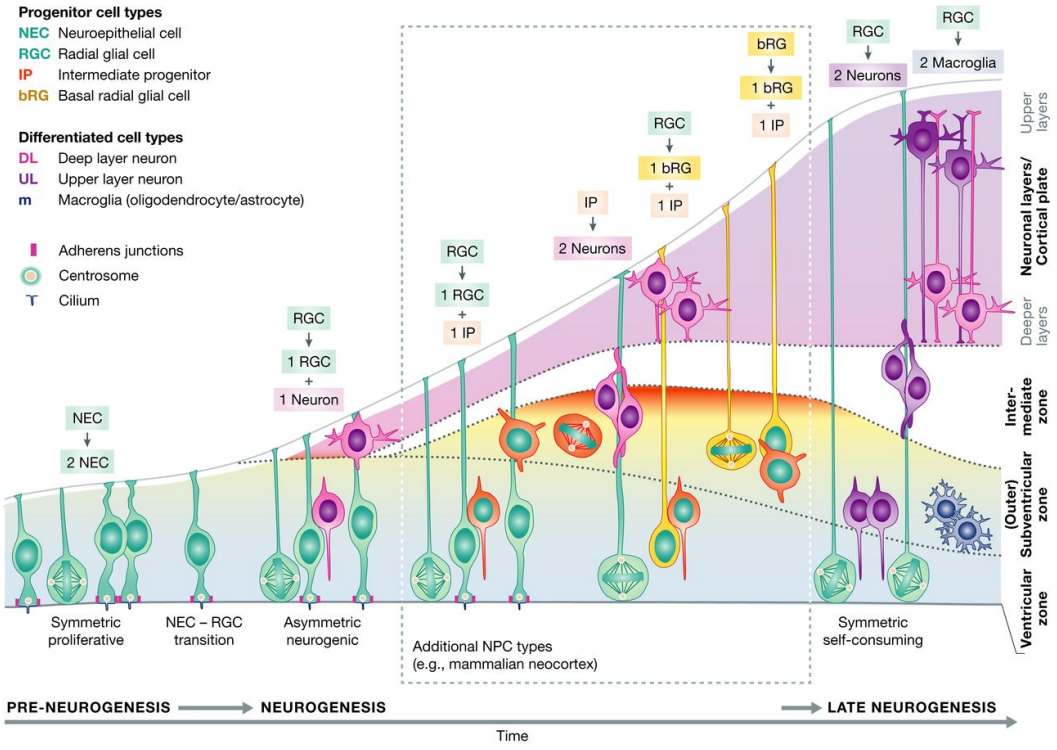

Fig. 2.18: Schematic diagram of neurogenesis and cortical differentiation. (Source: Paridaen and Huttner, 2014).

2.4.4.4 Deep and Upper Layer Formation of the Neocortex

Typically, the CP is often subdivided into two categories: upper layers (II-IV) and deep layers (V–VI) (Toma and Hanashima, 2015). In mammals, the stratified layout of the neocortex is a methodical sequelae of the migration of newborn neurons following their "birthdays" (Gilmore and Herrup, 1997). For this to occur, these newborn neurons must migrate radially and tangentially from the VZ to their final destination where neural connectivity will be established in the developing neocortex. They do this in an "inside-out" fashion by circumventing previously established neuronal layers to get to the top of the CP. (Super *et al.,* 2000; Toma *et al.,* 2014; Toma and Hanashima, 2015) (Fig. 2.13).

2.4.4.5 Neuronal Differentiation in the Developing Neocortex

Axonal and dendritic sprouting are meticulously-controlled programmed events which occur after the completion of neuronal migration in order to ensure proper neural circuit assembly and connectivity during development (Gilbert, 2000a; Hoshiba *et al.,* 2016). Indeed, Hoshiba *et al.,*(2016)posited that new born neurons express Sox11 which inhibits dendritic morphogenesis while conversely promoting movement of neurons to the CP of the developing neocortex.

2.4.4.6 Cellular Migration and Neocortical Layer Stratification

Cellular migrations form the cerebral cortex. Hence, the cortex is composed of undulating cortical grey mater surface (several ridge-like surfaces – gyri, and interspersing depressions –sulci) that is laminated into 6 heterogeneous layers histologically (Jacobson and Marcus, 2008). Each layer is established by the migration of radial glial cells from the VZ/SVZ to their final location in the neocortex (Germain *et al.,*2010) (Fig. 2.13).

1. **Layer I (molecular layer):** This is the foremost layer to emerge in neocortical formation at embryonic day (ED) 10.5 to 12.5 in the mouse. It is also the most external layer of the neocortex containing Cajal–Retzius cells and pyramidal cells (Muralidhar*et al.,* 2014). The migration pattern seen in Layer I differs from the remaining layers II-VI. Furthermore, this layer releases Tbr1, reelin, and markers for cortical migration (Meyer, 2007).
2. **Layers II and III** (External Granular layer and External Pyramidal layer respectively): they are usually the last layers to emerge; seen between ED 13.5 and 16 in the mouse. These layers contain radial glial cells, astrocytes, stellate cells and pyramidal neurons. The last two cell types express two DNA binding proteins - SATB2 and CUX1 which are implicated in the determination of cortical cells fate (Gaspard *et al.,*2008)
3. **Layers IV, V and VI:** also labelled as the Internal Granular layer, Internal Pyramidal layer, and Polymorphic/Multiform layer respectively. They appear in the mouse between ED 11.5 and 14.5. They also contain stellate cells, pyramidal neurons and radial glia cells. transcription factors. Tbr1, OTX1, CTIP2, or cortico-neuronal zinc finger proteins are expressed during the formation of these layers (Germain *et al.,*2010).

2.4.4.7 Cortical Gliogenesis

Timed genesis (sequential generation) of the different nervous cell populations is a highly conserved and programmed event in brain development with neurogenesis preceding gliogenesis (Qian *et al.,* 2000; Shen *et al.,* 2006). This allows for the early establishment of the brain neural circuitry, which is followed by a matching of glial cell populations and of their spatiotemporal locations to the already laid down neural

connections (Miller and Gauthier, 2007) (Fig 2.19). A delicate interplay of both intrinsic developmental biasing of multipotent NSCs and extrinsic signalling cues has been noted to be pivotal to the timing of this neurogenic-to-gliogenic switch (Miller and Gauthier, 2007; Alfonso, 2017). So far three different extrinsic cues - cardiotrophin-1 (CT-1), bone morphogenetic proteins (BMPs), and Notch ligands - have been identified to act together in initiating the gliogenic switch via the CT-1/gp130/JAK/STAT pathway.

Specifically, CT-1, a gliogenic cytokine released by the first-born cell lineage (neurons) binds to gp130 and LIFRβ co-receptors which then signals JAKs to trigger STAT3. Following this, STAT3 binds with the Smads (a downstream of activated BMP receptors) and p300/CBP. This Smad:p300/CBP:STAT complex transactivates gliogenic genes (*gfap* and *s100β*), thus ensuring the neurogenic-to-gliogenic switch (Chen *et al.,* 2004; Ernst and Jenkins, 2004; Miller and Gauthier, 2007).

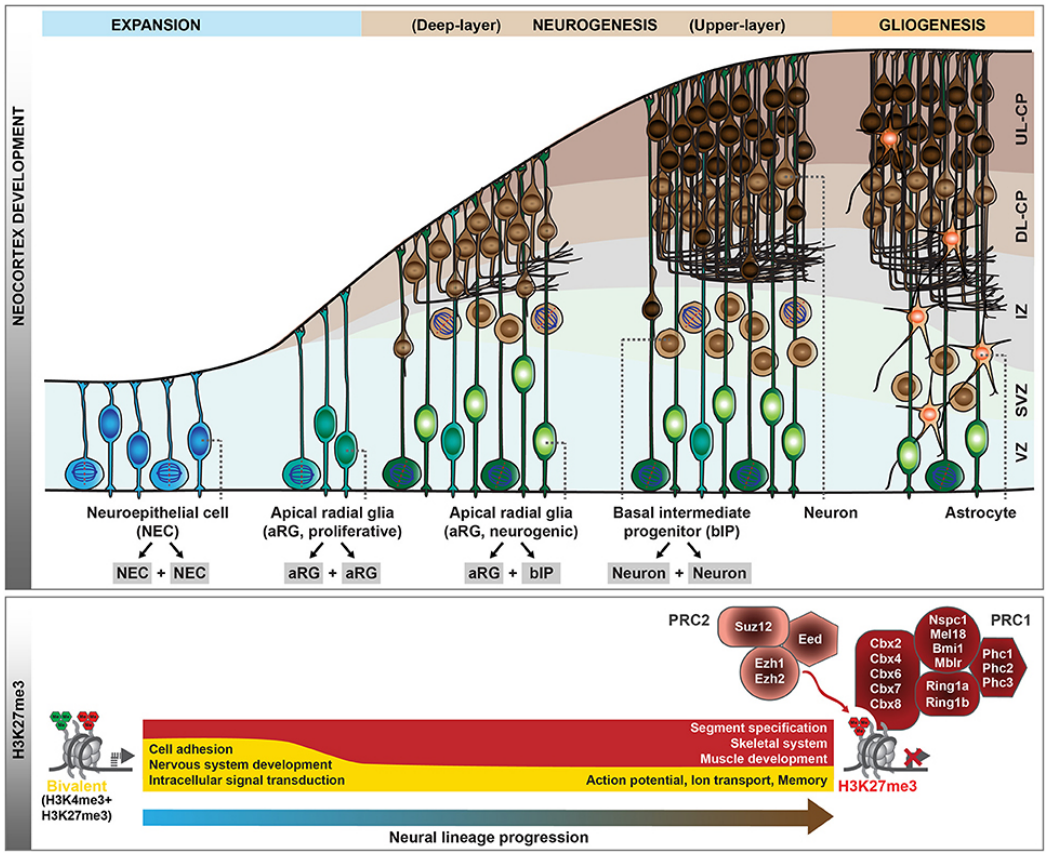

Fig. 2.19: Schematic chart of cortical neurogenesis and gliogenesis in the prenatal mouse. CP, cortical plate; DL, deep-layer; IZ, intermediate zone; SVZ, sub-ventricular zone; UL, upper-layer; VZ, ventricular zone. (Source: Albert and Huttner, 2018).

2.4.4.8 Cortical Myelinogenesis

Precocial animals give birth to their pups with some level of motor coordination already established at birth. This motor coordination has been observed in new born AGCR pups being noted to follow their mother within 32-40 minutes after their birth (Addo, 2002; Opara, 2010). Dobbing and Sands (1970) reported that most major brain developmental events in the developing guinea pig brain predate myelinogenesis; with appearance of the earliest myelin very close to birth – at day 63 of gestation.

CHAPTER THREE

3.0 MATERIALS AND METHODS

Ethical Approval

Prior to the commencement of this study, ethical clearance was secured from the ethical committee of the University of Ibadan (UI-ACUREC) with reference number: UI-ACUREC/17/0066.

3.1 EXPERIMENT ONE

3.1.1 Sonographic and Developmental Horizons in the Developing AGCR

This study was conducted with purpose of determining the sonographic features and measurements at different stages of gestation in the AGCR. It also characterized distinct external developmental features in the prenatal AGCR across its entire length of gestation, providing baseline ontogenetic attributes for AGCR embryos and foetuses.

3.1.2 Experimental Animals and Housing

Nineteen timed primi-graivd AGCR does from Gestation (GD) 10 to 140 (every 10 days) were used. They were purchased from two commercial farms (Pavemgo Farms® Lagos State and Onileola Farms® Osun State, South West, Nigeria) with mean age (1.2±0.5years) and mean body weight of 3.2 ± 0.4kg were used for this study.On the farm, the animals were housed in 80cm x 40cm x 35cm concrete pens. They were maintained on twelve hours of day light and darkness cycle and, prior to commencement of the study.

3.1.3 Mating and Pregnancy Detection

The female AGCRs were naturally mated; with one sexually matured male boarded with four nulliparous females per mating pen. Signs of successful copulation was noted by changes in the perineum after mating, some of which include vaginal wall protrusion, vaginal membrane perforation, vulval congestion, vulval oedema, evidence of copulatory vaginal plug and/or markings on the body of the doe's torso commonly meted by the buck as described by Addo (2002) and Opara (2010). African greater cane rats are known to be induced ovulators with the length of their gestation estimated from the time of observed copulation or evidence of copulatory plug and parturition (Opara, 2010; Adu *et al.,* 2017). The does were meticulously examined twice daily and they were separated from the male once these signs are noticed with the date of successful mating marked as day one of pregnancy. Gravidity was ascertained by digital palpation of abdomen as illustrated by Addo (2002) and was further confirmed by ultrasonography.

3.1.4 Ultrasound Examination

Each rat was examined sonographically using a portable ultrasound machine with a 5.0 MHz transducer (Kaixin KX 2000^{R}, GmbH, Ellfestrass, Hamburg, Germany). The transducer has four windows of frequency range. In addition, the machine was programmed with software for obstetric and cardiac calculations, as well as having a digital imaging and communication in medicine (DICOM) facility for image storage. Prior to examination, the AGCR were anaesthetized with parental injection of 2mg.kg of Xylazine Hydrochloride (2%, Xylazine 20 Inj®, Kepro, Holland) and 10mg/kg of Ketamine hydrochloride (5%, Ketanir®, Kepro, Holland). Basic preparation including clipping of the hairs on the ventral abdomen and application of acoustic gel were performed. Once an appropriate image and position were obtained, it was paused for

the measurements of the gestational sac, embryonal sac, crown-rump length, bi-parietal diameter, foetal length and foetal diameter. In addition, the presence of foetal heart beat and/or movement were noted.

3.1.5 Surgical dissection

Gravid AGCRs spaced at 10 days interval [with gestation days (GD): 10, 20, 40, 50, 60, 70, 80, 100, 110, 120, 130 and 140] were used for this study. Prior to dissection, anaesthesia was achieved with the administration of xylazine hydrochloride (10mg/kg; Xylazine 20 Inj®, KEPRO, Holland) and ketamine hydrochloride (100mg/kg; Ketanir®, Gujara, India). Hysterectomies were carried out on GD10-40 dams while caesarean section was performed on GD50-140 dams (GD 50, n=2; GD 60, n=2; GD 70, n=4; GD 80, n=3; GD 100, n=6; GD 110, n=4; GD 120, n=2; GD 130, n=2; GD 140, n=4) and embryos/foetuses were explanted in line with procedures outlined by Ibe (2016). Concisely, a 3cm post-umbilical mid-line incision (caudal laparotomy) was done and peritoneal folds of the small intestine and colon were reflected to reveal the uterus. Subsequently, each uterine horn was exteriorized, followed by a 2cm longitudinal incision that was made on its anti-mesenteric margin to allow for easy milking out of the embryos/foetuses. Surrounding extraembryonic sheaths were then gently separated.

3.1.6 Foetal measurements

Quantitative foetal body measurements viz: body weight, the length of the head, length of the trunk and length of the tailof the AGCR embryos/foetuses were obtained and recorded immediately following explantation, before post- fixation in 4% paraformaldehyde. Body weightswere obtained with digital weigh balance (KERN

EW 820-2NM). Using a fine thread, the length of the head, trunk and tail were outlined by following the body outline and generating their equivalent metric values.

Head length was evaluated from rostralmost tip on the head to the crown of the head. Trunk length was measured from the nuchal crest to the developing tail base while tail length was evaluated from the developing tail base to the caudal tip of the tail. Crown rump length was recorded to be the point from the apex of the head to the root of the tail (Ohuma *et al.,* 2013). Ano-genital distance was computed as described by Adu *et al.,* (2002), Owusu *et al.,* (2010) and Opara (2010).

3.1.7 Developmental Horizons of the AGCR Embryos and Foetuses

Developmental horizons of AGCR embryos/foetuses were observed, noted and described by visual assessment and digital palpation as detailed by Shehu *et al.,* (2012). They include:

- Integument pigmentation
- Integument transparency
- Integument pigmentation distribution
- Sprouting and spread pattern of hairs
- Appearance of distinctive blood vessels underlying the skin
- Skull consistency
- Development of limbs, tail and sense organs
- Development of external sex organsand
- Dental eruption

3.1.8 Embryo and Foetal Staging

Staging and aging of embryos/foetuses were done according to the morphogenetic features of sequential stages of prenatal development in mammals Embryos and

foetuses were classifiedusing the grossfeatures of timedstages of prenatal development in mammals as defined by the Carnegie system (O'Rahilly and Muller, 1987; Hill, 2016; Hill, 2019a) and Štěrba comparable ontogenetic system (Štěrba, 1995; Štěrba *et al.,* 2000; Witter *et al.,* 2005; Hampe *et al.,* 2015; Lanzetti *et al.,* 2018).

3.1.9 Statisticalanalysis

All morphometric data were presented in descriptive statistics (Mean ± S.E.M.). Inferential statistics was done using linear regression analysis and one-way Analysis of Variance (ANOVA).All analysis was done with GraphPad (v4.0).

3.2 EXPERIMENT TWO

3.2.1 Morphological Characterization of the Developing Prenatal AGCR brain

This study was designed to identify and describe distinctive gross developmental features in prenatal brain across the entire gestational length in the AGCR.

3.2.2 Animals

Explanted foetuses and embryos from Experiment One (from GD50-140) were examined to eliminate embryos/foetuses with any gross developmental anomalies, GD50 embryos were post-fixed in 4% paraformaldehyde while the head of the remaining explanted embryos and foetuses (GD60-140) were dissected to harvest their brains.

3.2.3 Brain Harvest

Craniotomy was done and the brains were extracted. Specifically, in all cases, the brains were extracted ina dorsoventral and caudorostral direction. A midsagittal longitudinal cut was made from the crown of the head to a point between the future eyes. After this, the fibrous cranium was cut into using a scalpel blade and then removed by gentle traction using thumb forceps to expose the underlying meningeal

covering (dura mater) of the brain tissue. In order to facilitate a smooth removal of the brain from the skull, the outer meninx (*dura*) was incised by means of a scalpel blade and was reflected away by carefully pulling the membrane from either side of the brain. Following which the intact brains were carefully extracted, first by making a transverse section at the level of the foramen magnum (which marked the point of transition on the brain to spinal cord) and followed by a gentle teasing off of attached cranial nerves (where present). Gross morphological observations and morphometric evaluations, based on the criteria explained below, were carried out on the harvested brains.

3.2.4 Brain Morphology

- **Brain topography and conformation:** The shape, outline, orientation, and emergence of some structures on the prosencephalon, mesencephalon and the rhombencephalon were noted and described across the entire gestation length of the AGCR.
- **Extent of the gyrification:** The degree of the sulci and gyri on the developing neocortex were noted as either gyrencephalic and lissencephalic across the entire gestation length of the AGCR.

3.2.5 Brain Morphometry

- **Absolute brain weight:** measures the whole brain weight having removed the meninges. Measured in the nearest grams (g).
- **Relative brain weight:** was computed by dividing the absolute foetal brain weight by the foetal body weight.

- **Maximum brain length:** the maximum longitudinal distance between the rostral-most part of the olfactory bulb to the caudal-most part of the brain, with the aid of Vernier calliper and recorded in centimetres.
- **Maximum brain width:** maximum transverse diameter of the temporal part/lobe of the cortex from left to the right side and recorded in centimetres.
- **Maximum brain height:** maximum height of the brain from the base and recorded in centimetres.

All linear measurements of the intact brain were obtained using a Vernier calliper with sensitivity of 0.01cm. Foetal brain weights (absolute) were taken with electronic weighting balance (KERN EW 820-2NM, Kern and Sohn GmbH, Germany). Afterwards, the harvested brains were preserved in 4% paraformaldehydefor 48 hours at $4^{o}C$, washed in PBS and stored in 0.02% PBS Sodium Azide at the same temperature.

3.2.6 Statisticalanalysis

Morphometric parameters generated were stated as Mean ± S.E.M. and analysed with one-way Analysis of variance (ANOVA). With linear regression analysis, the degree of relationship between parameters were evaluated with Graph Pad prism 4.0. Significance level was set at $p<0.05$.

3.3 EXPERIMENT THREE

3.3.1 Corticogenesis Profiling of the Developing Prenatal AGCR Brain

This study was conducted to elucidate the developmental pattern and timing (most especially the onset and peak periods) of neurogenesis, neuronal differentiation, gliogenesis and myelinogenesis in the developing AGCR neocortex. The timing of

deep and upper layer formation of the developing AGCR neocortex was also investigated.

3.3.2 Brain Tissue Processing

3.3.2.1 Reagents for immunohistochemistry protocol

- **30% Sucrose Preparation**

  Thirty grams (30g) of Sucrose was weighed using Mettler Toledo® analytical balance (AG204 DeltaRange; Readability of 0.1 mg with repeatability of 0.1 mg and linearity of ±0.2 mg) and was dissolved in 100ml of 1X PBS.

- **2M Citric acid preparation**

  In this preparation, 420.28g of citric acid (molecular weight: 210.14g/mol) was dissolved in 1 litre distilled water and stored at room temperature.

- **0.1M Sodium citrate buffer stock solution preparation (pH 6)**

  29.4g sodium citrate (molecular weight: 294.1g/mol) was dissolved in 1 litre distilled water. pH was adjusted with 2M citric acid and stored in refrigerator at 4^{o}C until use.

- **0.01M Citrate Buffer Preparation (200mls)**

  20mls of stock solution of sodium citrate (0.1M, pH 6) was diluted in 180mls of distilled water.

- **1M Tris preparation**

  121.14g Tris (molecular weight: 121.14g/mol) was dissolved in 1 litre distilled water and stored at room temperature.

- **0.1M Glycine buffer preparation (pH 7.4)**

  7.5g of glycine (molecular weight: 75.07g/mol) was dissolved in 1 litre distilled water. pH was adjusted with 1M Tris and stored in the refrigerator at 4^{o}C until use.

- **2% Gelatine buffer stock solution preparation**

  20g of gelatine was dissolved in 1 litre PBS and stored in refrigerator at 4^{o}C until use.

- **0.2% Gelatine buffer preparation (ready to use)**

  17.53g of sodium chloride (molecular weight: 58.442g/mol) and 20mls of 2% gelatine stock solution were dissolved in 1 litre of distilled water using a magnetic stirrer. The solution was then stored in the refrigerator at 4^{o}C until use.

3.3.2.2 Sectioning for Immunocytochemistry

For this study, the whole fixed embryos of GD50 and the cerebral hemispheres of the fixed intact brains of GD60-140 were used for cryosectioning. Dehydration was then achieved in thirty percent sucrose in phosphate buffered saline and afterward, placed on a rocker (ROTH, JKIKA Labortechnik, HS250 Basic) at 30 motions/minute until they sank to the bottom (around 48-72hours). The sucrose solution (30%) was then decanted and replaced with the embedding medium - Tissue-Tek (Sakura Finetek®) for 2hours.Thereafter, they were transferred into a peel-a-way disposable plastic tissue embedding molds (R-40) (22mm×40mm×20mm; Polysciences Inc., USA). containing Tissue-Tek®. The moulds were placed in a tyrofoam containing dry ice and allowed to solidify and preserved at −20 °C until use. Brain cryosections were sliced at 20µm and 30µm for GD50 and GD60-140 respectively. Complete serial coronal sections of the telencephalon were done. Mid-ventricular sections along the rostro-caudal axis were used for the immunohistochemical staining. Immunohistochemical procedure according to methods prescribed by Fietz *et al.,* (2010) was carried out on these brain

slices and processed with a battery of immunofluorescence biomarkers. The biomarkers are:

- Paired box gene 6 (Pax6) for apical progenitors and basal radial glia - neural stem cells (NSC)
- T-box Brain-2 (Tbr2) for basal intermediate progenitors - neural progenitor cells (NPC)
- T-box Brain-1 (Tbr1) for deep and upper layer neurogenesis
- HuC/D for neuronal soma
- Microtubule-associated protein 2 (MAP2) for dendritic processes
- Neurofilament (NF) for axonal extensions
- Glial Fibrillary Acid Protein (GFAP) for astrocytes
- Oligodendrocyte transcription factor (Olig2) for oligodendrocytes
- Myelin Basic Protein (MBP) for myelin

3.3.2.3 Protocol for Immunofluorescent Labelling with Biomarkers

Immunofluorescent labelling were done in accordance with methods prescribed by Fietz *et al.,* (2010). Representative brain sections at different time points across the entire gestation length of the AGCR were selected and placed in plastic slide racks containing 0.01M Citrate buffer and cooked at 90^{o}C for 90 minutes. This was done to expose the antigenic epitopes. The slides were cooled to room temperature for 20minutes. Next, limiting boundaries were drawn on the slides on either poles of the slides with the Liquid Barrier Marker (Roti®Art-Nr. AN 921). The slides were rendered permeable with TritonX (in PBS) for 40minutes. Thereafter, sections were blocked with glycine buffer (0.1M, pH 7.4) for 60 minutes so as to minimize non-specific antibody binding and to prevent endogenous peroxidase activities.

Subsequently, they were then washed once in 1X PBS for 10minutes and incubated with primary antibodies overnight at 4°C.

Single, double and triple immunofluorescence labelling was done using the following primary antibodies: Pax6 (1:100, rabbit, Biozol, BLD-901301), Tbr2 (1:100, sheep, RandD Systems, AF6166), Tbr1 (1:200, rabbit, Millipore, AB10554), MAP2 (1:100, chicken, Abcam, ab5392), HuC/HuD (1:100, rabbit, Abcam, ab96474), NF (1:100, rabbit, Abcam, ab204893), GFAP (1:225, rabbit, Antibodies, A85419), Olig2 (1:100, mouse, Abcam, ab236540), MBP (1:100, rat, Abcam, ab7349). Single immunofluorescence labelling was done using Tbr1 (for deep and upper layer neocortical characterization) and GFAP (for characterizing astrocyte development and differentiation). Double immunofluorescence labelling was done combining Pax6 and Tbr2 (for profiling the onset and peak periods of neurogenesis); Olig2 and Pax6 (for oligodendrogenesis), MBP andNF (for myelinogenesis). Triple immunofluorescence primary antibody labelling was carried out with Map2, HuCD and NF for mapping and characterizing neuronal soma, dendritic and axonal differentiation.

Following this, the slides were brought to room temperature for 2hours, washed with gelatine buffer twice for 10 minutes each and a repeat of wash with same buffer was done twice, this time for 5minutes each. They were subsequently incubated with secondary antibodies coupled to Alexa Fluor 488, 555, 647 (400µL, 1:500, Life Technologies) at room temperature for 1hour. Slides were subsequently washed in gelatine buffer twice for 10 minutes each and the washing step was repeated twice for 5 minutes each. Counterstaining with DAPI (1:500, Sigma) was done for all sections and coverslipped with Mowiol and preserved at 4°C.

3.3.3 PhotomicrographCapturing and Stereological Analysis

Immunofluorescence pictures were captured with Leica SP8 confocal laser-scanning microscope (×20 or ×40 objectives). Images were gotten as 3.121µm (×20) or 1.271µm (×40) single-optical sections.The VZ was defined as the layer of tightly stacked cell with radial nuclei lining the lateral ventricle. The landmark for SVZ identification was defined as the layer adjacent to the VZ with less tightly stacked and relatively sparser cells compared to VZ. The intermediate zone (IZ)/subplate (SP) was delineated as the cell layer between the SVZ and cortical plate (CP) with very low cell density while the CP was identified as a layer of densely packed cells dorsal to the IZ/SP. Images captured were processed with Fiji software. Quantitative analysis of individual NSCs/NPCs and Olig2+ cells, and their relative abundance was done with Fiji software using a Multiclass Cell Counter plugin (Schindelin *et al.,* 2012). The fluorescence signal of single channels was counted using grayscale colour. All quantifications were performed on images from the dorsolateral telencephalon. Radial thickness of the germinal zones and length of the ventricular surface were determined by tracing using Fiji software. Data obtained were further analysed with Prism software (GraphPad Software version 4.0).

Table 3.1: Immunofluorescence Biomarkers

Primary Antibody	**Manufacturer**	**Dilution**	**Wavelength**	**Secondary Antibody**	**Dilution**
Rabbit Polyclonal anti-Pax6	Biozol, BLD-901301	1:100	555	Anti-rabbit IgG Alexa Fluor 555	1:500
Sheep Polyclonal anti-Tbr2	RandD Systems, AF6166	1:100	647	Anti-sheep IgG Alexa Fluor 647	1:500
Rabbit Polyclonal anti-Tbr1	Millipore, AB10554	1:200	555	Anti-rabbit IgG Alexa Fluor 555	1:500
Chicken Polyclonal anti-MAP2	Abcam, ab5392	1:100	488	Anti-chicken IgG Alexa Fluor 488	1:500
Rabbit Polyclonal anti-HuC/HuD	Abcam, ab96474	1:100	555	Anti-rabbit IgG Alexa Fluor 555	1:500
Rabbit Polyclonal anti-NF	Abcam, ab204893	1:100	555	Anti-rabbit IgG Alexa Fluor 555	1:500
Rabbit Polyclonal	Antibodies, A85419	1:225	555	Anti-rabbit IgG Alexa	1:500

anti-GFAP				Fluor 555	
Mouse Monoclonal anti-Olig2	Abcam, ab236540	1:100	488	Anti-mouse IgG Alexa Fluor 555	1:500
Rat Monoclonal anti-MBP	Abcam, ab7349	1:100	488	Anti-rat IgG Alexa Fluor 488	1:500

CHAPTER FOUR

4.0 RESULTS

4.1 Experiment One

4.1.1 Sonographic Features of Gestation in the Developing AGCR

The sonographic features at different timed points of gestation in the AGCRs are shown in Table 4.1. The earliest detectable sonographic feature of pregnancy in the AGCR was the gestational sac. It was first detected by GD20 and was characterized by oval-shaped anaechoic sac containing bipolar hyperechoic band (Fig. 4.1). Gestational sac was observed also at GD40 (Fig. 4.2).

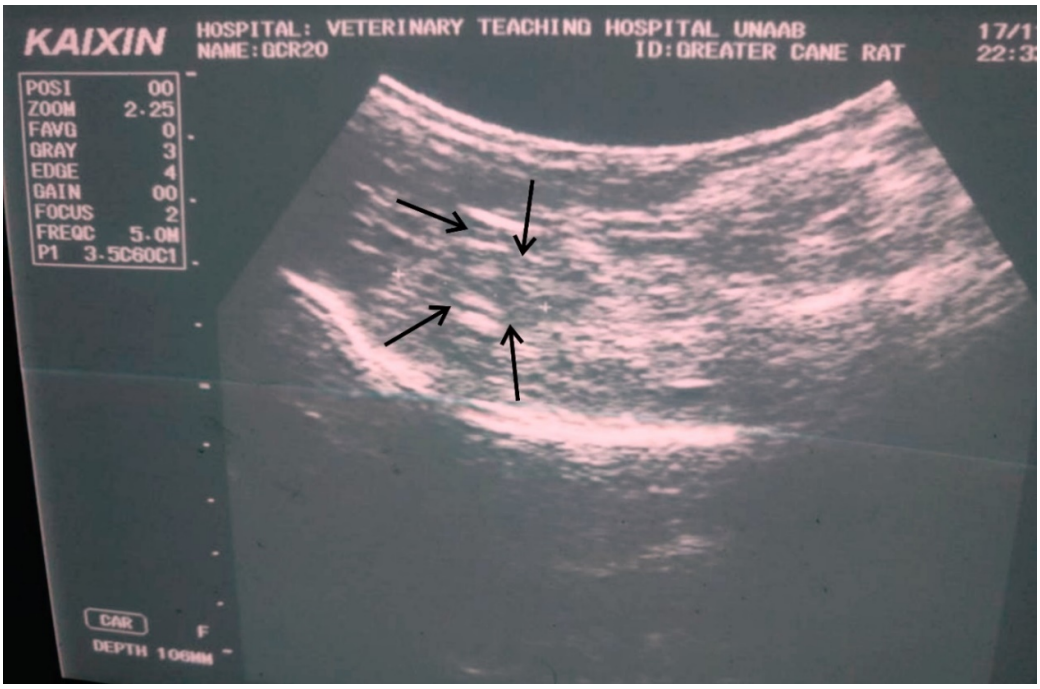

Figure 4.1: B-mode abdominal ultrasound of AGCR at gestation day 20 showing gestational sac (arrows)

Table 4.1: Sonographic features of gestation in African Greater Cane Rat.

Gestation Day	**Observable sonographic features**
10	No detectable sonographic features of gestation
20	Gestational sac (bi-polar hyperechoic structure) measuring 2mm in diameter
40	Gestational sac (bi-polar hyperechoic structure) measuring about 6mm in diameter
50	Embryonal sac represented as an oval shaped anaechoic structure bounded by hyperechoic rim with a central hyperechoic structure (embryo)
70	Embryonal sac represented as an oval shaped anaechoic structure bounded by hyperechoic rim with a central hyperechoic structure (embryo)
80	Embryonal sac represented as an oval shaped anaechoic structure bounded by hyperechoic rim with a central hyperechoic structure (embryo)
100	Foetal sac observed with distinct foetal structure without recognizable limbs and organs
110	Distinct foetal structures with recognizable foetal limbs and organs
120	Distinct foetal structures with recognizable foetal limbs and organs
130	Distinct foetal structures with recognizable foetal limbs and organs

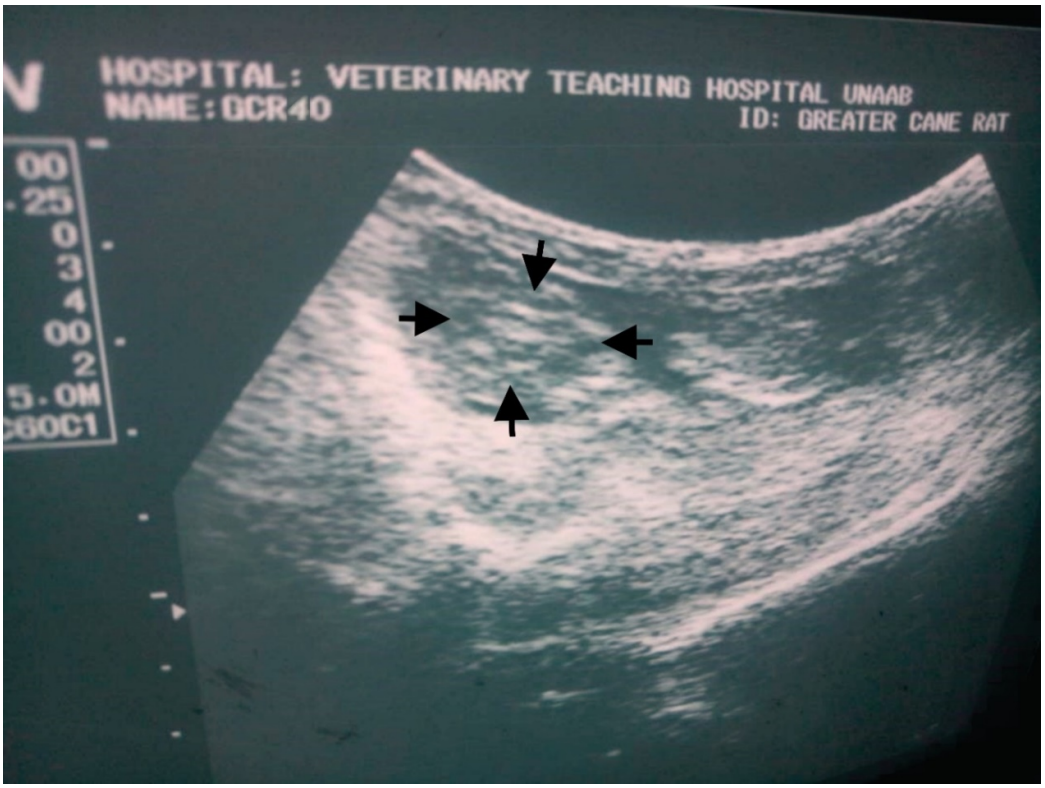

Figure 4.2: B-mode abdominal ultrasound of AGCR at GD40 showing gestational sac (arrows)

Sonographic features of the embryo were first detected by GD50 and was characterized an oval-shaped anaechoic structure bounded by hyperechoic rim with a central hyperechoic structure (embryo) (Figs. 4.3, 4.4 and 4.5).

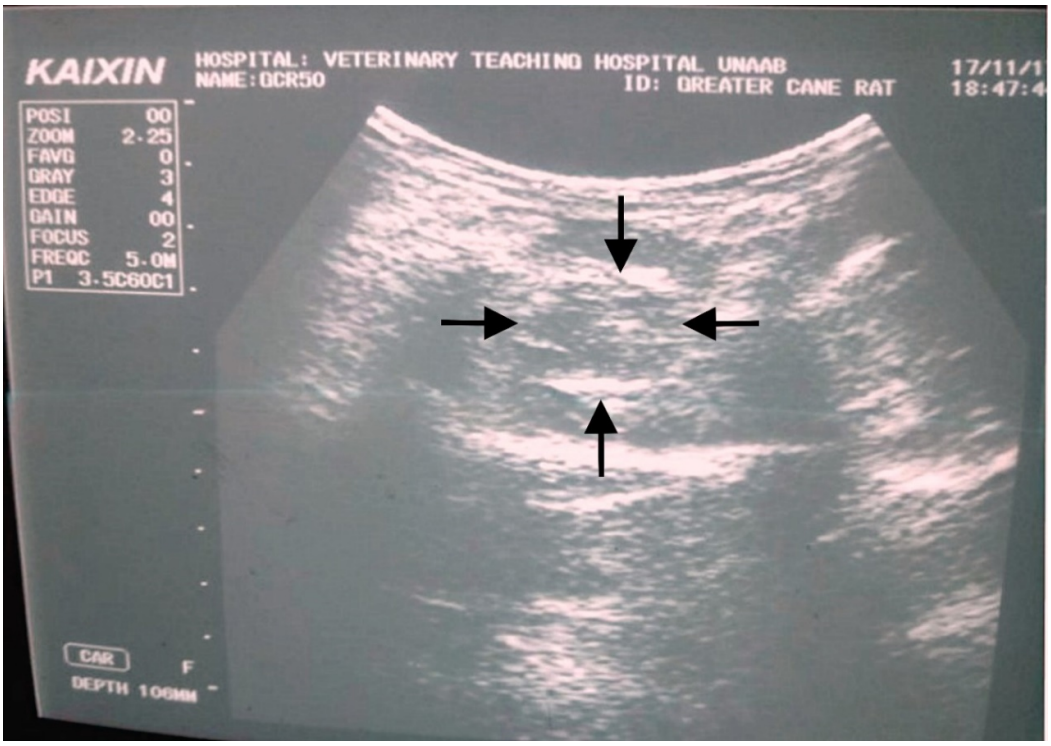

Figure 4.3: B-mode abdominal ultrasound of AGCR at GD50 showing embryonal sac (arrows)

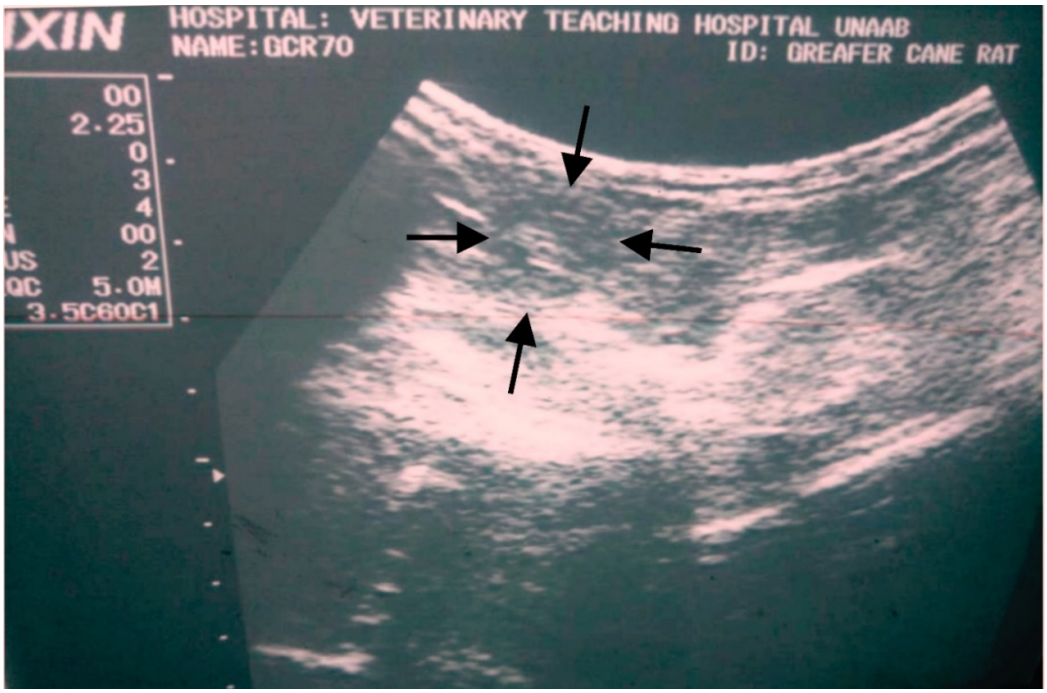

Figure 4.4: B-mode abdominal ultrasound of AGCR at GD70 showing embryonal sac (arrows)

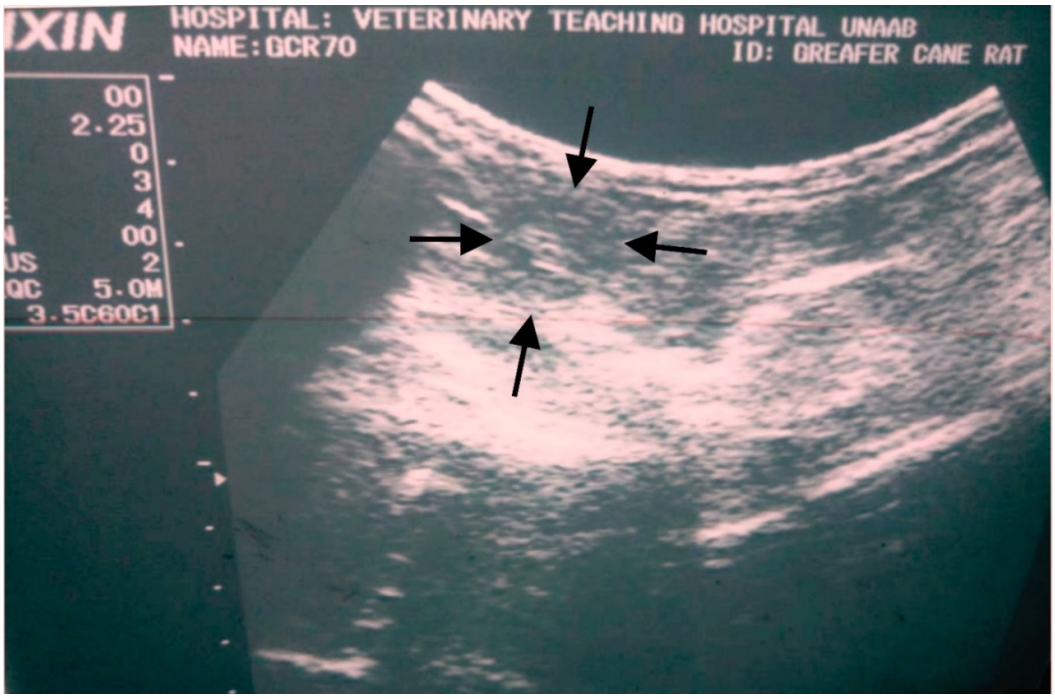

Figure 4.5: B-mode abdominal ultrasound of AGCR at GD80 showing embryonal sac (arrows)

Distinct foetal structures without recognizable foetal limbs and organs was observed by GD100 (Fig. 4.6), while foetal structures with recognizable foetal limbs and organs was observed from GD110 up to GD130 (Figs. 4.7, 4.8 and 4.9).

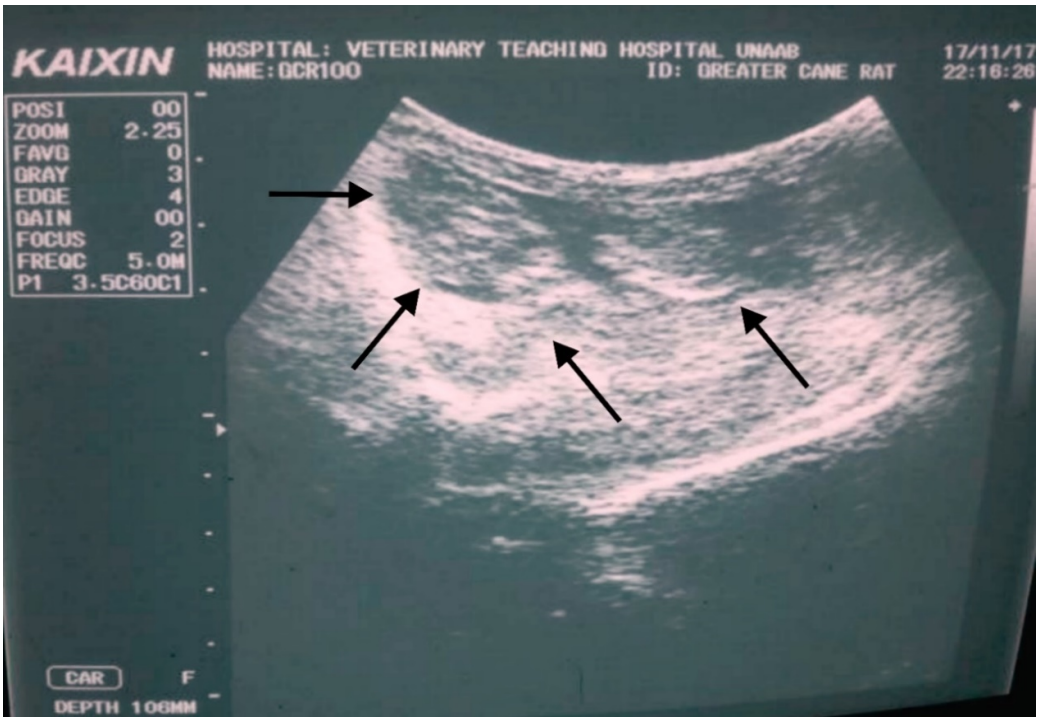

Figure 4.6: B-mode abdominal ultrasound of AGCR at GD100 showing foetal sac (arrows)

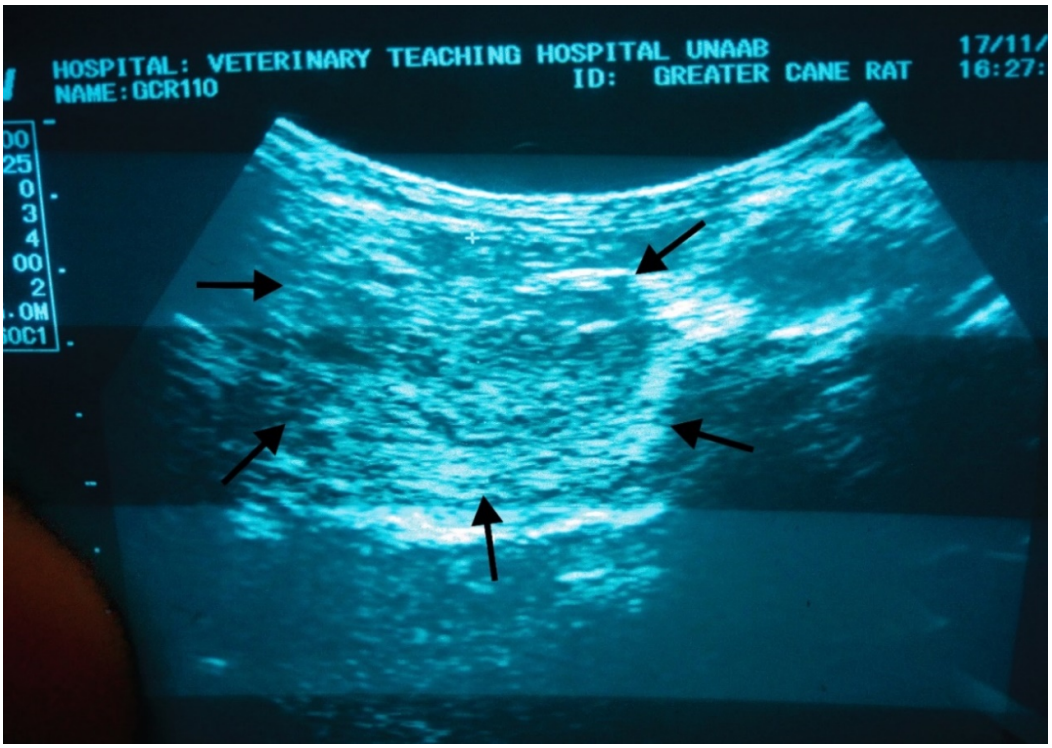

Figure 4.7: B-mode abdominal ultrasound of AGCR at GD110 showing a foetus (arrows)

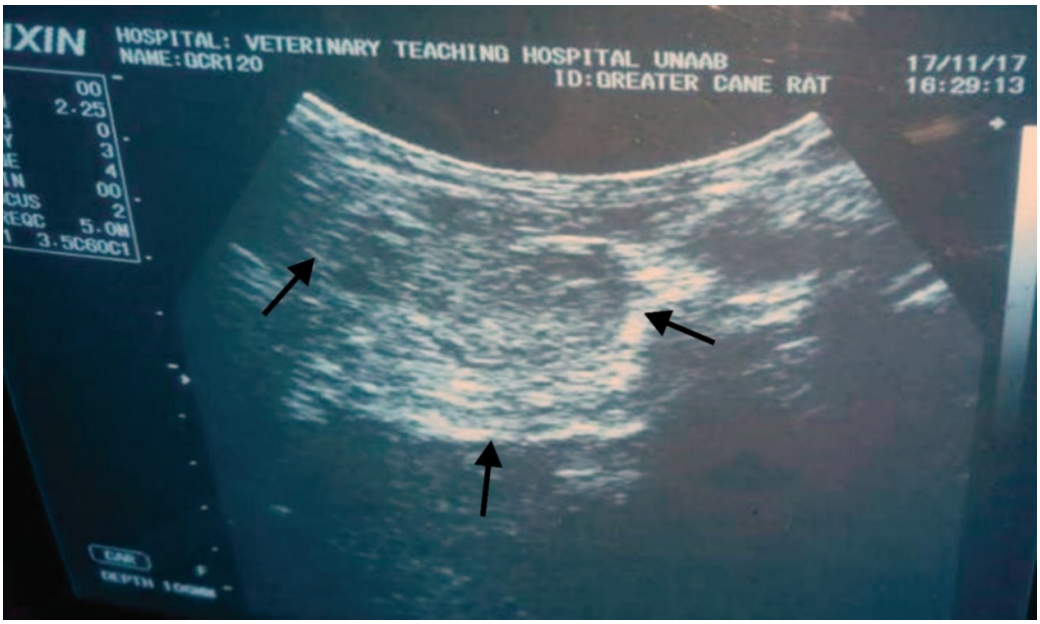

Figure 4.8: B-mode abdominal ultrasound of AGCR at GD120 showing a foetus (arrows)

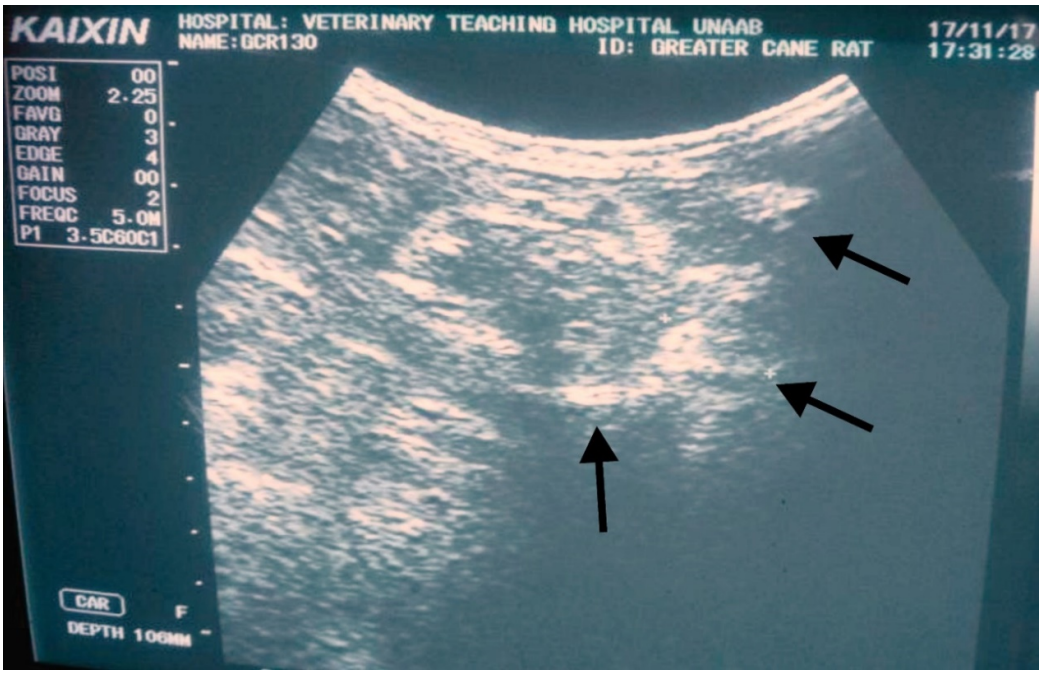

Figure 4.9: B-mode abdominal ultrasound of AGCR at GD130 showing a foetus (arrows)

4.1.2 Sonographic Parameters of Gestation in the Developing AGCR

The sonographic measurements at specified timed points across the gestation length in AGCR is shown in Table 4.2. Gestational sac at day GD20 was 2mm in length and 4mm in diameter, while at GD40 gestational sac length was 4mm and the diameter was 6mm. The embryonal sac length was 10mm, while the embryonal sac diameter was 14mm by GD50. Embryonal sac length ranged between 10mm and 14mm, while embryonal sac diameter ranged between 14 mm and 20mm.

The sonographic dimensions of AGCRfoetuses at scheduled timepoints of gestation are shown in Table 4.3. The crown rump length ranged between 36 mm and 56mm. The bi-parietal diameter ranged between 14mm and 29mm in diameter, while the foetal length ranged from 30mm to 50mm. Also the foetal width ranged between 17mm and 25mm.

Table 4.2: Sonographic measurements of gestational and embryonal sacs at different stages of gestations of African Greater Cane Rat.

Gestation Day	Gestational Sac Length (GSL)	Gestational Sac Diameter (GSD)
20	2mm	4mm
40	4mm	6mm
50	10mm	14mm
70	12mm	18mm
80	14mm	20mm

Table 4.3: Sonographic determination Sonographic determination of foetal parameters at different stages of gestation in AGCR. Bi-Parietal Diameter (BPD), Crown Rump Length (CRL), Foetal Length (FL) and Foetal Width (FW)

Gestation Day	CRL(mm)	BPD(mm)	FL(mm)	FW(mm)
100	36.0	14.0	30.0	17.0
110	43.0	22.0	43.0	25.0
120	48.0	25.0	49.0	25.0
130	56.0	29.0	50.0	25.0

4.1.3 Developmental Horizons in the Developing AGCR

4.1.3.1 First Trimester Developmental Milestones/Features

Macroscopic examination of the AGCR GD10 uteri revealed massively expanded mesometrial vessels and hyperaemic uterine walls (Fig. 4.10). Their uterine horns had a beaded appearance representing foci of implantation sites(Fig. 4.10). Howbeit, when the uteri were dissected, no visible gross structures bearing resemblance to gestational sacs were found.

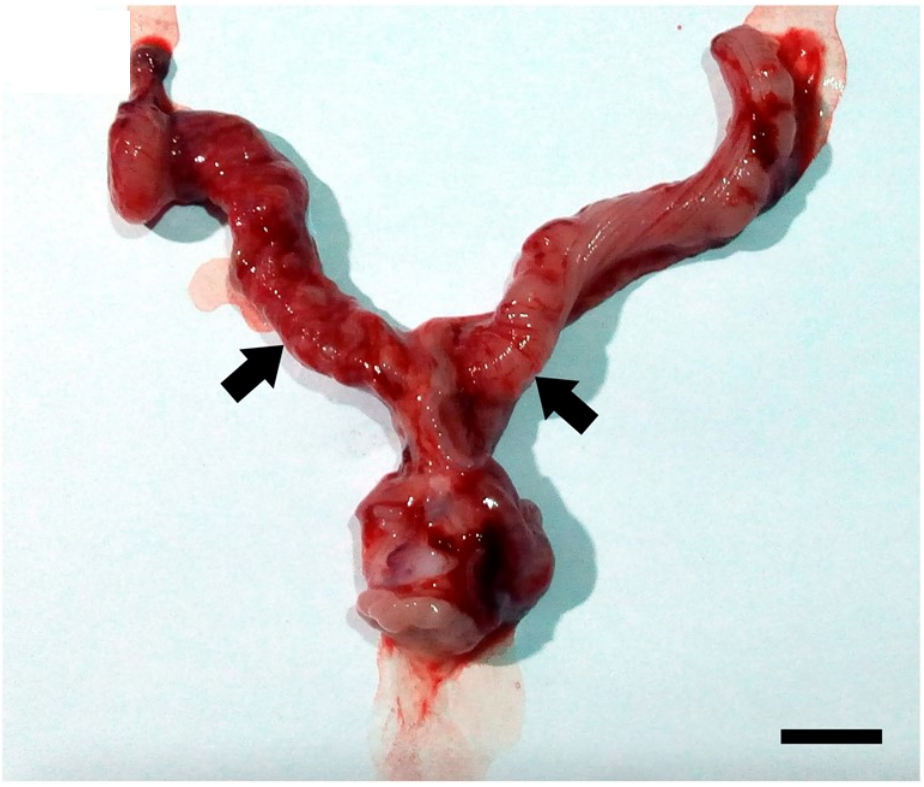

Figure 4.10: Dorsocaudal view of the AGCRuterus at GD10. Arrows are pointing to the bilateral bead string presentation of the uterine horns. Scale bar: 1 cm.

By day 20 of gestation (GD20), the general presentation of the uteri was much like what was observed at GD10. However, there was a significant increase in the sizes of the "bead-like" structures of the *cornu* at GD20 (Fig. 4.11). The earliest evidence of gestational sacs in the AGCR uterus was seen at day 40 of gestation. Upon gross examination and dissection, these sacs were noted to contain clear fluids which had no clearly visible enclosing embryos (Fig. 4.12a and b).

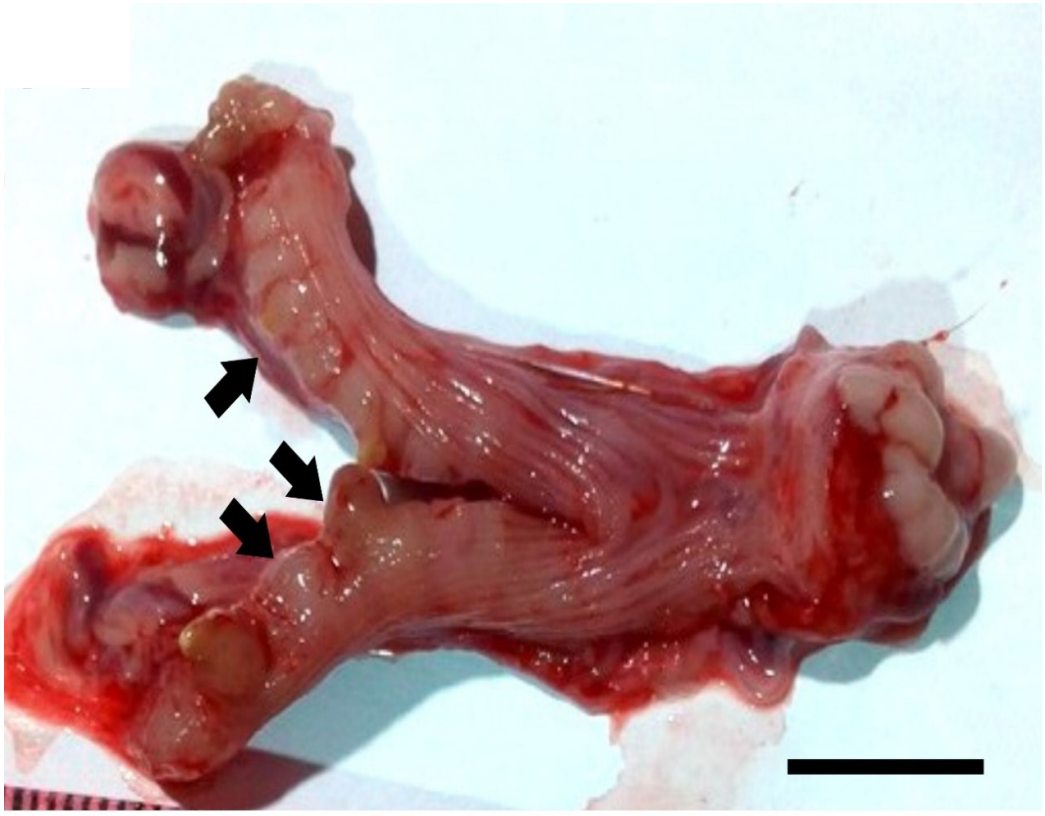

Figure 4.11: Close-up view of the AGCR uterus at GD 20 with arrows pointing at the beaded appearance of the uterine horns. Scale bar :1cm.

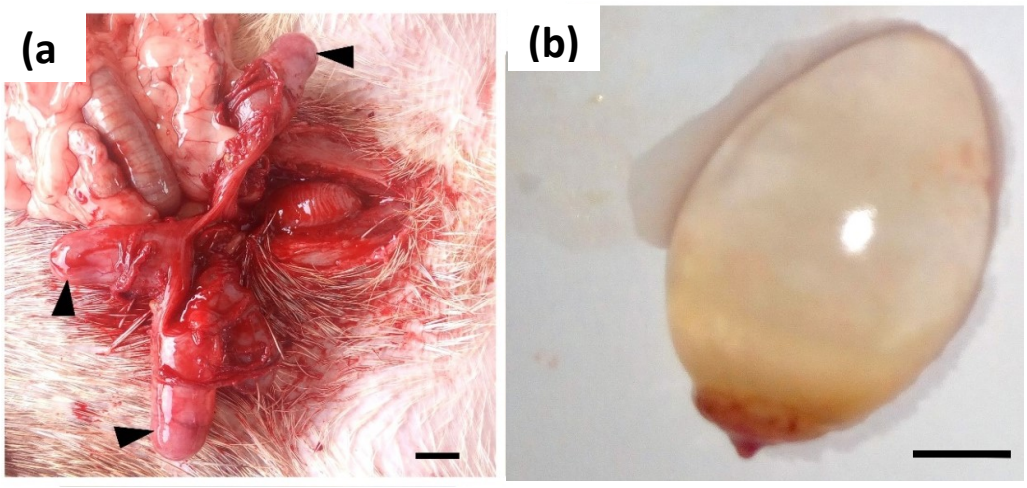

Figure 4.12: (a) Close-up view of the AGCR uterus at GD 40 with arrows pointing at the gestational sac within the uterine horn. Scale bar:1 cm (b) Gestational sac at GD40 (lateral view). Scale bar: 0.5cm

By GD50, there was an appreciable increase in the size of the gestational sacswith an accompanying change in colour of the containing fluid; from its initial clear colour to cloudy (Fig. 4.13). Embryos, approximately 5mm in body length, were explanted from these sacs. These embryos had a very thin transparent skin membrane. (Fig. 4.13b).

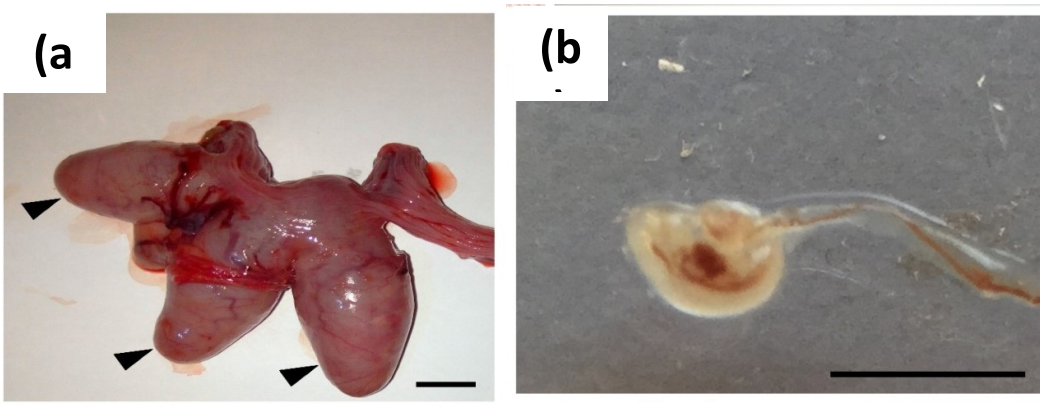

Figure 4.13: (a)Close-up views of the AGCR uterus at GD 50 with arrows pointing at the gestational sac within the uterine horn. Scale bar:1 cm. (b) AGCR embryo at GD50 (lateral view). Scale bar: 0.5cm.

4.1.3.2 Second and Third Trimester Developmental Milestones/Features

All AGCR uteri examined and dissected (GD60-140) had about 2 - 6 distinct embryos/foetuses *in utero*. Each of these embryos had individual gestational sac (Fig. 4.14 – 4.19).

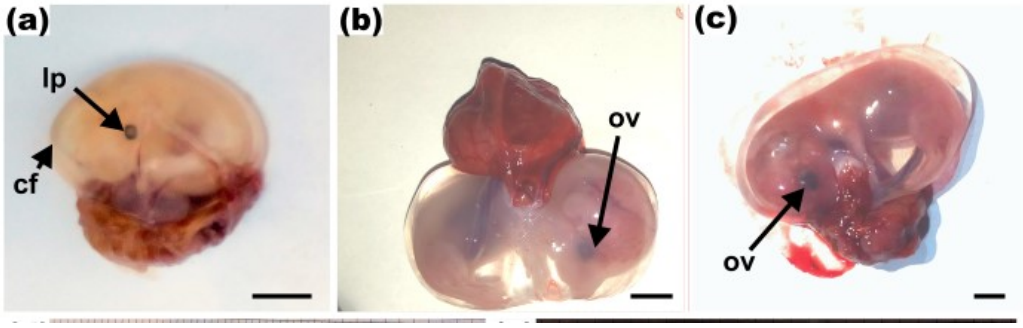

Figure 4.14: Lateral views of the prenatal AGCR at (a) GD 60, (b) GD70 and (c) 80. (Arrows indicate lp, lens placode; cf, cephalic flexure; ov, optic vesicle). Scale bar: 0.5cm.

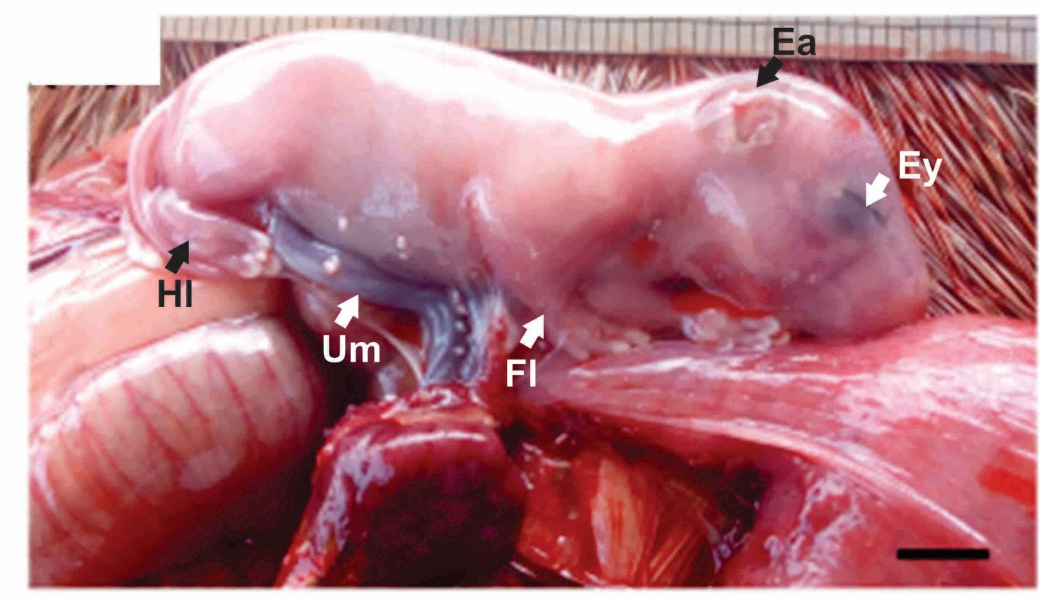

Figure 4.15: Lateral view of the prenatal AGCR at GD 100. Scale bar: 0.5cm. Note the close eye (Ey), unpigmented pinna (Ea), forelimb (Fl), Umbilical cord (Um) and the hindlimb (Hl).

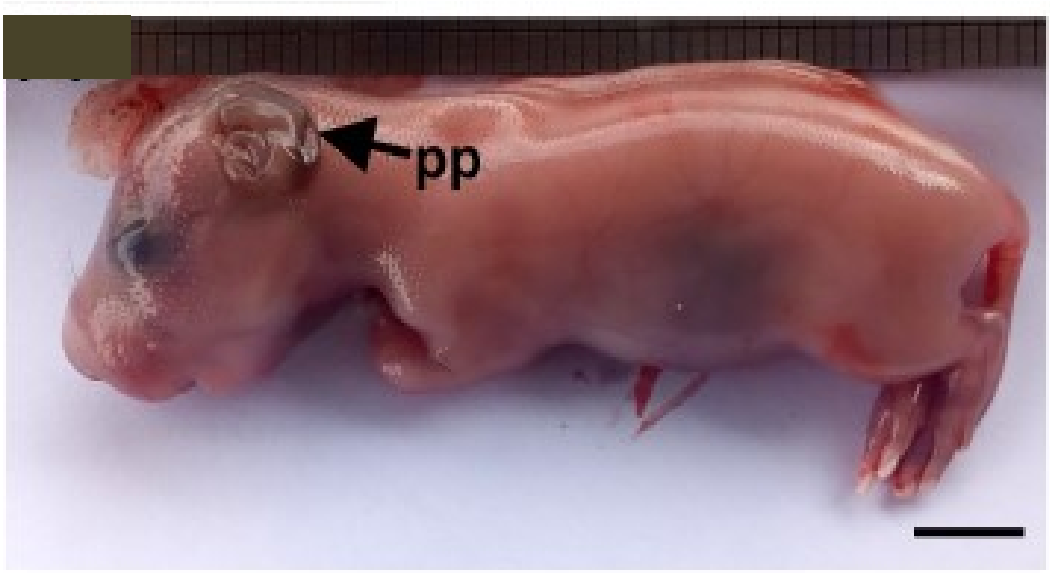

Figure 4.16: Lateral view of the prenatal AGCR at GD 110(Arrow indicate: pp, pigmented pinna)Scale bar: 0.5cm

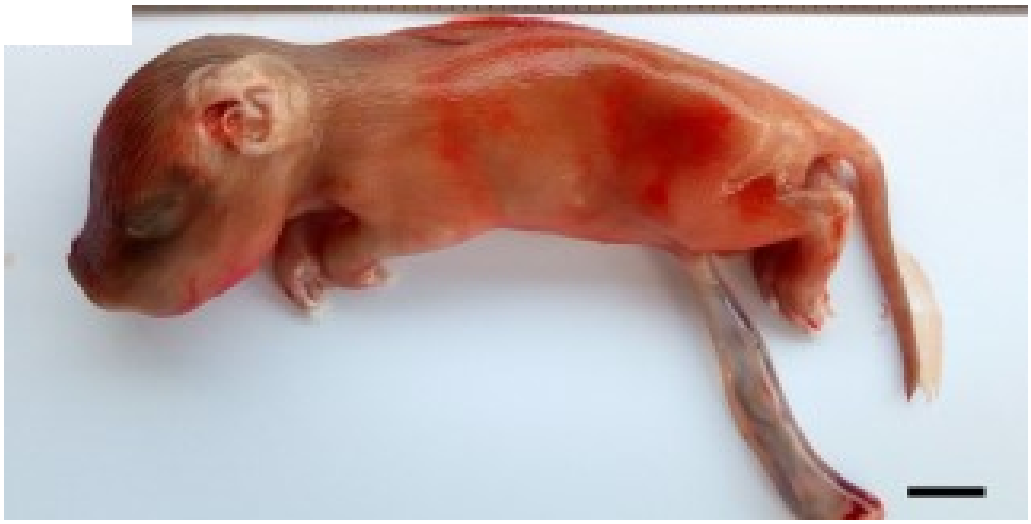

Figure 4.17: Lateral view of the prenatal AGCR at GD 120. Scale bar: 0.5cm.

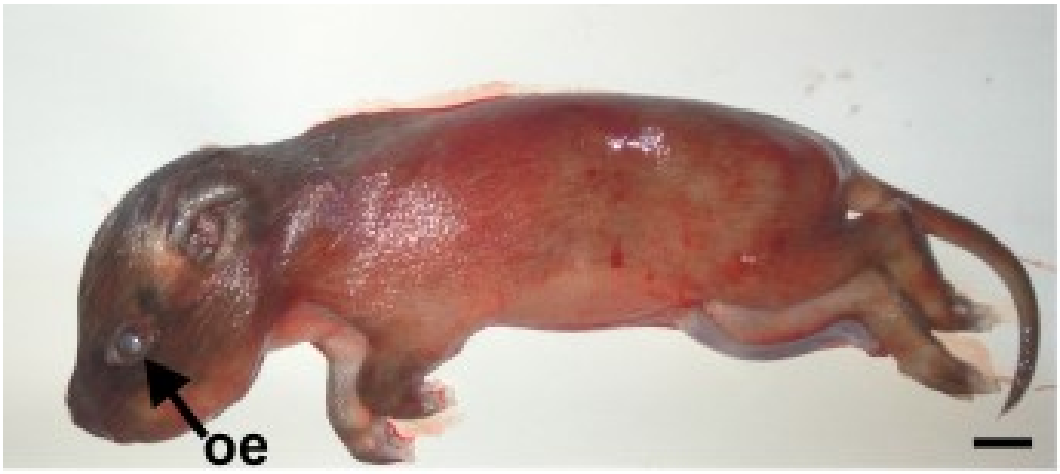

Figure 4.18: Lateral view of the prenatal AGCR at GD 130(Arrow indicate: oe, opened eyelid). Scale bar: 0.5cm

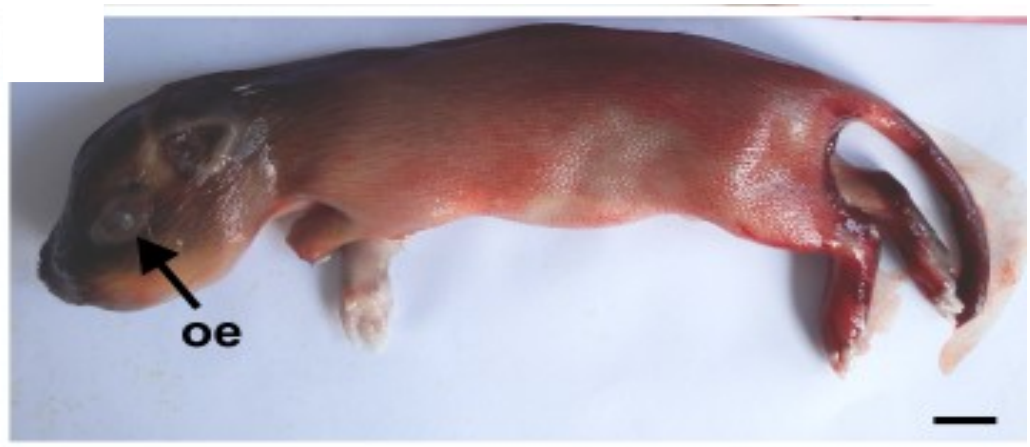

Figure 4.19: Lateral view of the prenatal AGCR at GD 140. Arrow indicate: oe, opened eyelid. Scale bar: 0.5cm

Metric linear measurements (body weight, CRL, lengths of the head, trunk and tail) were evaluated throughout the gestation length of the prenatal AGCR. This showed that there was a progressive increase in these quantitative parameters from day 60 of gestation (GD60) till day 140 of gestation (GD140) (Fig. 4.20 and 4.21). Moreover, a gadational increment in the average body weight of the prenatal AGCR with progressing gestational age was observed, peaking at day 130 of gestation (GD130) (Fig. 4.22). There were no statistically significant differences in the mean body weight between GD130 and GD140.

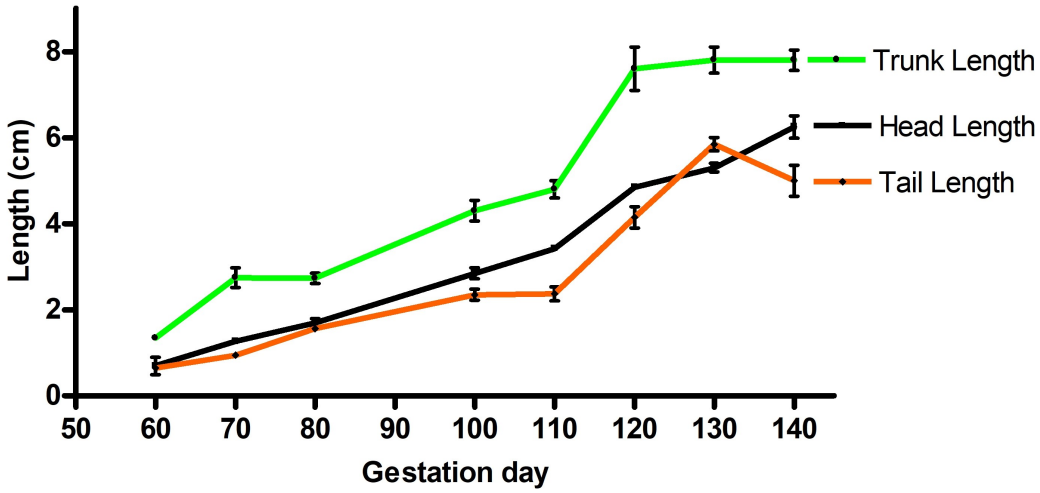

Figure 4.20: Graphical representation of mean body parameters in the prenatal AGCRfrom GD 60-140

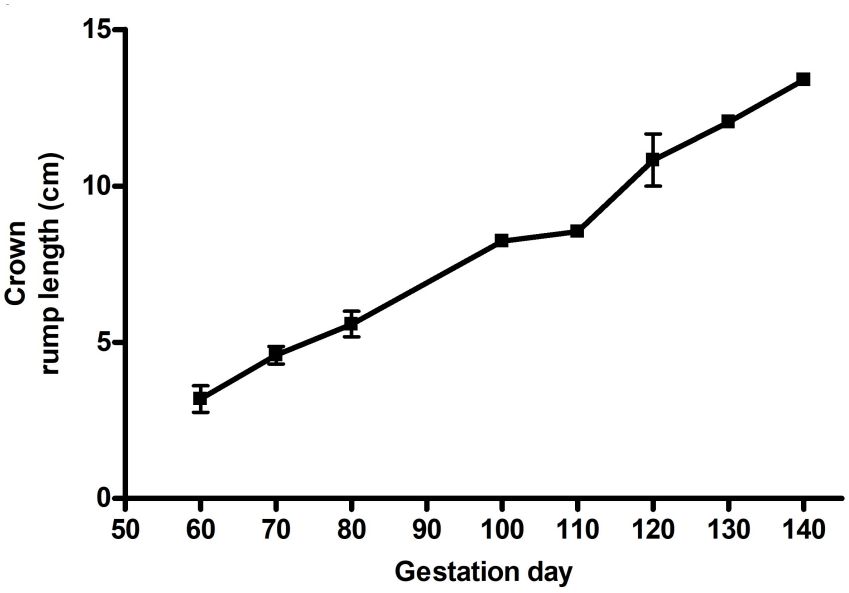

Figure 4.21: Quantification of crown rump length in the prenatal AGCR between GD60-140

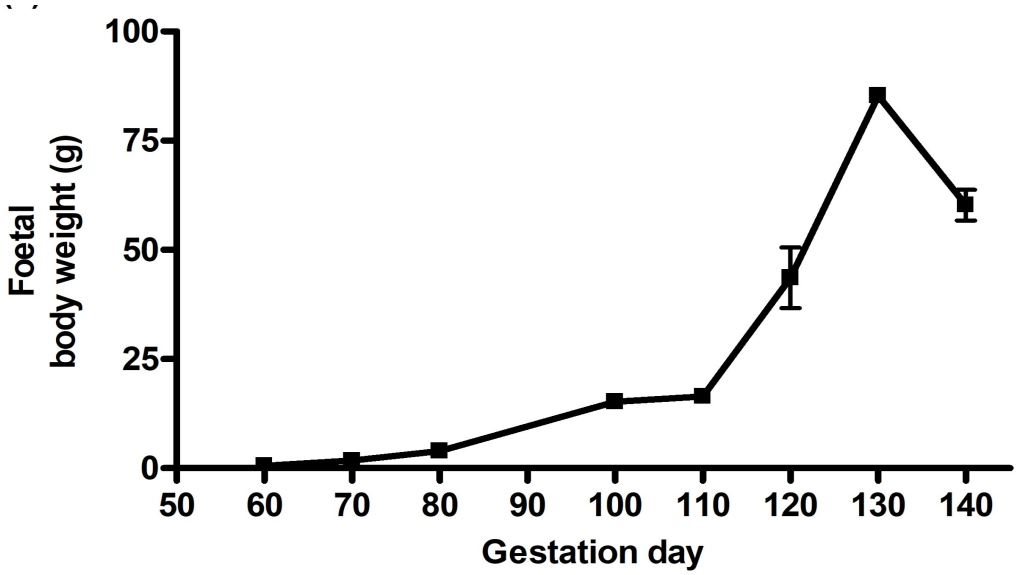

Figure 4.22: Quantification of body weight in the prenatal AGCR between GD60-140.

Definitive developmental milestones investigated in the prenatal AGCR from day 60 (GD60) to day 140 (GD140) of gestation comprise of calvarium consistency, integument pigmentation, dental eruption, appearance and spreadpattern of hairs, budding of limbs, visibility of distinctive underlying blood vessels, development of sense organs and external sex organs.

4.1.3.2.1 *Integument pigmentation*

The integument of the prenatal AGCR was observed to be transparent with the skin colour transiting from "off-white" as at GD60 to light pink by GD70 (Figs. 4.14a and b). With progressing gestational age, the integument between GD80-100 became less transparent and by GD100 had become translucent while still retaining its pink colour (Figs. 4.14c and 4.15). By the 110thday (GD110), a change in the skin colouration of the prenatal AGCR was noticed, where it had become ruby in colour with the exception of the external ear and the regions around eyes, which had brown pigmentations (Figs. 4.16 and 4.23).

The pigmentation pattern of the integument in the prenatal AGCR followed a craniocaudal wave, becoming progressively more pronounced between GD120-140. The whole integument of GD120 was dark brown and had become intransparent with hazel colouration on the dorsum and dorsolateral aspects of the head (Figs. 4.17 and 4.25). The last body parts noted to be pigmented were the footpads of both the fore limbs and hind limbs (Fig. 4.28). The volar surfaces of the limbs were observed to have been pigmented by GD130 (Figs. 4.28c and d).

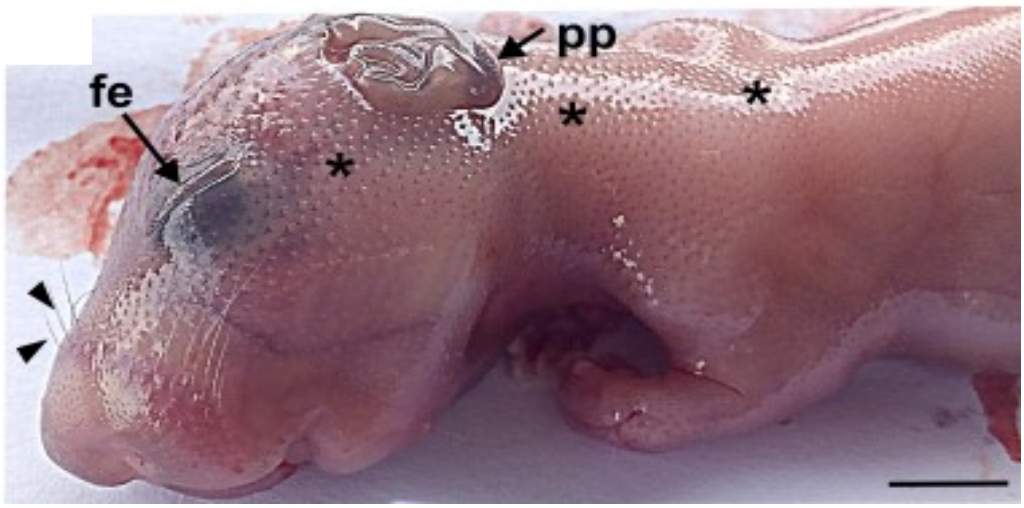

Figure 4.23: Lateral view of a prenatal AGCR at GD110. Note the fused eyelids (fe) and pigmented pinna (pp) on the head as well as presence of body hair follicles (black asterisks). First tactile hairs around the snout indicated by black arrow heads. Scale bar:1 cm

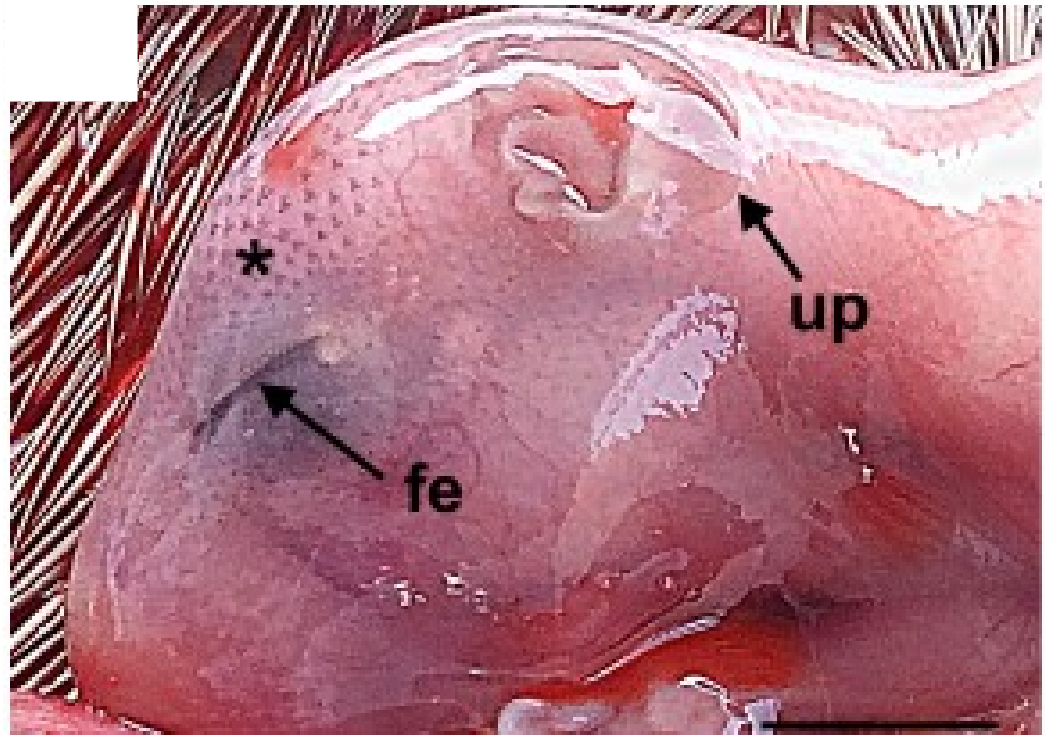

Figure 4.24: Lateral view of a prenatal AGCR at GD100. Note the fused eyelids (fe) and unpigmented pinna (up) on the head as well as presence of body hair follicles (black asterisk) restricted to the head, neck and cranial trunk region. Scale bar:1 cm

4.1.3.2.2 *Sproutingand spread pattern of hairs*

Tactile hair follicles initiallywere observed around the prenatal AGCR's snout at day 80 of gestation (GD80), however tactile hairs weren't visible on the upper lip until GD110 (Fig. 4.23). Body hair follicles were first seen on the head at day 100 of gestation (GD100) andextended to the rest of the body in a craniocaudal fashion by day 110 of gestation (Figs. 4.23 and 4.24). Fine hairs had emerged on the integument of the prenatal AGCR by day 120 of gestation, with abundance of these hairsmostly on the head and neck region of the body (Fig. 4.25). Dense long hairs covered the entire body of this developing rodent by GD130. The ventral part of the body was less pigmented than that of the back and thus with hairs lighter in colour (Figs. 4.18 and 4.26).

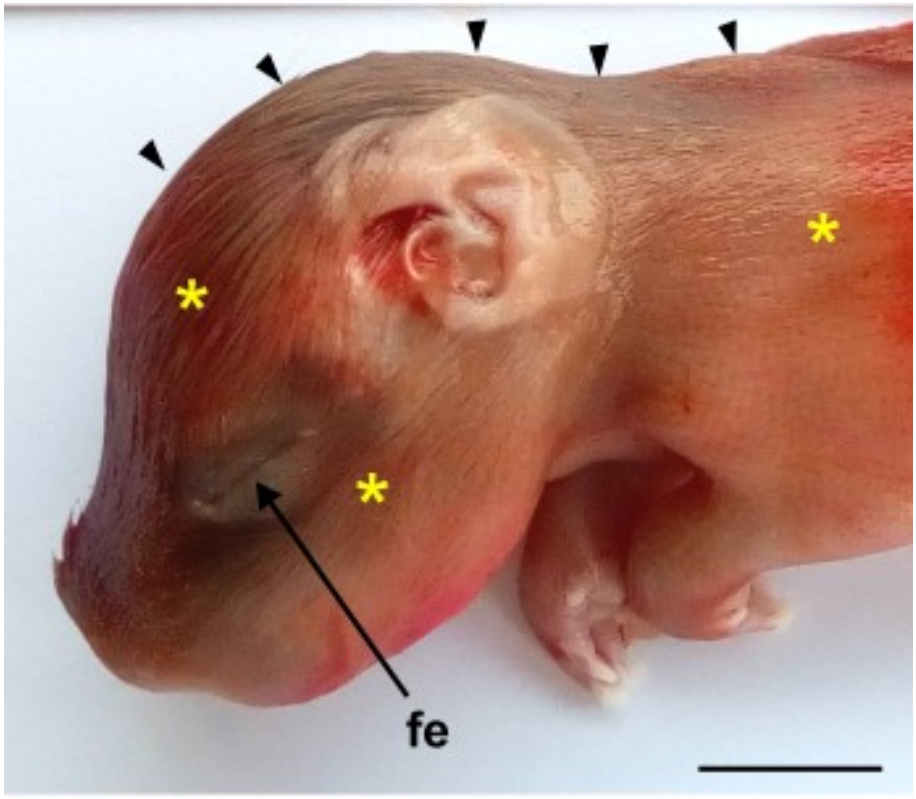

Figure 4.25: Lateral view of a prenatal AGCR at GD120. Notice the eyelids are still fused (fe) and the pigmented integument (yellow asterisks) on the head, neck and trunk. Scale bar:1 cm

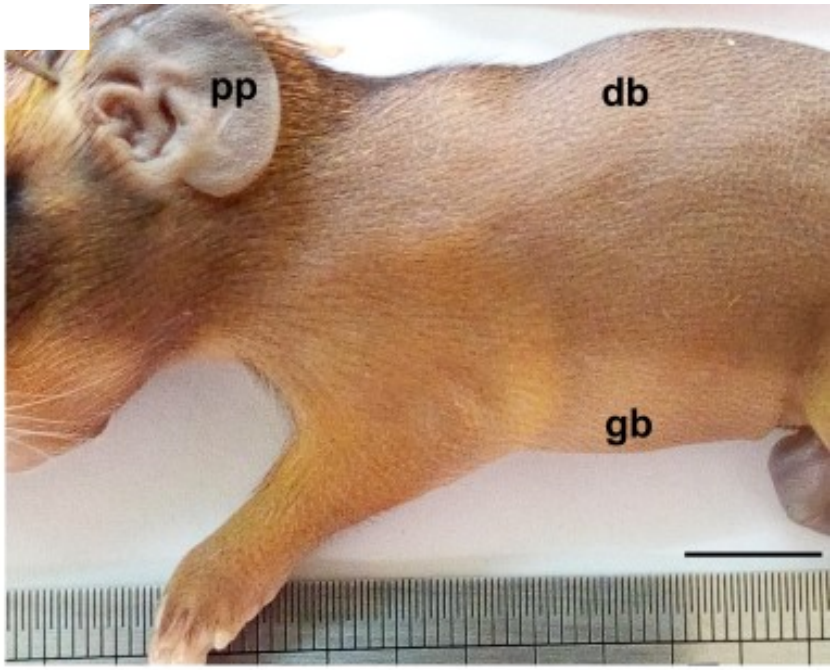

Figure 4.26: Lateral view of the head, neck and trunk region of a prenatal AGCR at GD140. Note the pigmented pinna (pp), dark brown pigmented dorsum (db) and ginger brown ventrum (gb). Scale bar:1 cm

4.1.3.2.3 *Appearance of distinctive blood vessels beneath the skin*

No blood vessels were seen underlying the skin of the prenatal AGCR as at GD60 (Fig. 4.14a). However, by GD70 the jugular vein was observed beneath the transparent integument (Fig. 4.14b). This vein became concealed by day 110 of gestation (Fig. 4.23). The coccygeal and lateral saphenous veins were visible underneath on the skin at GD100 until GD110 and became obscured by GD120 (Fig. 4.27).

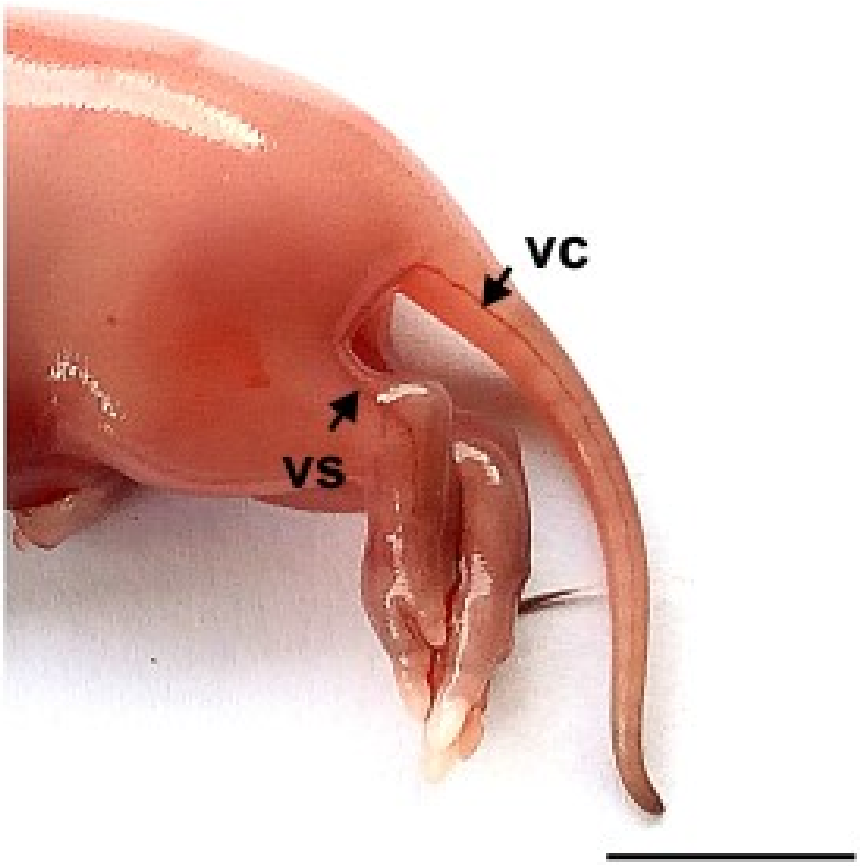

Figure 4.27: Lateral view of the hind limbs of a prenatal AGCR at GD110. Observe the visible blood vessels underlying the skin of the tail. coccygeal vein (vc) and saphenous vein (vs). Scale bar: 1 cm.

4.1.3.2.4 *Calvarium consistency*

The calvarium of the prenatal AGCR at GD60 and 70 was soft and fragile in consistency similar to a thin delicate membranous tissue. The consistency had become pliable by GD100. By day 120 of gestation, there was a progressive ossification of the cranial bones and expectedly, a change in the consistency of the calvarium. It had become hard and firmer similar to a bony structure. This continuous hardening (ossification) of the calvarium occurred along a time-dependent course with the calvarium of day 140 of gestation being the hardest compared to GD120 and GD130.

4.1.3.2.5 *Emergence of limbs, tailand sense organs*

In the developing AGCR, tail and limb buds first emerged at day 60 of gestation (GD60) (Fig. 4.14a). The extremities of these appendages had differentiated into digits by GD80 (Fig. 4.29a). These digits have been clearlydelineated; bearing cartilaginous claws by GD100 (Fig. 4.29b). Lens placodes were first observed at GD60 (Fig. 4.14a). Between GD70-80; the lens vesicles had become closed and separated from the surface (Fig. 4.29a). Eyelids (upper and lower) which were first noticed at GD100 were initially fused (Fig. 4.24) and were separated from GD130 until birth (Fig. 4.18). Otic vesicles of the prenatal AGCR were sealedbyday 60 of gestation. By GD80, the pinna was seen to have slightly emerged with visible external acoustic pores (Figs. 4.14c and 4.29a). The external ears of the prenatal AGCR had become well formed by GD100 and resembledthose of the adult (Figs. 4.15 and 4.24).

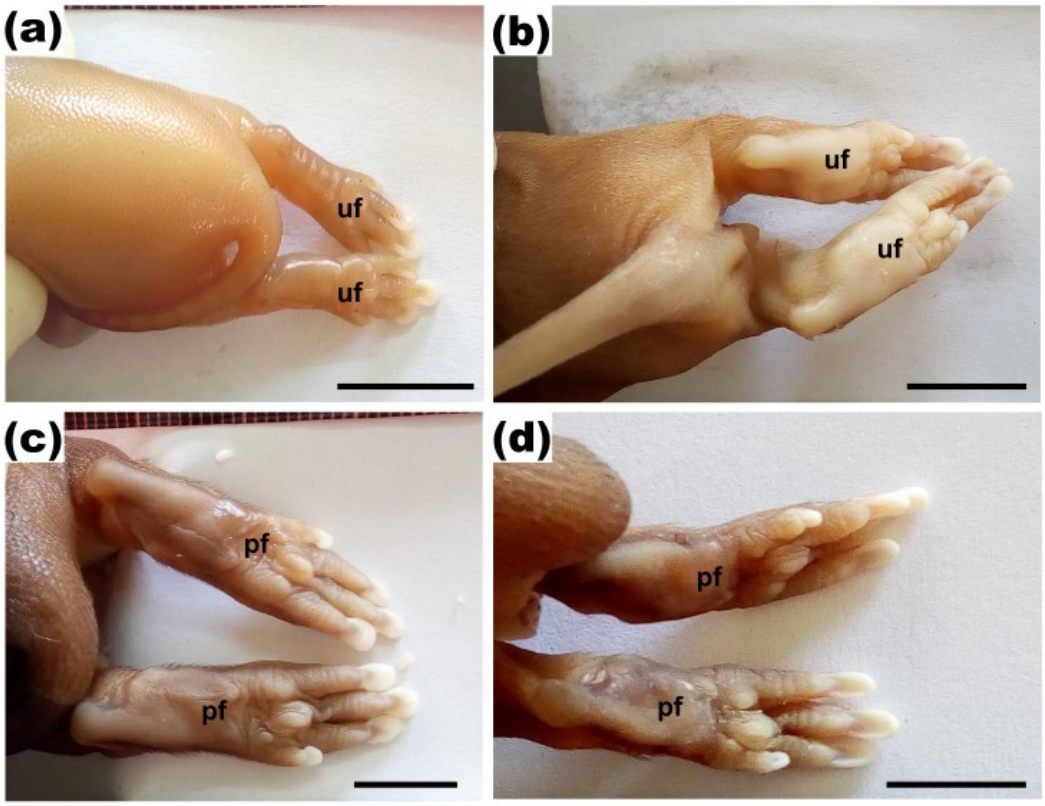

Figure 4.28: Plantar views of the prenatal AGCR showing hind limbs at (a) GD110, (b) GD120 (c), GD 130 and (d) GD140. Note the unpigmented footpads (uf) and pigmented footpads (pf). Scale bar:1cm

4.1.3.2.6 *Development of external sex organs*

The earliestclueof gross sex differentiation in the developing AGCR was observed at GD70. This was indicated by the emergence of a small protuberance between the hind limbs - the genital tubercle. This signalled the earliest time point of phenotypic sex differentiation (Figure 4.29c). At this stage, however, differentiation of sexual phenotypes into males and females was not achievable. They became easy to differentiate at day 80 of gestationutilizing the ano-genital distance. This distance was estimated as the measured interval fromthe anal openingtothe genital tubercle and it progressively increased in the prenatal AGCR between day 80 and 140 of gestation (Figs. 4.29d and 4.31, Table 4.4). It was observed that the ano-genital distance was consistently higher in the males than in the females with the highest difference recorded at GD140.

Furthermore, for all the time points from GD70, the prenatal sex ratio consistently favoured more of the males over the females (Fig. 4.33). Paired mamillae were found seen on either side of the ventrolateral parts of the trunk and this was first detected at GD130 (Fig. 4.30).

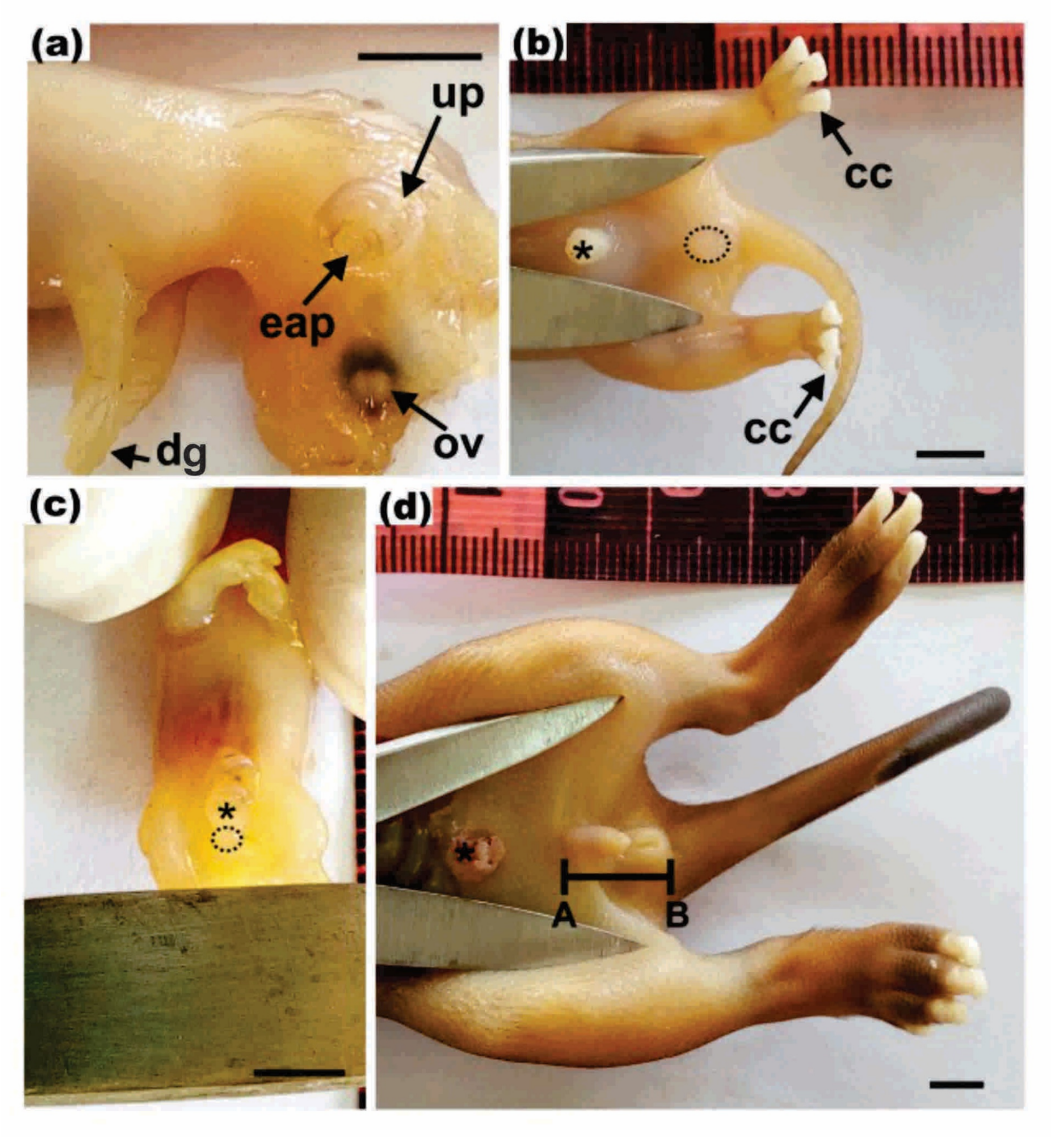

Figure 4.29:[a] Lateral view of the head, neck and cranial trunk of a prenatal AGCR at GD80. Note the unpigmented pinna (up);optic vesicle (ov); external acoustic pore (eap); digits without claws (dg) at the extremities. Scale bar: 0.5 cm. (b) Ventral view of a prenatal AGCR at [b] GD100, [c] GD 70 and [d] GD 130. Umbilical cord (asterisks); cartilaginous claw (cc); dotted circle circumscribes the genital tubercle. Note he anogenital distance (A – B). Scale bar:0.5 cm.

Figure 4.30: Lateral view of the prenatal AGCR at GD 130 showing the emergence of the teat of the mammary gland (arrow heads). Scale bar:0.5cm

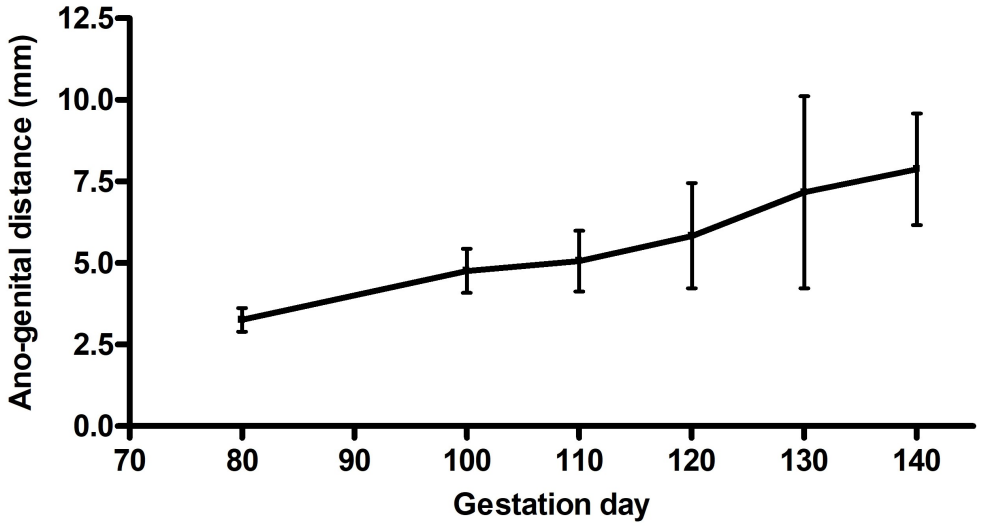

Figure 4.31: Graphic representationof the ano-genital distance in the prenatal AGCR between GD80 and 140. Data presented as mean ± s.e.m.

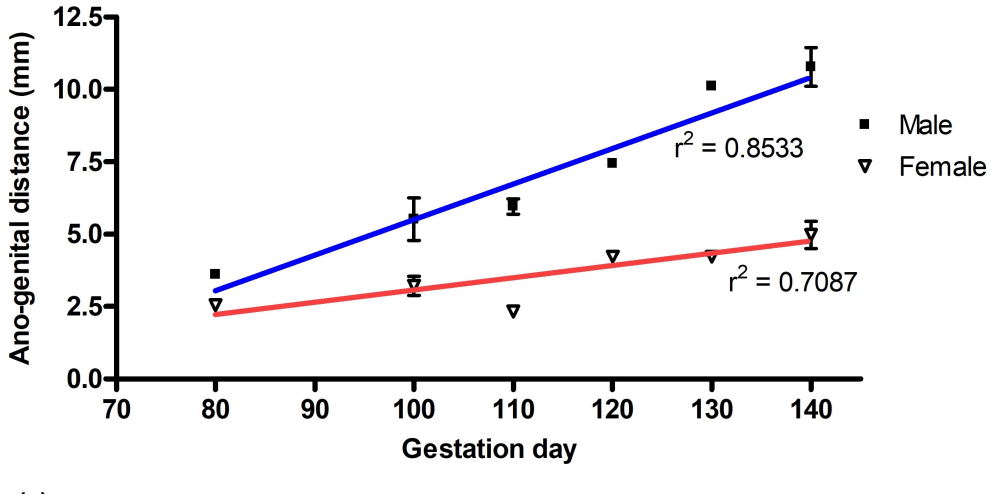

Figure 4.32: Graphic presentation of the ano-genital distance in the prenatal AGCR between GD80 and 140.

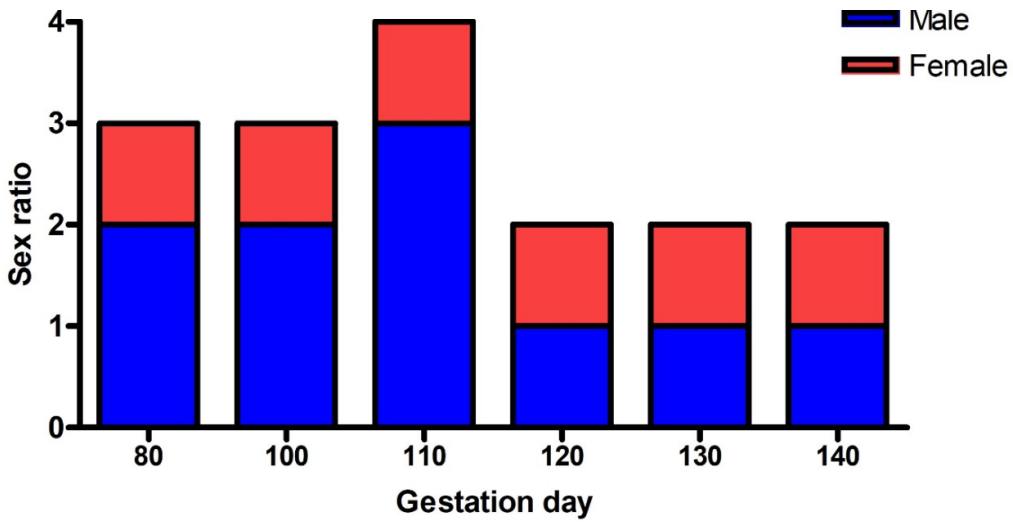

Figure 4.33: Sex ratio graph in the prenatal AGCR between GD80 and 140.

Table 4.4: Ano-genital distance in the developing AGCR. Data represent Mean ± S.E.M.

Gestation Day	Male ano-genital distance (mm)	Female ano-genital distance (mm)
80	3.60±0.17*	2.60±0.0
100	5.50±0.74	3.21±0.34
110	5.96±0.27**	3.30±0.0
120	7.40±0.0**	4.20±0.0
130	10.00±0.0**	4.20±0.0
140	10.78±0.67**	4.97±0.47

** Statistically significant difference at $p<0.05$*

4.1.3.2.7 *Dental eruption*

The first two incisors, both on the upper jaw and lower jaw, were the only prenatal teeth that erupted prior to birth. The incisor on the lower jaw were the first to erupt and was observed at GD80, while the upper jaw incisors did not erupt earlier than GD100 (Figs. 4.3a and b).

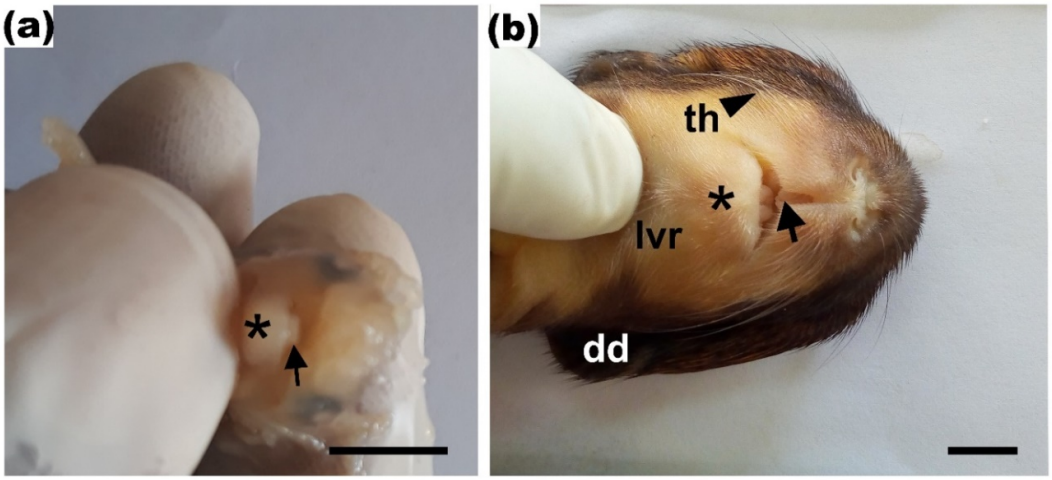

Figure 4.34: Ventral views of the prenatal AGCRhead revealing first pair of erupted incisors indicated by arrows (a) of the lower incisor at GD80 and (b) upper jaw at GD130. Lower jaw (asterisks); lighter ventral region (lvr); dark dorsum of skin (dd); tactile hairs on the upper lip (th). Scale bars: 1 cm.

4.1.4 Staging of embryos and foetuses

The AGCR embryos and foetuses of GD10-140 were staged based on the phenotypic features generated from this study adopting the Carnegie and Štěrba systems (Tables 4.4 and 4.5). This staging showed the embryogenesis in the AGCR (Štěrba stages 1-6 and Carnegie stages 1-23) terminates at GD90, followed by foetogenesis (Štěrba stages 7-13) that spans till parturition (Tables 4.4 and 4.5). The timing of these periods (embryonic and foetal developments) when compared with those of other precocial rodent mammals like guinea pig and non-rodent mammals like sheep, pig and human revealed that embryogenesis ends at a relatively belated time point (GD90) (Fig. 4.35a). The relative period of foetal development in the AGCR was observed to be comparatively shorter (40%) to those of sheep (78%), pig (71%) and humans (79%), and marginal compared to other precocial rodent such as the European hare (52%), agouti (55%) and guinea pig (57%) (Fig. 4.35b). On the contrary, the AGCR had the longest relative interval for embryonic development among all mammals examined (Fig. 4.35b).

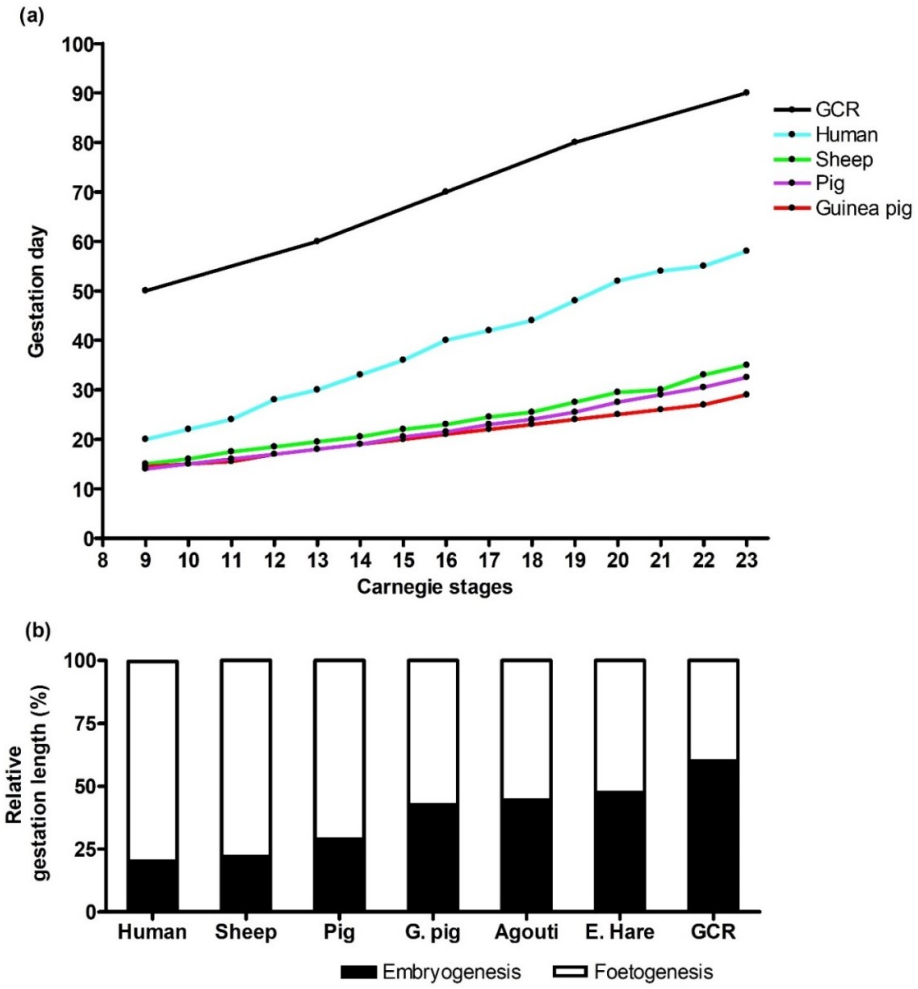

Figure 4.35: Comparative graphical representation of the Staging of the embryogenesis and foetogenesis in the prenatal AGCR compared with other selected mammals (a) by computing stages 9-23 of the Carnegie staging system and (b) the relative period of embryogenesis and foetogenesis (represented in percentages of the total length of gestation). Data of other mammals used for comparison were obtained from established literature (Sivachelvan *et al.,* 1996; Roellig *et al.,* 2010; Fortes *et al.,* 2013; Hill, 2018, 2019b & 2019c).

4.2 Experiment Two

4.2.1 Morphological Characterization of the Developing Prenatal AGCR Brains

Due to the reproductive delay and consequent prolonged period of embryogenesis seen in the AGCR, no gross observable embryo was seen until GD50 where the embryos were seen with transparent integuments. This marked the earliest time point of gross body formation and delineation of the somites, cephalic and caudal regions of the embryos. Not until GD60 were the embryos appreciable for gross morphological descriptions. Thus, description of the gross developmental features of the AGCR prenatal brain was done from its earliest visually recognizable time point (GD 60) until birth.

4.2.1.1 Brain Morphology

Gestation Day 60:

The developing brain at GD 60 was grossly lissencephalic. Although the three primordial brain vesicles – the prosencephalon, mesencephalon and rhombencephalon were readily identified, differentiation into secondary brain vesicles had begun. The prosencephalon was noted to had differentiated into a paired cranio-laterally directed telencephalic vesicles, two optic sulci and an unpaired relatively small and partly concealed diencephalon dorsally (Fig. 4.36a).

A median hemispheric sulcus was observed and separated the two telencephalic vesicles and later runs laterally on either sides to separate the telencephalic vesicles from the mesencephalon. The optic sulci appeared as an indentation on either side of the prosencephalon which bear the optic stalks and extend towards the surface ectoderm as the optic cup. The diencephalon concealed to a large extent by the telencephalic vesicles dorsally, however it was better appreciated ventrally. The

emergence of the paired olfactory vesicles were noticed ventrally. The mid brain (mesencephalon) was at this stage of development observed to be undifferentiated and was located caudal to the fore brain (precisely caudal to the diencephalon). It occupied approximately about half of the entire brain length. At this stage of development, the mesencephalon represents the highest point of the brain. This summit is a direct consequence of the brain flexion at this point and corresponds to the cephalic or midbrain flexure.

The hind brain (rhombencephalon) had differentiated into the rostral metencephalon which was seen as small dilatation just caudal to the midbrain and a caudal small stalk, the myelencephalon. Both of which were separated by the pontine flexure. This flexure is best appreciated on the ventral view of this developing brain (Fig. 4.36b). The brains were severed at the cervical flexure and as such are not best demonstrated in the figures provided. This flexure was found at the transition of the hind brain into the spinal cord. It is however worthy of note that these flexures were identified before the brains were severed from the cord.

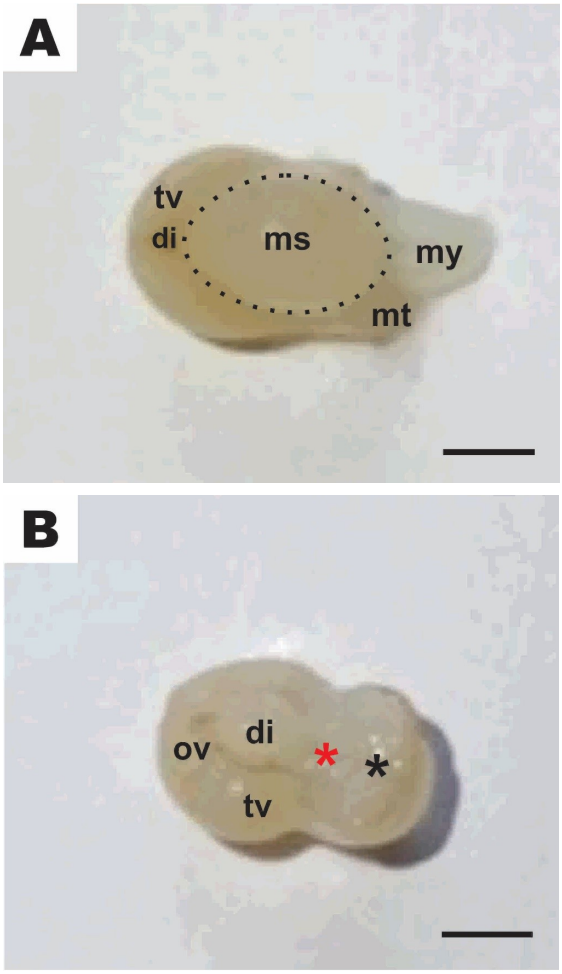

Figure 4.36: Prenatal brain of the AGCR at GD60 (a: dorsal and b: ventral views). Note the telencephalic vesicle (tv), olfactory vesicle (ov), diencephalon (di), mesencephalon (ms), metencephalon (mt), myencephalon (my), cephalic flexure (red asterisk) and the pontine flexure (black asterisk). Scale bar: 1cm

Gestation Day 70:

The developing brain GD 70, the fore brain (telencephalon) remained grossly lissencephalic. There is however, an appreciable increase in the size of the telencephalic vesicles. These vesicles were observed to have expanded in lateral, parietal and longitudinal directions reaching as far as about the mid length of the midbrain. The hemispheric sulcus appeared more distinct and relatively extensive, occupying from its rostral limit about one-third of the total inter-telencephalic fissure and terminates where it forms the rostral border of the diencephalon. The diencephalon is moderately more distinct with little appreciable differentiation noticed from the dorsal view grossly (Fig. 4.37a).

There was slight elongation in the length of the mid brain with a shallow midsagittal longitudinal depression noticed on its roof plate and also a corresponding floor plate – an indication of the differentiation and emergence of the tectum. The cephalic/midbrain flexure still observable at this stage, caudal and somewhat ventrolateral to the mesencephalon are the emerging rhombic lips of the differentiating metencephalon. These rhombic lips are widely separated located on either side on the dorsolateral side of the metencephalic alar plate. A noticeable increase in length of the myelencephalon was also noted with the emergence of a slight median longitudinal groove on its dorsum (Fig. 4.37a). There was a substantial enlargement of the diencephalon which was more visible on the ventral plane of the developing brain. At this stage of development, the olfactory vesicles had differentiated into a pair of olfactory bulbs. The pontine flexure was further deepened and the cervical flexure also persisted (Fig. 4.37b).

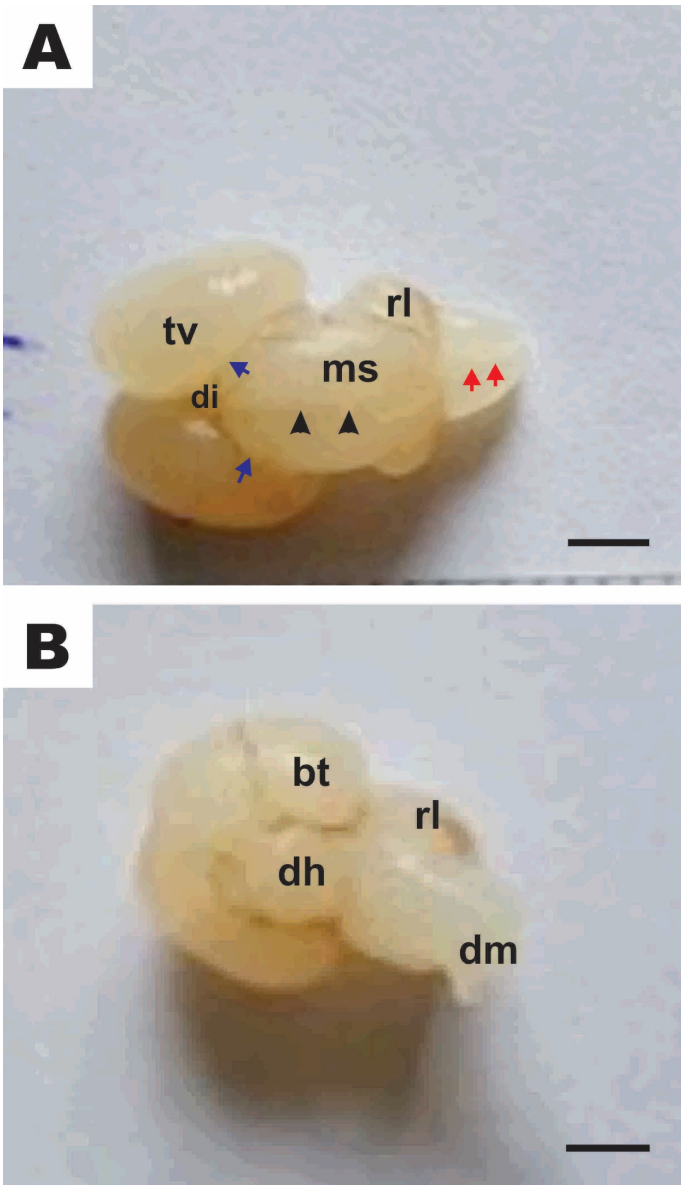

Figure 4.37: Prenatal brain of the AGCR at GD70 (a: dorsal and b: ventral views). Note the telencephalic vesicles (tv), mesencephalon (ms), diencephalon (di), rhombic lips(rl), developing medulla (dm), basal telencephalon (bt), developing hypothalamus (dh), hemispheric sulcus (blue arrows), mid-sagittal longitudinal mesencephalic groove (black arrowheads) and median longitudinal groove on developing medulla (red arrows). Scale bar: 1cm

Gestation Day 80:

The forebrain of the AGCR foetus at GD 80 still appeared grossly smooth with no gyri, however the telencephalic vesicles had grown extensively, both laterally and caudally, and enveloped more of the diencephalon. Also sequelae to the lateral enlargement of the telencephalic vesicles, the contact surface area of these vesicles at the inter-telencephalic fissure had also increased remarkably. The median longitudinal groove on the roof plate of the mid brain, separating two longitudinal elevations, persist however still slightly noticeable. The rhombic lips of the metencephalon which were initially far apart, have migrated towards to the midline to form a transverse cephalo-caudally compressed thickening which extends over the roof plate. This thickening was identified as the cerebellar plate (Fig. 4.38a).

Ventrally, paired olfactory bulbs were seen on the rostral most part of the telencephalon alongside with slight bulging appearance of the corresponding paired olfactory striae. All three brain flexures (cephalic, pontine and cervical) persisted, with particularly a deeper invagination of the pontine flexure. The alar plate of the diencephalon was identified as a distinct rounded eminence bounded laterally by the telencephalic vesicles on either side and rostrally by the paired olfactory bulbs and olfactory striae. There were no apparent observable changes in the gross morphology of the developing medulla at this stage of development (Fig. 4.38b).

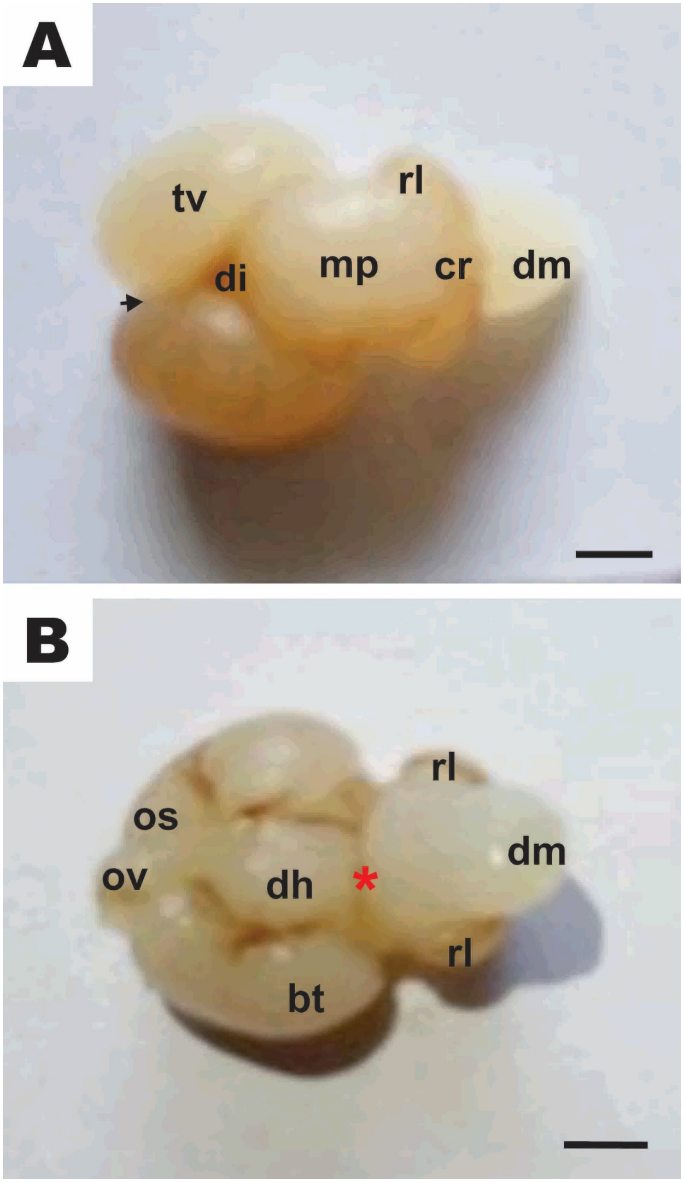

Figure 4.38: Prenatal brain of the AGCR at GD80 (a: dorsal and b: ventral views). Note the telencephalic vesicles (tv), olfactory vesicle (ov), olfactory striae (os), mesencephalon (ms), diencephalon (di), midbrain roof plate (mp), rhombic lips(rl), developing medulla (dm), cerebellar plate(cr), basal telencephalon (bt), developing hypothalamus (dh) and inter-telencephalic fissure (black arrow). Scale bar: 1cm

.

Gestation Day 90:

At gestation day 90 of AGCR development, the forebrain still remained lissencephalic. There was a further increase in the size of telencephalic vesicles along lateral, longitudinal and parietal planes, with the vesicles completely overlying the diencephalon and corresponding increase in the inter-telencephalic fissure length. A transverse groove was seen over the roof plate of the mesencephalon perpendicular to the median longitudinal groove and thus dividing the roof plate into four quadrants of colliculi (the paired rostral and caudal colliculi) (Fig. 4.39a). With a further deepening of the pontine flexure (as evidenced by slight concealment of the myelencephalon on the dorsal plane), the metencephalon appeared more dorsal compared to the more caudo-ventrally displaced myelencephalon. The transverse cerebellar plate of the metencephalon had differentiated into a small central vermis and a pair of protruding lateral masses (the paired lateral lobes).

The ventral view of the developing AGCR brain at prenatal day 90 revealed paired olfactory bulbs with more distinctly delineated medial and lateral olfactory striae and piriform lobes on either side of the telencephalon. The ventral surface of the developing hypothalamus (seen on the floor of the bulging diencephalon) had on either side of its midline two slightly rounded elevations called the mammillary bodies. Caudal to this, is the emergence of the differentiating cerebral peduncles on the ventral surface (tegmentum) of the mesencephalon. These peduncles form the rostral limit of the primordial pons; a median rounded protrusion on the ventral surface of the metencephalic floor plate (Fig. 4.39b).

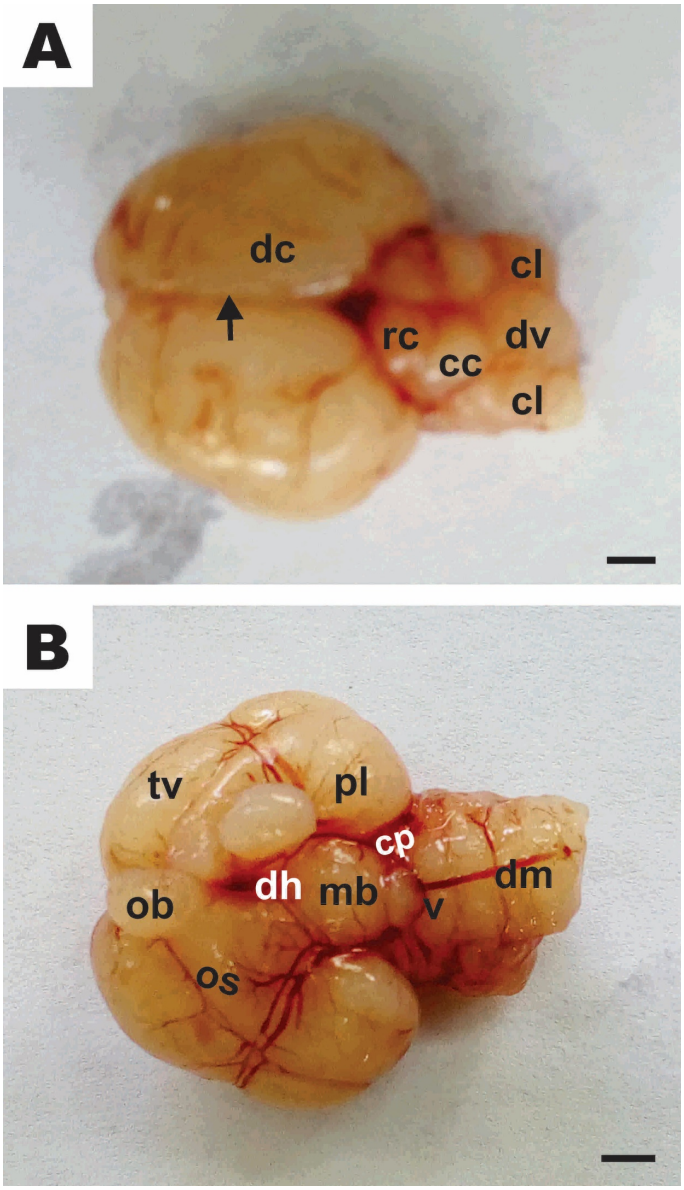

Figure 4.39: Prenatal brain of the AGCR at GD90 (a: dorsal and b: ventral views). Note the olfactory striae (os), developing cortex (dc), rostral colliculus (rc), caudal colliculus (cc), lateral cerebellar lobes (cl), developing vermis Idv), olfactory bulb (ob), piriform lobe (pl), developing hypothalamus (dh), mammillary bodies (mb), developing pons (dp), cerebral peduncle (cp), developing medulla (dm) and inter-telencephalic fissure (black arrow).Scale bar: 0.5cm

Gestation Day 100:

This stage (GD 100) of prenatal brain development marked the beginning of the forebrain gyrencephalization, observed as slight depressions and elevations on the surface of the telencephalic vesicles. There was further increase in sizes of the telencephalic vesicles, laterally and caudally, reaching beyond the diencephalon and extending over parts of the metencephalon. There was a further deepening of both longitudinal and transverse grooves on the tectum thus, making the paired rostral and caudal colliculi more delineated and better appreciated. The slight caudoventral inclination of the mesencephalon is a direct consequence of the further deepening of the cephalic (mid brain) flexure. A substantial increase in the sizes of the vermis and paired lateral lobes of the metencephalon was noted on the dorsal part of the brain. A shallow transverse fissure separates a budding nodule arising from the vermis. As a result of the deepening pontine flexure, the myelencephalon appeared more concealed when viewed from the dorsal plane, directed more caudoventral to the differentiating metencephalon (Fig. 4.40a).

The olfactory bulb was observed on the rostral portion of the telencephalon on the ventral view with both medial and lateral olfactory striae identified. The developing hypothalamus still appeared as a round bulging mass on the diencephalon floor plate and is bounded caudally by the developing cerebellar peduncles of the mesencephalon. Just beyond these peduncles, the developing pons was observed as a gradual prominent structure on the floor plate of the metencephalon. Caudal to this, is the developing medulla with a prominent cervical flexure separating it from the spinal cord (Fig. 4.40b).

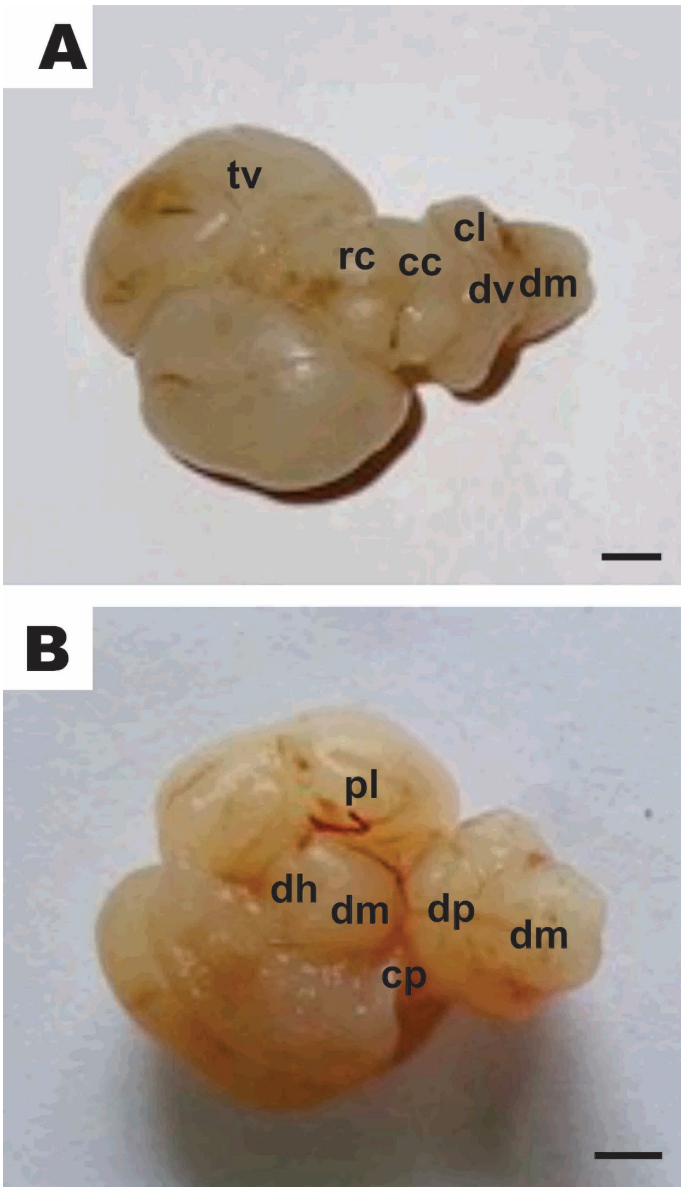

Figure 4.40: Prenatal brain of the AGCR at GD100 (a: dorsal and b: ventral views). Note the telencephalic vesicle (tv), olfactory striae (os), rostral colliculus (rc), caudal colliculus (cc), lateral cerebellar lobes (cl), developing vermis (dv), olfactory bulb (ob), piriform lobe (pl), developing hypothalamus (dh), mammillary bodies (mb), developing pons (dp), cerebral peduncle (cp) and developing medulla (dm). Scale bar: 0.5cm

Gestation Day 110:

There was an observable progression in gyrification of the forebrain at GD 110. The tectum of the mesencephalon at this stage of development was observed to be more differentiated with a clear demarcation into two paired structure (rostrally and caudally). More transverse fissures were noticed on the dorsal portion of the developing cerebellum. The pontine flexure is further elaborated at the point of transition of the differentiating metencephalon into the myelencephalon, thus displacing the latter further into a more caudo-ventral orientation, making it almost impossible to visualize from the dorsal aspect (Fig. 4.41a).

Ventrally, the olfactory tracts (medial and lateral) became more prominent on the basal telencephalon. Caudal to the ventral surface of the developing hypothalamus is a more expansive cerebral peduncles marking the rostral limit to the developing pons. The latter is more pronounced on the floor of the metencephalic region. Little to no observable changes were observed in the developing medulla (Fig. 4.41b).

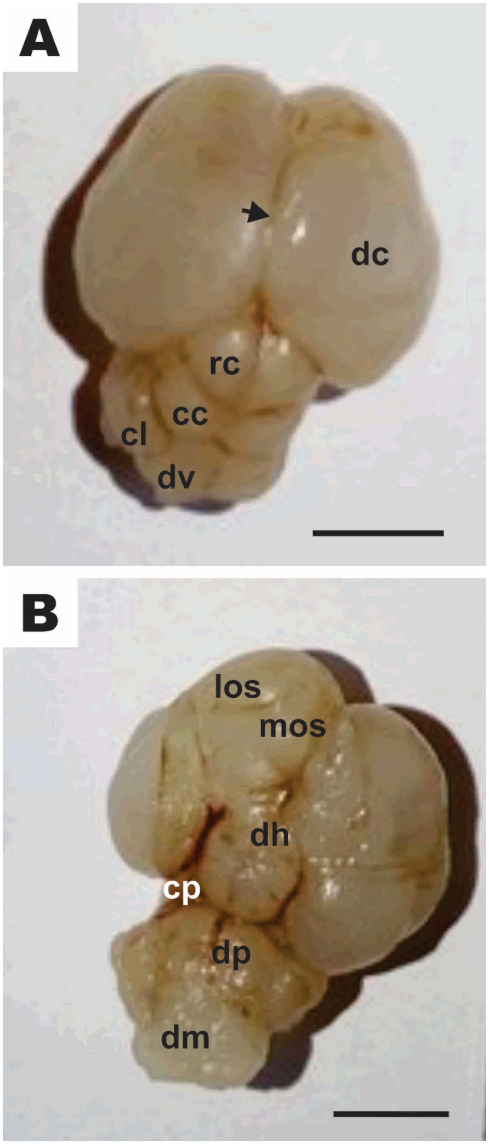

Figure 4.41: Prenatal brain of the AGCR at GD110 (a: dorsal and b: ventral views). telencephalic vesicle (tv), lateral olfactory striae (los), medial olfactory striae (mos), rostral colliculus (rc), caudal colliculus (cc), lateral cerebellar lobes (cl), developing vermis (dv), developing hypothalamus (dh), developing pons (dp), cerebral peduncle (cp) and developing medulla (dm). Scale bar: 0.5cm

Gestation Day 120:

The forebrain had become more visibly gyrencephalic at GD 120. A rostral to caudal expansion of the longitudinal groove was noted to have demarcated the left and right colliculi on the tectum leading to a wider longitudinal groove separating the caudal colliculi. Consequently, the left and right caudal colliculi appeared farther apart compared to the rostral colliculi. Also, the former had become relatively bigger in size compared to the latter. The differentiating cerebellum was beginning to look more like the post-natal brain with deepening and increase in the numbers of transverse fissures. The flocculonodular lobe could be well delineated from the corpus cerebelli at this stage of development by the caudolateral fissure. A primary fissure separating the rostral and middle lobes of the corpus cerebelli was also noticed. The paired lateral lobes of the cerebellum seemed to have differentiated grossly into recognizable cerebellar hemispheres bounding the vermis on either side (Fig. 4.42a).

On the ventral surface, the olfactory bulbs and tracts (medial and lateral) were visibly prominent on the basal telencephalon with the piriform lobes (caudal to the olfactory tracts) also identifiable. The hypothalamic floor and cerebral peduncle were also observed to be similar to state of development in GD 110. More strikingly on the ventral surface was that the cranial nerves were easily identified on the diencephalon and brain stem. The trapezoid body was also easily identified caudal to the pons. The ventral sides of the cerebral hemispheres could also be noticed lateral to the pons and trapezoid body. Continuing from this (trapezoid body), caudally is an emergence of two slightly raised ventral longitudinal streaks on both sides of the developing medulla – the medullary pyramids (Fig. 4.42b).

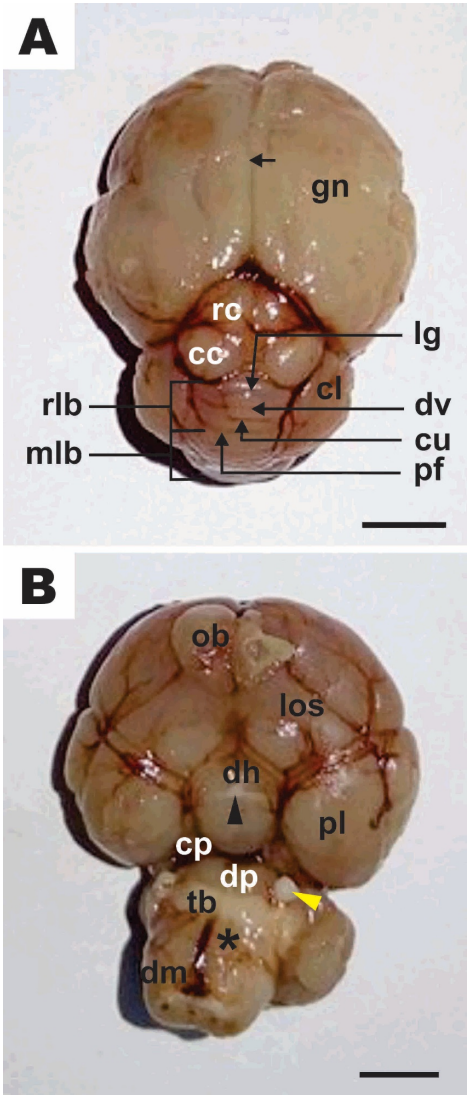

Figure 4.42: Prenatal brain of the AGCR at GD120 (a: dorsal and b: ventral views). Note the developing hypothalamus (dh), developing pons (dp), olfactory striae (os), developing medulla (dm), cerebral peduncle (cp), gyrencephalic neocortex (gn), rostral colliculi (rc), caudal colliculi (cc), lingula (lg), culmen (cu), developing vermis (dv), primary fissure (pf), rostral cerebellar lobe (rlb), middle cerebellar lobe (mlb), lateral cerebellar plate (cl), piriform lobe (pl), olfactory bulb (ob), trapezoid body (tb), intertelencephalic fissure (black arrow), cranial nerve on the pons (yellow arrow head), cranial nerve on the diencephalon (black arrow head). Scale bars: 0.5cm.Scale bar: 0.5cm

Gestation Day 130:

The forebrain of the developing AGCR at GD130 appeared more gyrencephalic grossly with more evidences of deeper sulci and gyri on the developing neocortex. The olfactory bulbs were seen as the most rostral structures and can be appreciated from the dorsal surface protruding from the underside of the forebrain. The curvature of mesencephalic tectum seems relatively less convex compared to the preceding time point (GD 120) as a result of the gradual decrease in depth of the cephalic (midbrain) flexure. The rostral portion of the rostral colliculi was covered by the caudal parts of the hemispheres of the cerebrum. The caudal colliculi seem farther apart compared to the preceding timed age point and abutting the commissure between these colliculi is the differentiated lingula of the cerebellum. The lobation pattern of the cerebellum at this time point of gestation was beginning to appear clearly for description. The lingual, central lobe and culmen of the rostral lobes of the corpus cerebelli can be well appreciated. Caudal to this culmen is the primary fissure that delineates the rostral lobe and the middle lobe of the cerebellum (Fig. 4.43a).

Ventrally, all developmental features/structures described for the developing AGCR brain at GD 120 appeared similar to observed features at this time point but with major differences being greater accentuations of the described features (Fig. 4.43b).

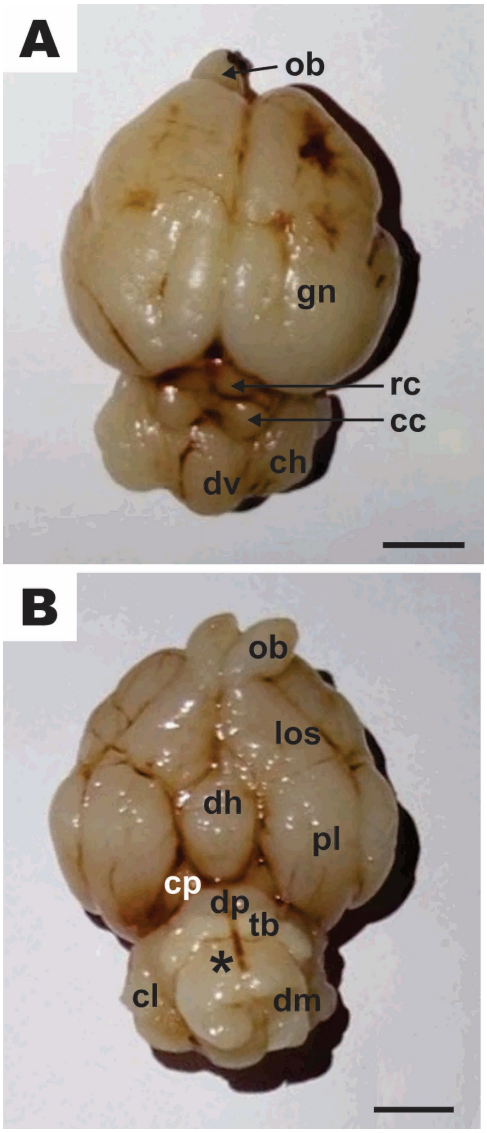

Figure 4.43: Prenatal brain of the AGCR at GD130 (a: dorsal and b: ventral views). Note the olfactory bulb (ob), olfactory striae (os), developing hypothalamus (dh), cerebral peduncle (cp), gyrencephalic neocortex (gn), rostral colliculi (rc), caudal colliculi (cc), developing vermis (dv), cerebellar hemisphere (ch), piriform lobe (pl), developing pons (dp), trapezoid body (tb), developing medulla (dm) and pyramid (asterisk).Scale bar: 0.5cm

Gestation Day 140:

The forebrain of the developing AGCR at GD140 appeared more gyrencephalic grossly compared to that of GD130 with more evidences of deeper sulci and gyri on the developing telencephalon (neocortex). The olfactory bulbs were seen as the most rostral structures and at this stage of development, it can be appreciated from the dorsal surface which appeared protruding from the underside of the forebrain. The mesencephalic tectum appeared slightly bulged as a result of the gradual decrease in depth of the cephalic (midbrain) flexure, contributing to the slight stretching out of the brain. The rostral and the caudal colliculi seem farther apart compared to the preceding timed age point and appeared slightly bulged.

The lobation pattern of the cerebellum at this time point of gestation appeared well demarcated (with the lingual, central lobe and culmen of the rostral lobes of the corpus cerebelli can be well appreciated) (Fig. 4.44a). The features observed at this stage of development appeared same as the previous time point but more developed with only a better delineation of differentiated brain structures (Fig. 4.44b).

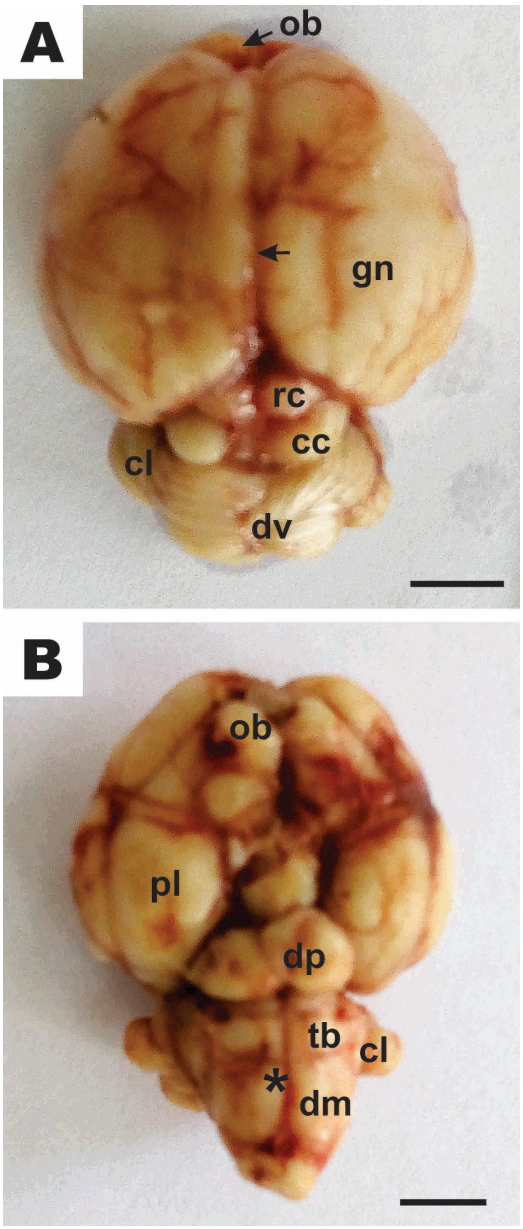

Figure 4.44: Prenatal brain of the AGCR at GD140 (a: dorsal and b: ventral views). Note the olfactory bulb (ob), piriform lobe (pl), gyrencephalic neocortex (gn), rostral colliculi (rc), caudal colliculi (cc), developing vermis (dv), lateral cerebellar lobe (cl), piriform lobe (pl), developing pons (dp), trapezoid body (tb), developing medulla (dm) and pyramid (asterisk).Scale bar: 0.5cm

4.2.1.2 Brain Morphometry

Evaluating the changes in the absolute brain weight with the progressing gestation in the developing prenatal AGCR, two growth spurts were recorded. The first growth spurt was observed between GD80-GD100 while the second spurt noted between GD110 and GD130 (Fig. 4.45). A negative slope was observed when the relative brain weigh of the prenatal AGCR brain was observed with increasing gestation length in the prenatal AGCR (Fig. 4.45)

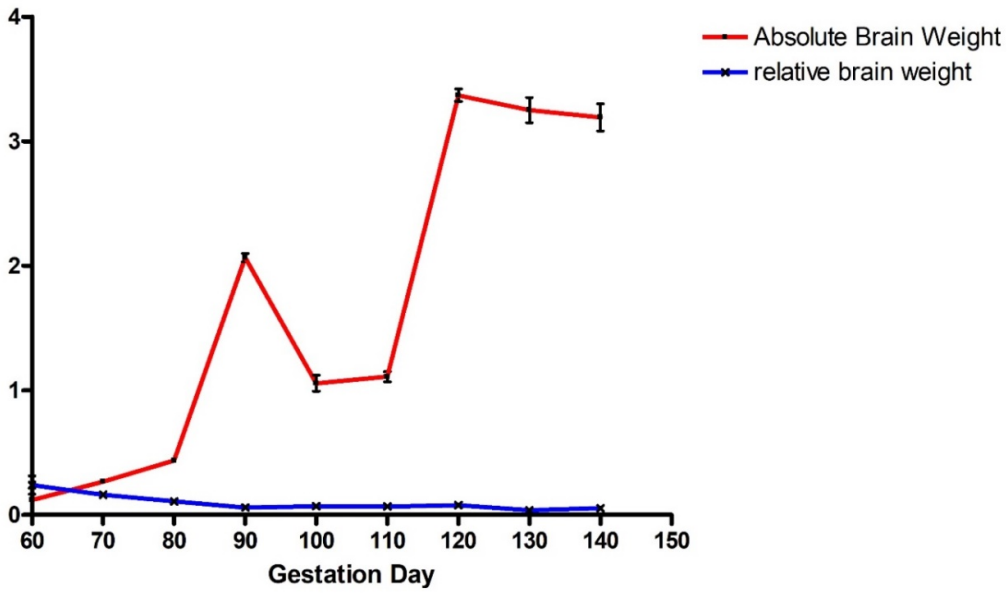

Figure 4.45: Graphical representation of the relationship between the prenatal AGCR brain weight (relative and absolute) across the gestational age.

Positive relationships, which turned out to be statistically significant ($p<0.05$), were found to exist across all the brain variables quantified (brain width: $r=0.87$; brain length: $r=0.86$; and brain height: $r=0.58$). (Figs. 4.46, 4.47 and 4.48).

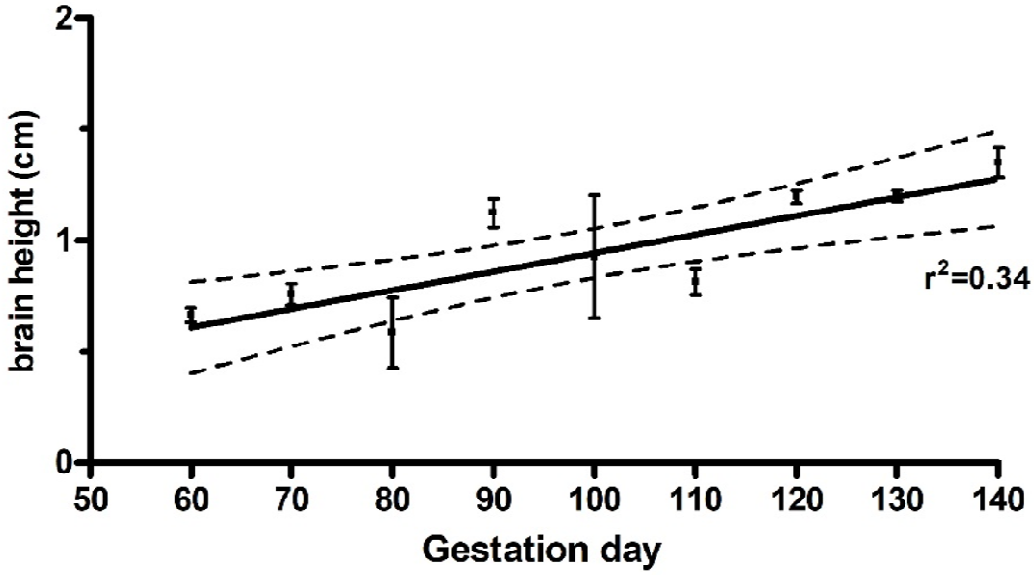

Figure 4.46: Allometric quantification of brain height in the prenatal AGCR brain between GD60 and GD140. showing the best-fit line (BH= 0.11+0.01*GD). Where BH= brain height, GD = Gestation day and r^2 = coefficient of determination

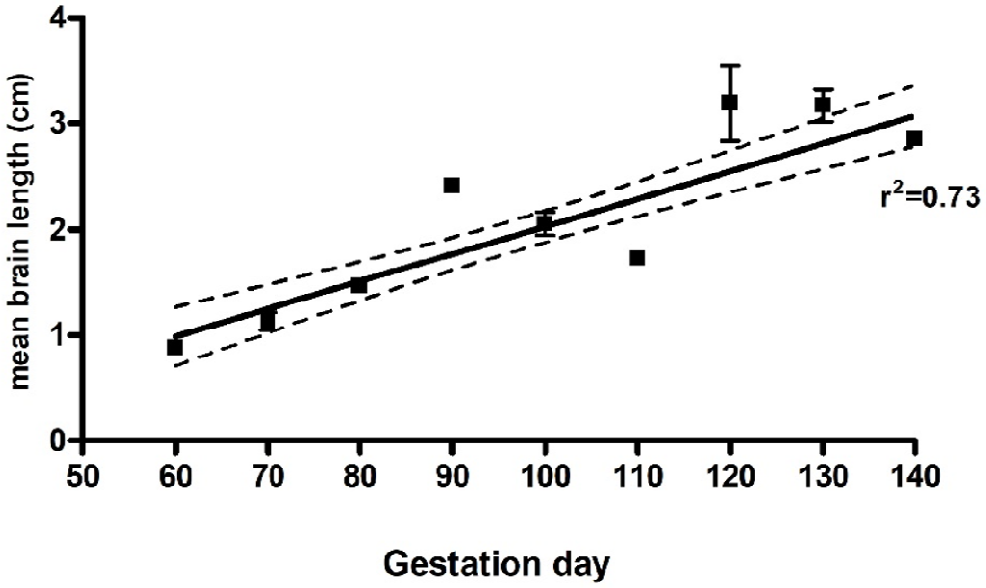

Figure 4.47: Allometric quantification of brain length in the prenatal AGCR brain between GD60 and GD140 showing the best-fit line (BL= -0.57+0.03*GD). Where BL= brain length, GD = Gestation day and r2 = coefficient of determination

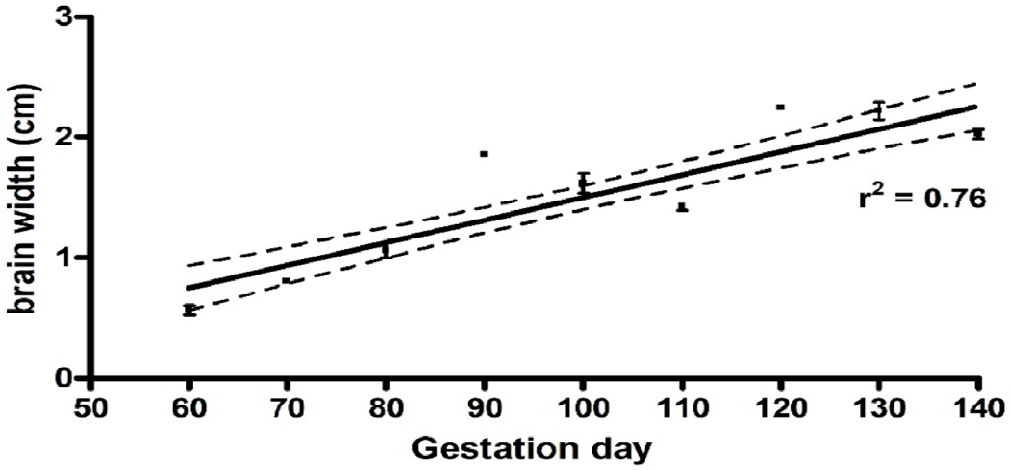

Figure 4.48: Allometric quantification of brain width in the prenatal AGCR brain between GD60 and GD140 showing the best-fit line (BW= -0.38+0.02*GD). Where BW= brain width, GD = Gestation day and r^2 = coefficient of determination.

4.3 Experiment Three

4.3.1 Corticogenesis Profiling of the Developing Prenatal AGCR Brain

This study gave a detailed report on the developmental pattern and timing (most especially the onset and peak periods) of neurogenesis, deep and upper layer formation, neuronal differentiation, gliogenesis and myelinogenesis in the developing AGCR neocortex across its gestation length (GD50 - 140).

4.3.1.1 Neurogenesis in the Prenatal AGCR (Pax6/Tbr2)

The Pax6 and Tbr2 biomarkers stain for neural stem cells (NSCs), basically radial glial cells and neural progenitor cells (NPCs), particularly intermediate neuronal progenitors respectively. At GD50, the neuroepithelium of the developing neural tube appeared as a pseudostratified layer with all cells staining positive for Pax6 and negative for Tbr2 (Fig 4.49). By GD60, ventricular zone (VZ) and sub-ventricular zone (SVZ) were already clearly established with the former reaching its maximum thickness and with the highest Pax6+/Tbr2- cell counts (Fig 4.50). Subsequently, there was a progressive decline in the Pax6+/Tbr2- VZ cell populations and thickness, having reached its peak at GD60 (Fig. 4.50).

By GD130, the VZ layer had been reduced and transformed to a single layer of ependymal cells. Concurrently at the SVZ, there was a gradual multiplication of the NPCpopulation(Pax6-/Tbr2+) as well as an increase in the thickness of this zone from GD60 reaching its peak at GD80 (Fig 4.50), thus representing the peak period of neurogenesis in the prenatal AGCR. Afterwards, a decline in the population of NPCs and the SVZ thickness was observed for the remainder of the gestation days in the prenatal AGCR brain (Fig 4.51).

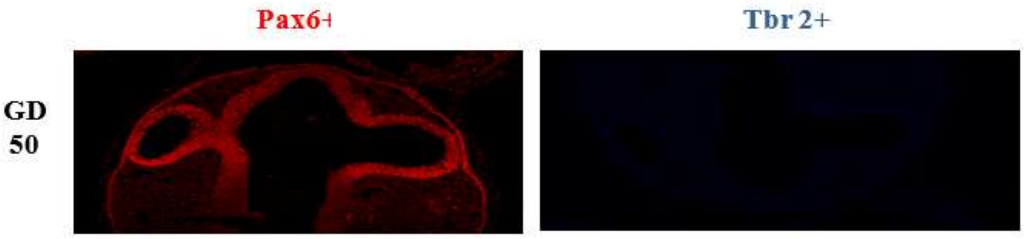

Figure 4.49: Pax6 and Tbr2 expression of the prenatal brain of the AGCR at GD 50

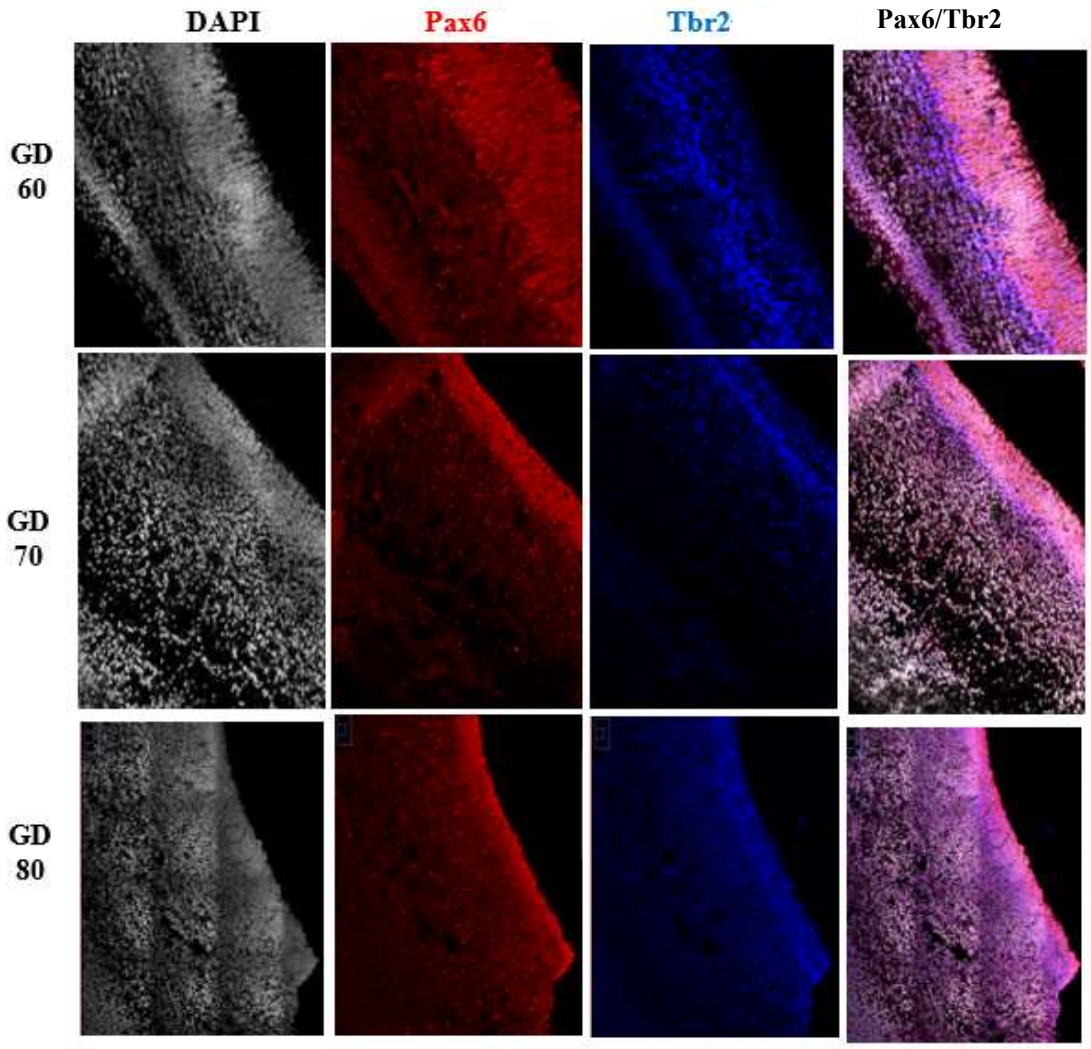

Figure 4.50: Expression of Pax6 and Tbr2in prenatal brain of the AGCR at GD 60, GD 70 and GD 80

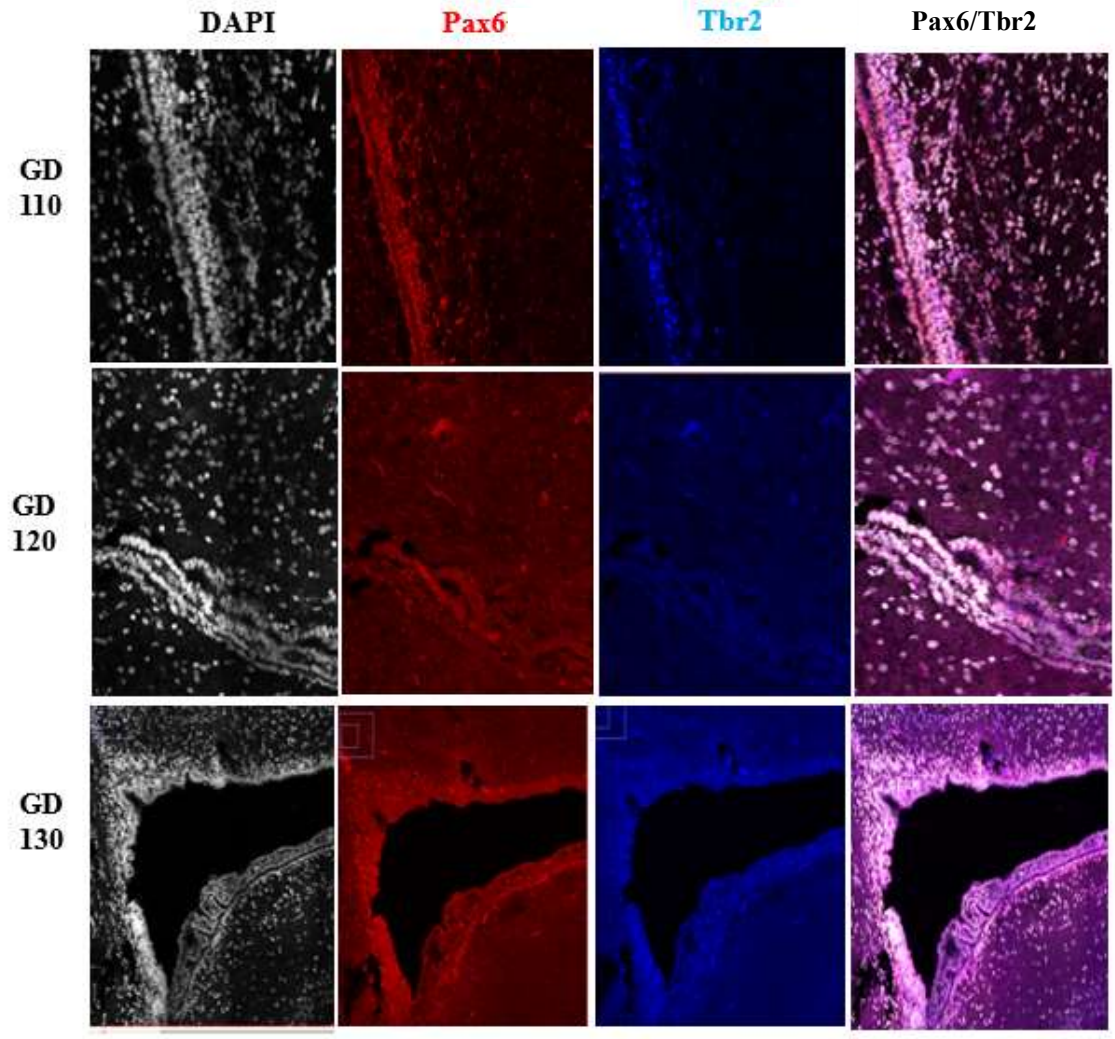

Figure 4.51: Expression of Pax6 and Tbr2 in prenatal brain of the AGCR at GD 110, GD 120 and GD 130

4.3.1.2 Timing of Deep and Upper Layer Formation in the developing AGCR Neocortex (Tbr1/DAPI)

Following the formation of the VZ and SVZ, neuronal migration and timing of the establishment of the deep layers (layers V to VI) and upper layers (II to IV) of the developing neocortex was investigated with Tbr1 biomarker. Results revealed that the establishment of these layers occurred in an "inside-out" manner with the layers V and VIbeing the first to be laid down and followed by layers II to IV.

At GD60, there was an emergence of the cortical plate with no clear delineation into deep and upper layers (Fig 4.52). However, a progressive increase in neuronal migrations (Tbr1+/DAPI) was noted from the SVZ into the destined deep layers of the developing neocortex from GD70, reaching its peak at GD120 (Fig 4.52). This neocortical expansion of the deep layer was further corroborated by the measurement of the thickness of the deep layer reaching its maximum at GD120 (Fig 4.52). Neuronal migrations into the destined upper layer of the neocortex, marked as Tbr1-/DAPI+ cells, progressed slowly but attained its maximum volume at about GD130 (Fig 4.53). This was further validated by the thickness of this layer reaching its greatest thickness at GD130 (Fig. 4.53).

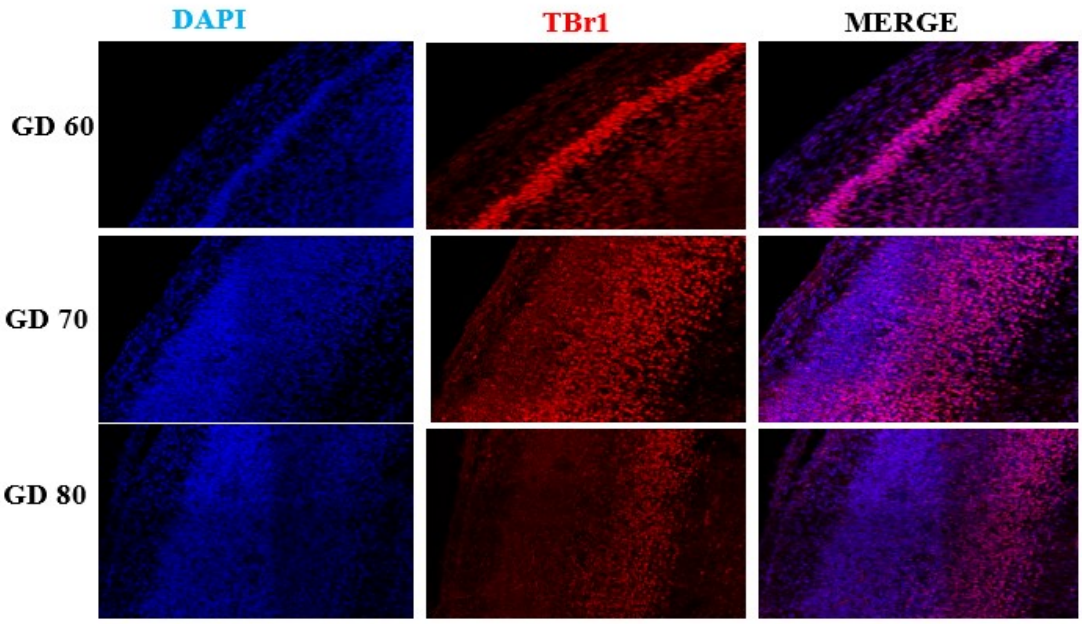

Figure 4.52: Tbr1 expression on the cortical zone of the prenatal brain of the AGCR at GD 60, GD 70 and GD 80

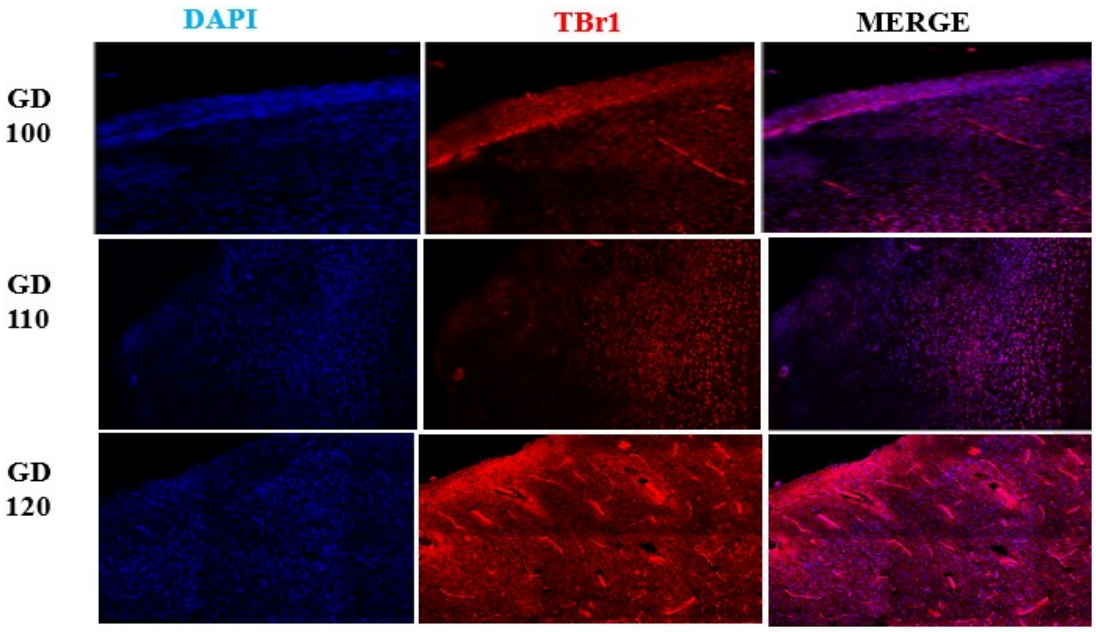

Figure 4.53: Tbr1 expression on the cortical zone of the prenatal brain of the AGCR at GD 100, GD 110 and GD 120

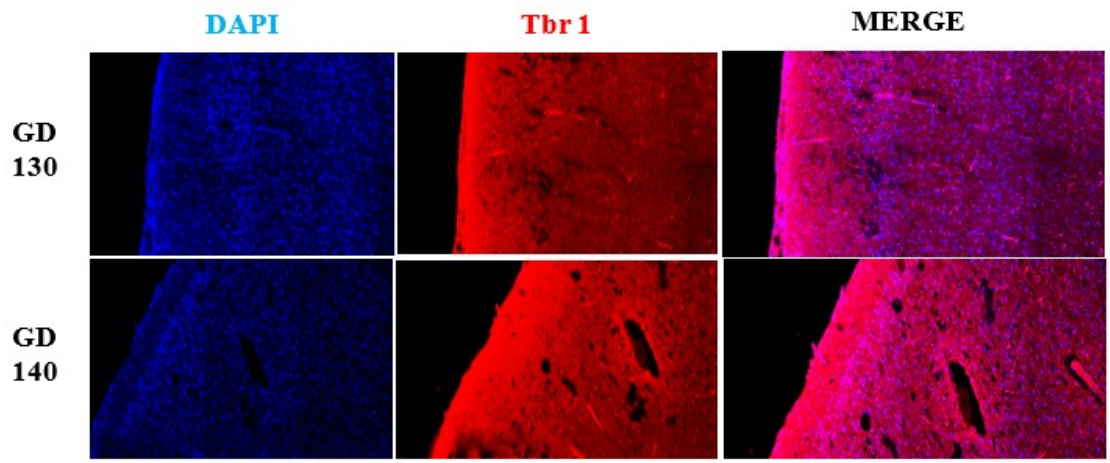

Figure 4.54: Tbr1 expression on the cortical zone of the prenatal brain of the AGCR at GD 130 and GD 140

4.3.1.3 Onset and Peak Period of Neuronal differentiation in the Prenatal AGCR Brain (MAP2/HuCD/NF)

With the establishment of the deep and upper layers of the neocortex characterized, it became necessary to define the period of neural circuitry assembling and network formation. This was identified as the time when the migrating neurons began to sprout dendrites and axonal processes. In the prenatal AGCR, the earliest time of neuronal differentiation was noted around GD70 at the deep layers only. This differentiation also progressed from the bottom of the cortical plate (layer VI) to the top of the plate (layer II). This differentiation appeared to be age dependent progressively increasing with gestation length until birth (Fig 4.55 and 4.56). A gradual transitioning of the IZ into the subcortical white matter tracts was noticed at GD100.

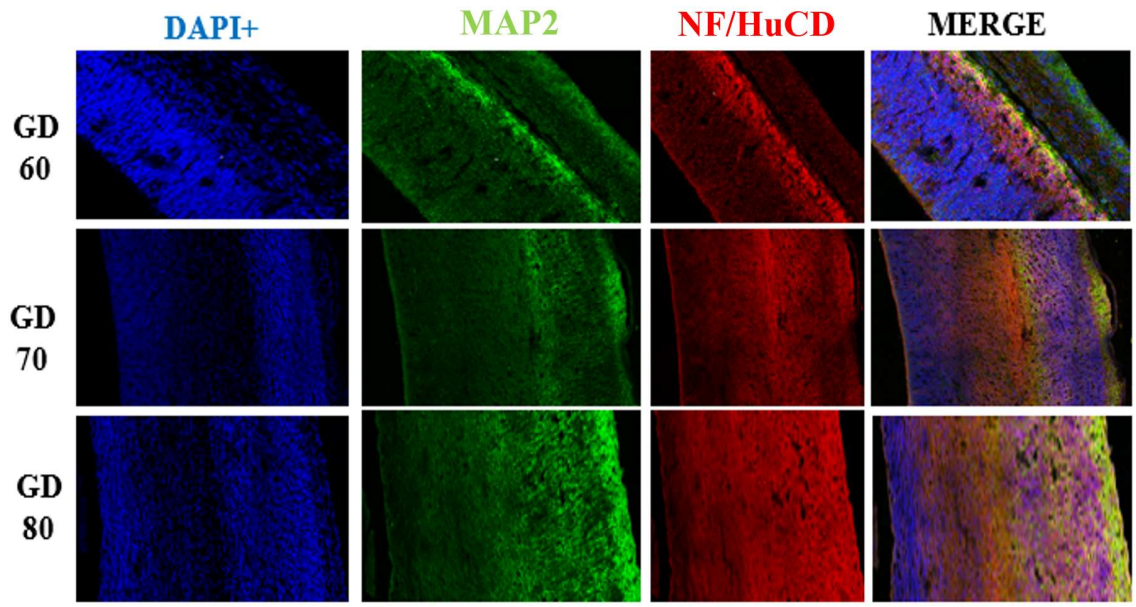

Figure 4.55: MAP and HuCD expression on the prenatal brain of the AGCR at GD 60, GD 70 and GD 80

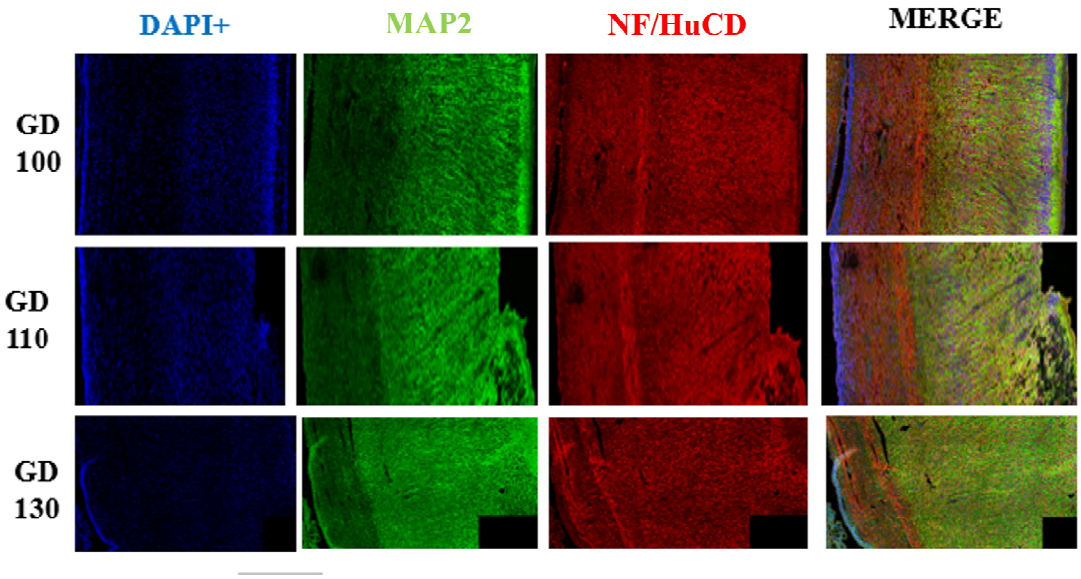

Figure 4.56: MAP and HuCD expression on the prenatal brain of the AGCR at GD100, GD110 and GD130

4.3.1.4 Gliogenesis Profiling in the Prenatal AGCR Brain

The window of precursor glial cell multiplication and differentiation from the VZ after the neurogenesis was defined and results given below.

4.3.1.4.1 Astrocyte Development and Differentiation (GFAP)

No positive immunosignalling was observed in the developing prenatal AGCR brain earlier than GD100 (Fig 4.57). By GD100, GFAP+ signalling was identified concentrated around the VZ and SVZ. These precursor astrocytic cells had no cytoplasmic processes (Fig 4.58). By GD110, a further differentiation was seen with radially oriented astrocytic process radiating from the VZ and also few tangentially oriented processes were also seen in the SVZ and intermediate zone (IZ) of the developing brain (Fig 4.58). The proliferation and differentiation of astrocytes reached its peak at GD130 (Fig 4.59).

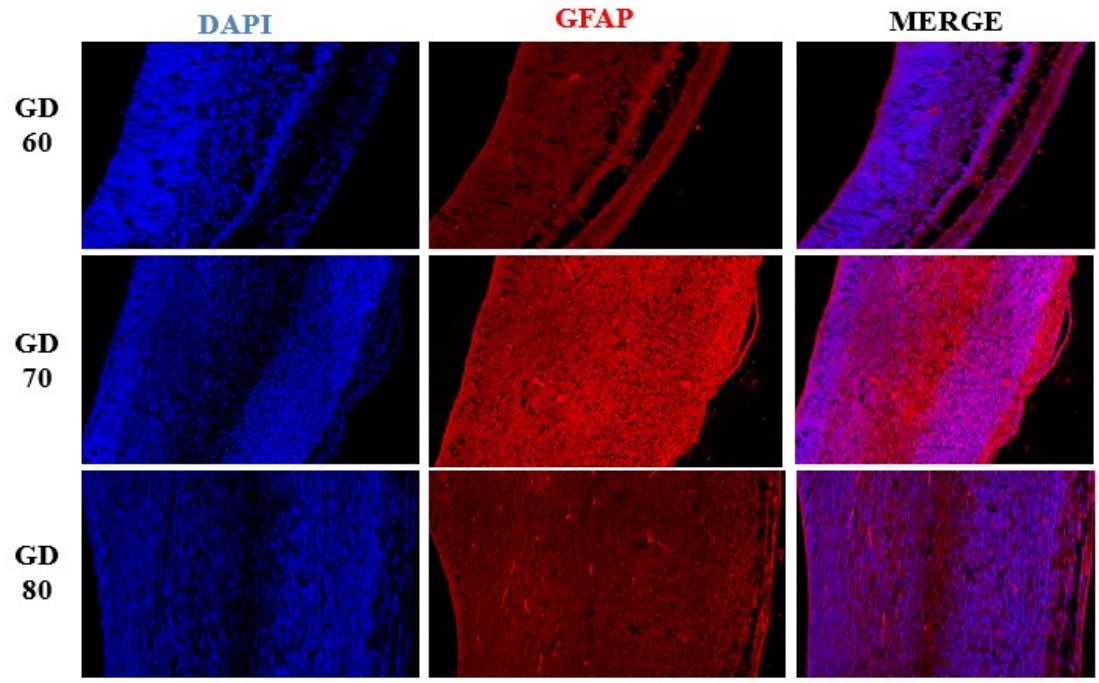

Figure 4.57: GFAP expression on the prenatal brain of the AGCR at GD 60, GD 70 and GD 80**.**

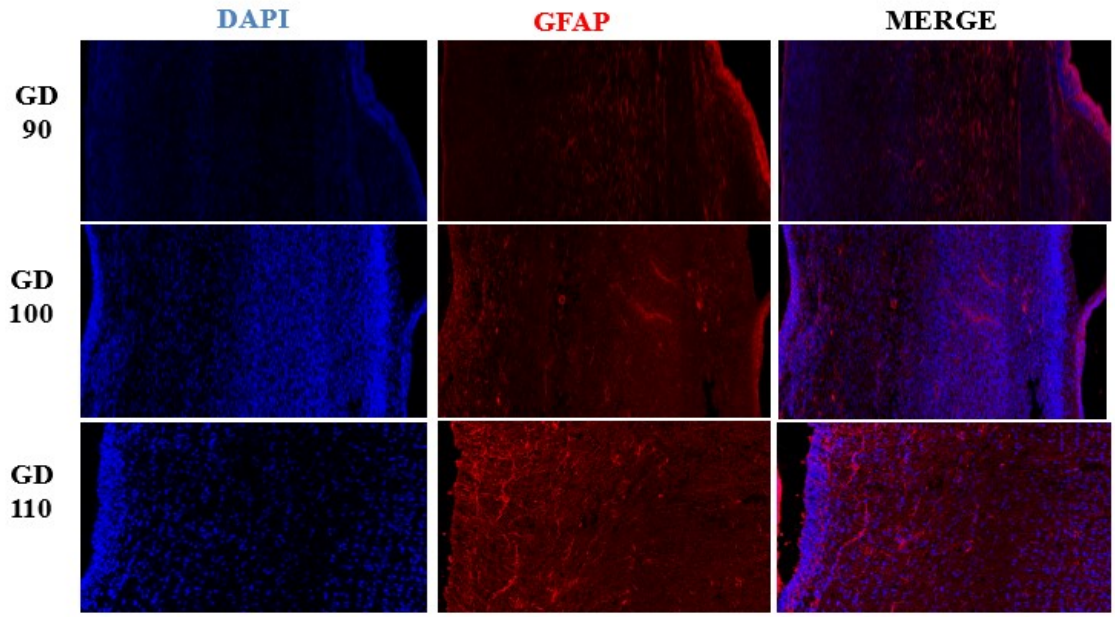

Figure 4.58: GFAP expression on the prenatal brain of the AGCR at GD 90, GD 100 and GD 110

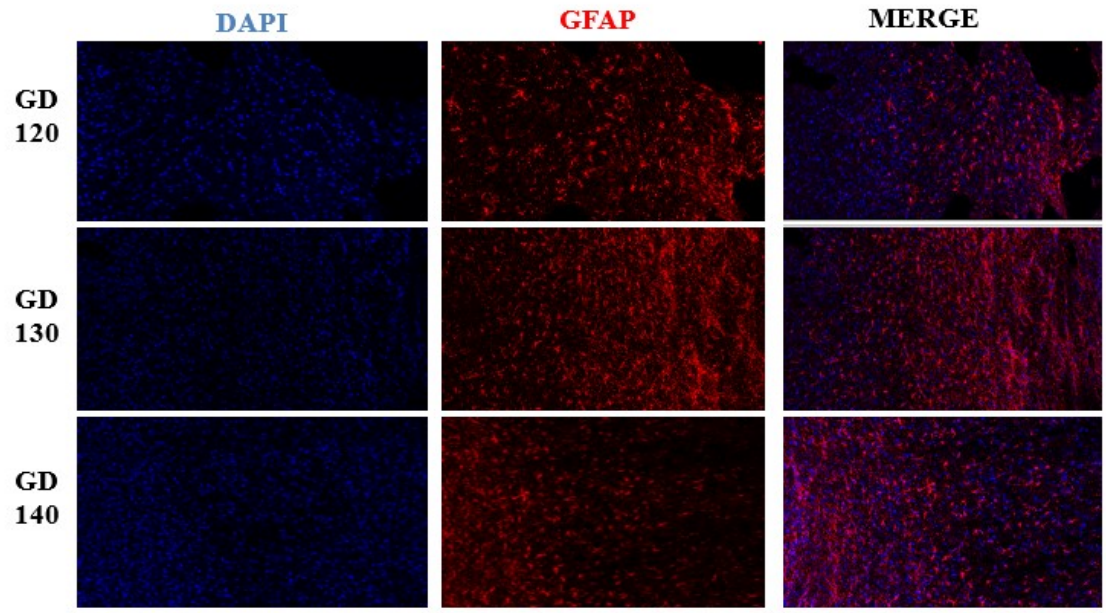

Figure 4.59: GFAP expression on the prenatal brain of the AGCR at GD 120, GD 130 and GD 140

4.3.1.4.2 Oligodendrogenesis (Olig2/Pax6)

Positive immunosignalling of Olig2 for oligodendrocyte progenitor cells (OPCs) around the SVZ by GD80 indicated the onset of oligodendrogenesis (Fig 4.60). The proliferation, differentiation and maturation of oligodendrocytes progressed with increasing gestation length spreading from the SVZ through the IZ/subcortical white matter layer into the deep and upper layers of the developing neocortex (Figs. 4.61 and 4.62).

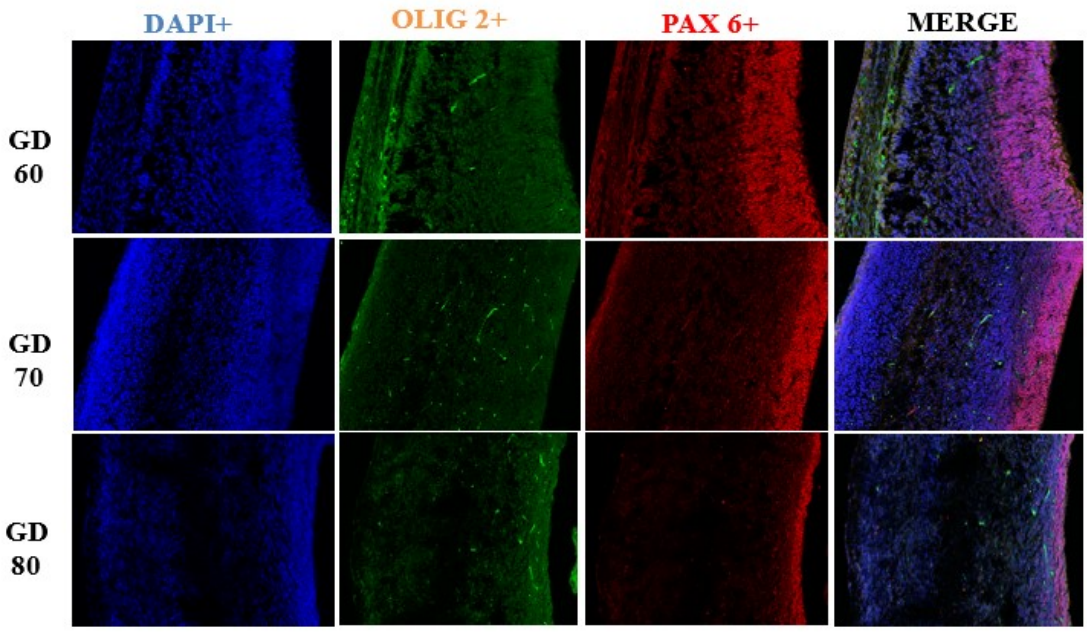

Figure 4.60: Olig2 and Pax6 expression on the prenatal brain of the AGCR at GD 60, GD 70 and GD 80

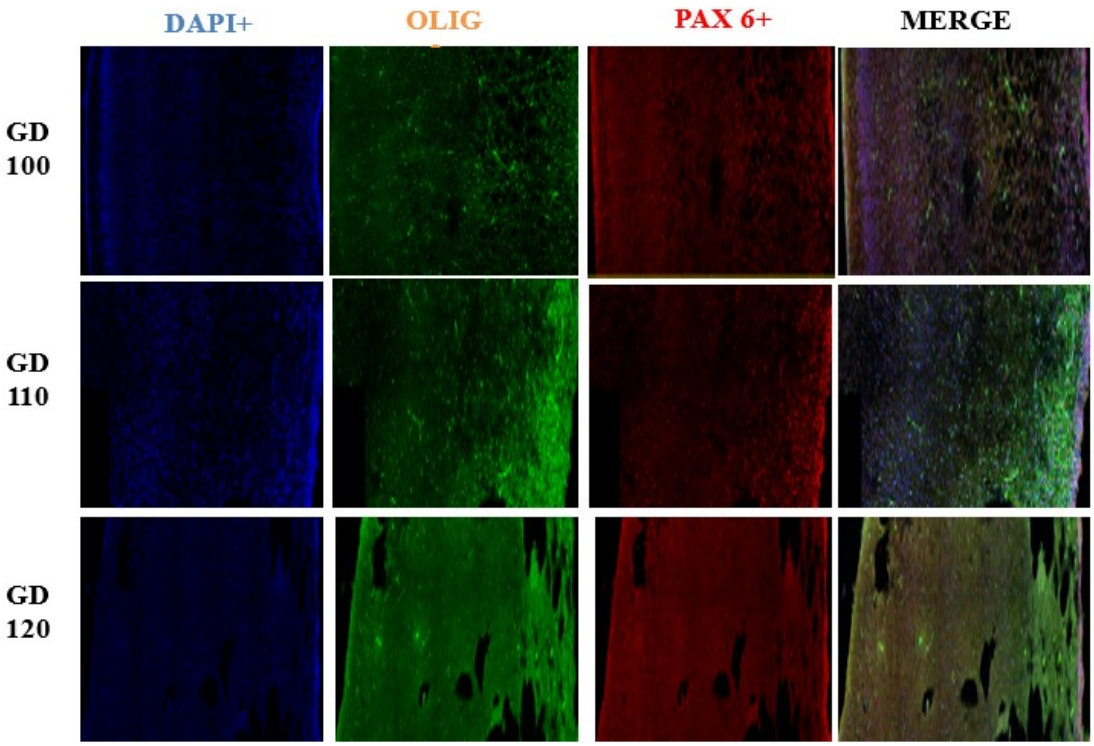

Figure 4.61: Olig2 and Pax6 expression on the prenatal brain of the AGCR at GD 100, GD 110 and GD 120

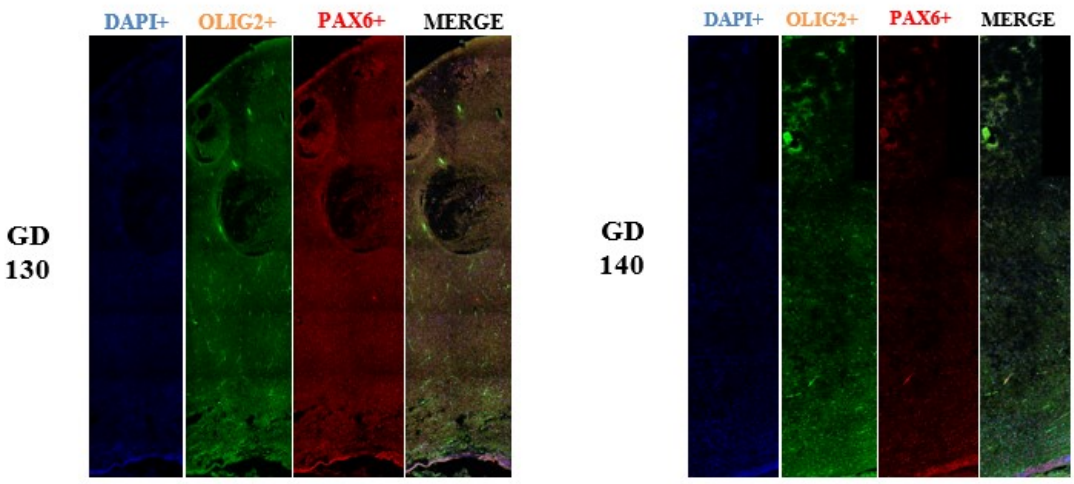

Figure 4.62: Olig2 and Pax6 expression on the prenatal brain of the AGCR at GD 130 and GD 140

4.3.1.5 Myelinogenesis (MBP/NF)

The period of the onset and duration of myelin sheath formation was investigated, having established the period of formation and proliferation of myelin-forming cells. Interestingly, although oligodendrogenesis had commenced at GD80 with subcortical white matter formation also noted at GD100, myelinogenesis was not noticed earlier than GD120. Myelin Basic Protein positive immunosignalling was first detected at the subcortical white matter. The myelination pattern seems to had progressed outwards toward the subplate zone of the neocortex with an intensification of MBP+ immunosignalling with increasing gestation days (Fig. 4.63).

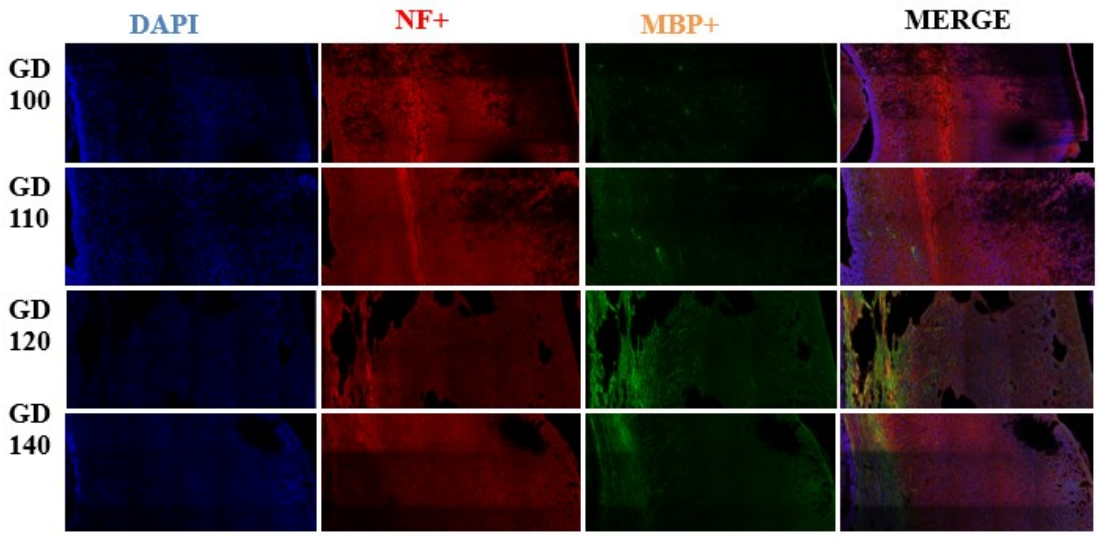

Figure 4.63: NF and MBP expression on the prenatal brain of the AGCR at GD 130 and GD 140

CHAPTER FIVE

5.0 DISCUSSION

5.1 Sonographic Features of Gestation in the Developing AGCR

This is the first study of sonographic evaluation of pregnancy in the AGCR. The sonographic features of gestational sac in the AGCR is similar to that reported for dogs (Luvoni and Grioni, 2000), and Agouti (Sousa *et al.,*2012). Part of the routine skin preparation for ultrasound examination is the shaving of the hair before application of ultrasound gel. The skin of the AGCR is furnished with individual thick spinous hairs which are sharp, pliable and pointed (Skinner and Chimimba, 2005). Thus, it is important to shave the hair on the ventral abdomen before gel application in order to ensure excellent image acquisition. Chemical restraint is necessary for the preparation process as the skin is delicate and easily gets stripped.

In this study, the gestational sac was the earliest observable sonographic evidence of pregnancy in the AGCR and was observed by GD20. Other features observed include embryonal sac from day 50 and foetal skeletal structures from GD100. This finding varied from that reported for Agouti in which gestational sac was first detected by day 14, embryonal sac by GD20 and foetus detected by GD55 (Sousa *et al.,*2012).The differences may be due to the longer gestational length in AGCR(150 days) compared with the 104 days reported for agouti and 59-72 days reported in guinea pigs (Fortes *et al.,* 2013; Hill, 2016).

The embryonal sac was first recognized at GD50. These embryonal sacs are easier to recognize sonographically than the gestational sac because they are bigger in size and

more anaechoic. Although early detection of pregnancy in AGCR is achievable by GD20, a confirmatory diagnosis can better be made around GD60 when both the presence of vaginal mucus plug and more easily detectable embryonal sac can be used.

Recognition of the foetal heart beat and foetal movement is useful in the assessment of foetal viability and to detect foetuses that are stressed. In the agouti, the foetal heart beat was detected by GD25, (Sousa *et al.,*2012). however, foetal heart beat and foetal movement were not detected in this study. This may probably be due to the agents (Ketamine and Xylazine) used to chemically restraint the AGCR. Both xylazine and ketamine have been reported to cross the placenta to cause foetal depression, although ketamine is reported to produce less depression than xylazine (Sumitra *et al.,*2004). In the sonographic detection of pregnancy in agouti, the animals were neither sedated nor anaesthetized.

This study confirms the reliability of B- mode ultrasound in the detection of pregnancy in the AGCR. Ultrasound examination can detect pregnancy as early as GD20, much earlier than the traditional detection of the vaginal mucus plug. However, it is better to perform detection of pregnancy around GD60 when sonographic detection of the embryonal sac and the presence of a vaginal plug can be better used to confirm pregnancy. The sonographic measurements obtained in this study will serve as baseline sonographic measurements during gestation in AGCR.

5.2 Developmental Horizons in the Developing AGCR

This work provides novel information on the developmental biology of the prenatal AGCR by characterizing well-defined developmental milestones across the entire period of gestation in this hystricomorphic rodent. These milestones include calvarium consistency, integument pigmentation, dental eruption, emergence and pattern of spread of the hairs, budding of limbs, development of sense organs and external sex organs. These developmental features were employed in the staging and aging of the AGCR adopting the Carnegie system - a standardized scale that illustrates a detailed sequence of morphogenetic attributes in the vertebrate embryo (O'Rahilly and Muller, 1987; Hill, 2016). Both Carnegie system, which do not go beyond the period of embryogenesis, and Štěrba ontogenetic system, whose scale encompasses a similar robust ontogenetic staging system that extends beyond period of embryonic development, spanning into the period of foetal development were used for staging of the prenatal AGCR (Štěrba, 1995). By adopting both systems, this work presents a robust benchmark reference for the AGCR embryos/foetuses using morphogenetic phenotypes, that can be utilized for aging and staging of the prenatal AGCR in future investigations.

From this study, male ano-genital distances were significantly higher than those of their female AGCR foetuses from day 80 till day 140 of gestation. Specifically, at day 140 of gestation the mean ano-genital distance of the male AGCR (10.78 ± 0.67mm) was approximately two-fold higher than the mean value of the female AGCR (4.97 ± 0.47mm). This agrees with what was reported by Opara (2010), where similar male-to-female ano-genital distance ratio was noted at parturition. Androgens have been implicated to influence the development of perineum and the caudal movement of the genital tubercles during the prenatal stage of development in rodents and humans

(Bowman *et al.,* 2003; Macleod *et al.,* 2010; Eisenberg *et al.,* 2011; Dean and Sharpe, 2013). Hence, this study does not only explain the contributory role of foetal androgen interaction in affecting the sex difference noted in prenatal AGCR ano-genital distance, it also posits that ano-genital distance can be used a reliable index for sex determination in this rodent.

The AGCR has a relatively long period of gestation of 150 days, divided into three trimesters (Opara, 2010). The first trimester starts from the day1 and ends at day 50 of gestation; second trimester spans from day 51 to day 100 of gestation while the third semester starts from day 101 of gestation till birth (Owusu *et al.,* 2010). It was noted from this study that the time of transition from the period of embryonic development to foetal development in the prenatal AGCR occurred during the late second trimester, specifically between day 80 and day 100 of gestation. This is however quite different from what has been reported in other precocial mammals such as in the sheep (which has a similar gestation period of about 150 days), pig and human, of which this transition was noted to have occurred during the late first trimester (Hill, 2019b; Sivachelvan *et al.,* 1996). This implies that the AGCR has a relatively shorter period of foetogenesis (measured in percentage of total gestation period) compared to that in the pig, sheep and human.

Much like in other precocial mammals, the AGCR have their bodies covered with hairs and eyes wide opened at birth (Opara, 2010). Intriguingly, the development of the eyelid (evaluated as the interval between the fusion of the eyelids and their separation) was noted to have occurred earlier in the prenatal AGCR spanning about 20% of the total length of gestation (30 of 150 days) unlike what was reported in humans (30% of the total length of gestation; 84 of 280 days) (Tawfik*et al.,* 2016) and

in the sheep spanning about 33% of the total length of gestation (50 of 150days) (Sivachelvan *et al.,* 1996).Furthermore, time taken for the development of hairs (evaluated as the time interval from folliculogenesis to the emergence of body hairs) appears to be shorter in the prenatal AGCR taking about 20 days (13% of total length of gestation) as against observations noted in the humans lasting for about 48 days (18% of total length of gestation), and in the sheep, it takes 43 days (about 29% of the total gestation period) (Lyne and Hollis, 1972; Bolla *et al.,* 1991; Sivachelvan *et al.,* 1996; Vogt *et al.,* 2008; Hill, 2019c). Altogether, these findings suggest that distinct developmental milestones recorded including the development of the eyelids and hairs may have progressed at a more rapid rate in the AGCR foetus in contrast with other mammals, case in point humans and sheep, thus making up for the relative brief period of foetogenesis. Additional investigation using broader scopes of developmental attributes and milestones and also a wider scale of gross and histological techniques is hereby recommended so as to explore and unveil more depths on specific developmental processes and timelines in the prenatal development of the AGCR.

Using gross examination, the earliest indication of an embryo was observed at day 50 of gestation with embryogenesis ending around late second trimester (about day 90 of gestation). In addition, this study has shown that the relative period of development of the embryo (calculated as a percentage of the entire period of gestation) in the AGCR was protracted as opposed to its precocial hystricognath rodents such as the guinea pig, European hare, and agouti. This prolonged period of embryonic development in the AGCR is indicative of a reproductive diapause – a delay in development that may take place between (i) mating and fertilization, (ii) fertilization and nidation and/or (iii) post-nidation (Orr, 2012). This phenomenon has been reported in some mammals including rodents (Roellig *et al.,* 2011; Orr, 2012; Orr and Zuk, 2014).

Delayed fertilization often encourages cryptic female choice behaviours and also enhances sperm competition, while delayed nidation promotes zygote selection or rejection resulting in embryonic resorption. In delayed development, on the other hand, there is an extension in the length of days an embryo/foetus spends in the uterus possibly enabling abortion or embryonic resorption (Bernard and Cumming, 1997). Adu and Yeboah (2000) and Owusu *et al.,* (2010) have previously documented that the rate of embryonic resorption is at its peak during the first trimester (GD1-50).

Interestingly, the rate of embryonic resorption in the AGCR is known to be notably higher compared to other mammals in which reproductive diapause have not been reported. For instance, in the guinea embryonic resorption rate is put at 7.2% (Hoar, 2005). The attending implication of this high rate of embryonic resorption in the AGCR may be targeted towards choice selection of specific blastocysts/embryos, thus prolonging the interval (i) between fertilization and nidation, and/or (ii) post-nidation (Owusu *et al.,* 2010). The latter tends to influence the size of the litter at birth and sexual selection after mating (Orr and Zuk, 2014). Hence, the male bias in sex ratio recorded in this work is suggestive of post-mating sex selection activity in the AGCR. Thus, this lends more credence to the notion that the type of reproductive diapause exhibited by the AGCR is more of a delayed nidation. More studies will be necessary to better characterize and confirm the exact kind of delayed reproduction in the AGCR and to elucidate if the type of delay in this rodent is unique to it or on the contrary a general occurrence in the precocial hystricomorph mammal. It is to be noted that the long gestation period and the required housing necessary for breeding and mating the domesticated AGCR posed some limitations to this work as the work had to be carried out on the farm where they were sourced from.

This work therefore has provided novel developmental reference data on the prenatal developmental biology of the AGCR, a native rodent of Africa. By utilizing external developmental attributes, a robust scale for the AGCR embryos/foetuses was generated that will be useful for aging, staging and estimation of the sex in future works. Furthermore, this study reported the first proof of evidence of a reproductive diapause in the AGCR.

5.3 Morphological Characterization of the Developing Prenatal AGCR Brains

5.3.1 Brain Morphology

The relationship of the biology of evolution and development illustrates that the schedule and series of early occurrencesin the development of the brain are notably conserved across mammalian species (Finlay and Darlington, 1995; Clancy*et al.,* 2007). Modes of development within the altricial-precocial context have been noted to potentially regulate definitive changes in the processes leading to the development of the brain (Charvet and Striedter, 2011). Therefore, there are variations in the timing of the maturations processes during the development of the brain in precocial and altricial animal. Specifically, precocials are noted to speed up certain phases of their brain development and maturation relative to altricials.

Altricials are usually born somatically immature, blind, hairless and with under developed nervous system largely at birth whereas precocials are born with eyes opened, with relatively well-developed body parts (e.g. formed furs, eye opened) and relatively matured nervous system (Sanchez-Villagra and Sultan, 2002; McGuire and Bernis, 2008). The AGCR belongs to the precocial spectrum, and from this study, the prenatal brain at GD140 appeared grossly gyrencephalic with most neural structures already established prior to birth.

The earliest time point in gestation where gross features of the primitive brain could be well appreciated for gross description in the prenatal AGCR was between late first trimester and early second trimester (GD 50-60). This period is suggestive of specific changes in neural patterning that will ultimately affect the transformation of the overall shape of the developing embryo (Stiles and Jernigan, 2010). The neural patterning that occurs during embryogenesis does not only provide a primordial layout of the ultimate nervous system architecture that marks the onset of a prolonged series of neural arrangement but also set the stage for later neural developments (Sur and Rubenstein, 2005).

No grossly observable brain development was observed until about 28% of the total gestation length (20 days' post copulation) in the guinea pig (Silva *et al.,* 2016). From this study, gross brain development was observed in the developing AGCR at a later time (GD50 - 33% of the total gestation length). This period also coincided with the emergence of the primary brain vesicles (prosencephalon, mesencephalon and rhombencephalon). Further differentiation of the primary brain vesicles to secondary brain vesicles was noted at GD60 in the AGCR which marked the beginning of the second trimester. This is consistent with the developmental trajectory reported in domestic mammals (Sinowatz, 2010; Ferreira *et al.,* 2018).

The most remarkable developmental features in the prenatal AGCR brain was noted between the mid and late second trimester (GD80 to GD100; about 60% of total gestation length). Some of these gross features include the emergence of the colliculi on the mesencephalon, differentiation of the cerebellar plate into the vermis and lateral lobes, emergence of the piriform lobes and mammillary bodies as well as the emergence of the cerebral peduncles and primordial pons amongst others. Silva *et al.,*

(2016) reported peak gross brain development in the guinea pig at day 45 post copulation (about 62.5% of the total gestation length).

First eye-opening, amongst all other vital traits in mammalian life history, was noted as the best predictor of the state of cerebellar development and a compelling relationship between first eye-opening and development of the cerebellum has been reported (Sanchez-Villagra and Sultan, 2002). Indeed, Stein and Glickstein (1992) pointed that the strong relationship between eye opening and development of the cerebellum is not surprising taking in account the important function of the cerebellum in visual sensorimotor control. This strong relationship has been correlated with locomotion performance as spatial navigation is controlled by visual perception. Taking into consideration that fine motor coordination is necessary in the early phase of life of precocials, then it comes as no surprise that a comparatively well-developed cerebellum is essential at birth (Nacher *et al.,* 2000). This strongly supports the observations made in this study as lobation patterning of the cerebellum was the last striking gross developmental feature noticed in the prenatal AGCR brain. This was observed at mid third trimester (GD130) after which no other significant development were subsequently observed. This pattern was also similar to what was reported in the guinea pig. However, this seemed to have happened relatively earlier in the latter where it occurred not later than day 50 post copulation (about 69% of the total gestation period) compared to GD130 in the AGCR (about 86% of the total gestation period). While the emergence and pattern of gross developmental features in the AGCR brain is similar to that of its precocial comparative (guinea pig), the timing of these events appeared to be slightly prolonged in the AGCR.

5.3.2 Brain Morphometry

The progressive increase in absolute brain weight with increasing gestation length and the decrease in relative brain weight values with advancing gestation age observed in the developing AGCR is typical of mammalian species. The decrease in relative brain weight is attributed to the early brain growth relative to that of the body (Dobbing and Sands, 1970). Thirty-four percent (34%) of the variability observed in the prenatal AGCR brain height can be explained by the gestation length during development. Also, seventy-three percent (73%) and seventy-six percent (76%) of the variability observed in the brain length and width respectively can be explained only by the gestation length of the AGCR.

Precocial animals, such as the guinea pigs and sheep, are usually regarded as prenatal brain developer (McIntosh *et al.,* 2008). Two notable brain growth phases have been identified in their brain development. This biphasic phenomenon suggests a period of proliferation of neuroblast during the early phase and proliferation of glial in the later stage of development. Consequently, these rapid growth spurts signify the most susceptible windows for developmental perturbations (Clancy *et al.,* 2007). In the sheep, for instance, this biphasic growth occurs from 40 to 80 days (for neuronal multiplication) and from 95 to 130 days (for glial multiplication) (McIntosh *et al.,* 2008). From this study, the biphasic growth occurred at between GD80-GD100 (for peak neuronal proliferation) and between GD120 and GD130 (for glial proliferation).

This work presents detailed chronology of the morphological features of the developing brain of the prenatal AGCR as a successive and conservative events. It serves to provides a baseline frame for evaluating and defining normality in the developing prenatal AGCR brain; to highlight significant marginal deviations, and also to create criteria for the assessment of pathologic/teratogenic changes. Thus, this study

provides a comprehensive foundation for later comparison with pathologic states, may assist in defining the scale of anomaly, and to define probable windows of susceptibility. The AGCR is also being advocatedto be suited as a model for neurodevelopmental investigations.

5.4 Corticogenesis Profiling of the Developing Prenatal AGCR Brain

5.4.1 Neurogenesis

Prior to neurogenesis, the neural tube is composed of a monolayer of neuroepithelial cells (NECs) that constitute the neural epithelium. During their cell cycle, nuclei of the NECs rove from top to bottom along the apical-basal axis thus giving the neural epithelium a pseudostratified appearance (Huttner and Brand, 1997; Wodarz and Huttner, 2003). The neuroepithelium in the prenatal AGCR brain was observed by GD50 as NECs consisting of pure NSCs (Pax6+/Tbr2-).

The germinal neuroepithelium or VZ is a temporaryembryonic layer of tissue consisting of NSCs, predominantly radial glia cells of the CNS and their derivative NPCs which will divide symmetrically and asymmetrically producing the cellular component of the mature neural system thus contributing to neurogenesis, gliogenesis and ependymal cell formation (Noctor *et al.,* 2001; Götz and Huttner, 2005; Rakic, 2009; Girard *et al.,* 2016). From this study, the proliferation of NSCs in the germinal VZ had reached its peak by GD60, with this zone also attaining its maximum thickness. By GD130, the multi-layered VZ had been transformed into a single layered ependymal zone. This pattern of neurogenesis is comparable to reports in the guinea pig.

The SVZ, a complementary proliferative layer, is next to the VZ and comprises of a pool of intermediate neuronal progenitors (NPCs) which are derivatives of the NSCs

that ultimately divide and differentiate into neurons that are unable to undergo mitosis again(Noctor *et al.,* 2004; Hevner and Haydar, 2012). Peak periods of neurogenesis represent the time point at which the SVZ reaches its maximum thickness with the highest NPCs (Pax6-/Tbr2+) cell populations, more specifically the basal progenitor cells (Florio and Huttner, 2014). In the AGCR, the SVZ was identified by GD60 and reached its maximum thickness by GD80. This time point also marked the peak stage of neurogenesis in the prenatal AGCR brain where NPC populations (Pax6+/Tbr2-) were most abundant.

The duration of the neurogenic period has been noted as one of the chief determinants which defines the outputs of neurons and influences interspecies variation. Delayed onset of neurogenesis allows for a greater expansion of NEC pool prior to commencement of neurogenesis. Furthermore, prolonged period of neurogenesis allows for expansion of the NPCs pool, most notably the basal radial glia thus increasing neuronal output. Together, they contribute significantly to the expansion of the neocortex (Florio and Huttner, 2014). From this study, the onset of neurogenesis was delayed occurring between the later stages of the first trimester and early second trimester (GD50 - GD60), a much later time in development as against what is observed in typical rodents (Rakic, 1995). More so, the duration of neurogenesis in the prenatal AGCR was much longer, spanning about 35% of the entire gestation length (50-60 days) when compared to the 6-day neurogenic period in the mice (Kornack and Rakic, 1998; Florio and Huttner, 2014). This differences probably accounts for a more expanded and gyrencephalic neocortex in the AGCR compared to the lissencephalic neocortex in the mice.

5.4.2 Deep and Upper Layer Formation

In mammals, the stratified layout of the neocortex is a methodical sequelae of the migration of newborn neurons following their "birthdays" (Gilmore and Herrup, 1997). For this to occur, these newborn neurons must migrate radially and tangentially from the VZ to their final destination where neural connectivity will be established in the unfolding neocortex. They do this from within outwards by circumventing previously established neuronal layers to get to the summit of the CP (Super *et al.,* 2000; Toma *et al.,* 2014). The establishment of the deep and upper layers of the developing neocortex followed a similar pattern, with the deep layers established first by GD120 while the upper layers were fully established by GD130. Both the deep and upper layers of the neocortex reached their maximum thickness at these time points.

5.4.3 Neuronal differentiation in the developing AGCR Neocortex

Axonal and dendritic sprouting are meticulously-controlled programmed events which occur after the completion of neuronal migration in order to ensure proper neural circuit assembly and connectivity during development (Gilbert, 2000a; Hoshiba *et al.,* 2016). Although neuronal differentiation had begun by mid second trimester and progressed increasingly until birth in the prenatal AGCR brain, intense signalling for dendritic and axonal markers (MAP2 and NF respectively) was not seen until around GD130. This agrees with what was reported by Hoshiba *et al.,* (2016), who noted that new born neurons express Sox11 which inhibits dendritic morphogenesis while conversely promoting neuronal migration to the cortical plate of the developing neocortex.

5.4.4 Gliogenesis Profiling in the Prenatal AGCR Brain

Timed genesis (sequential generation) of the different nervous cell populations is a highly conserved and programmed event in brain development with neurogenesis preceding gliogenesis (Qian *et al.,* 2000; Shen *et al.,* 2006). This allows for early establishment of brain neural circuitry, which is followed by a matching of glial cell populations and of their spatiotemporal locations to the already laid down neural connections (Miller and Gauthier, 2007). This was consistent with the timeline of nervous development observed in the prenatal AGCR. From this work, gliogenesis began later after neurogenesis; with peak window of the former occurring between early to mid-third trimester (GD110-GD130) compared to peak window of the latter occurring between mid to late second trimester (GD80-GD100).

A delicate interplay of both intrinsic developmental biasing of multipotent NSCs and extrinsic signalling cues has been noted to be pivotal to the timing of this "neurogenic-to-gliogenic" switch (Miller and Gauthier, 2007; Alfonso, 2017). So far three different extrinsic cues namely cardiotrophin-1 (CT-1), bone morphogenetic proteins (BMPs), and Notch ligands are already identified to act together in initiating the gliogenic switch via the CT-1/gp130/JAK/STAT pathway. Specifically, CT-1, a gliogenic cytokine released by the first-born cell lineage (neurons) attaches to LIFRβ co-receptors and gp130 which subsequently signals JAKs to activate STAT3. Following this, STAT3 binds with the Smads (a subsequent productof activated BMP-receptors) and p300/CBP. This Smad:p300/CBP:STAT complex transactivates gliogenic genes (*gfap* and *s100β*), thus ensuring the neurogenic-to-gliogenic switch (Ernst and Jenkins, 2004; Chen *et al.,* 2004;Barnabe-Heider *et al.,* 2005; Miller and Gauthier, 2007). These mechanisms probably explain the timed genesis of glia cells (specifically astrocytes and oligodendrocytes) in the developing prenatal AGCR brain.Using astrocytic and oligodendrocyte progenitor biomarkers (GFAP and Olig2 respectively),

the timing and progression of astrocytogenesis and oligodendrogenesis in the prenatal AGCR brain were mapped with the former preceding the latter.

5.4.5 Myelinogenesis

Precocial animals give birth to their pups with some level of motor coordination already established at birth. This motor coordination has been observed in new born AGCR pups being noted to follow their mother within 32-40 minutes after their birth (Addo, 2002; Opara, 2010). This motor coordination indicates that some degree of myelination may have begun prior to their birth. Although oligodendrocyte progenitor cell proliferation had started by GD80, myelinogenesis did not start earlier than GD120. The timing differential observed between the onset of oligodendrogenesis and myelinogenesis is considered necessary as the axonal infrastructure needed to be myelinated must have been first established.

Furthermore, this timing differential also reveals the time course of differentiation and maturation of oligodendrocyte precursor cells to mature oligodendrocytes (between GD80-GD120) in the prenatal AGCR brain. The successive sequences of these developments in connection to the time of parturition is consistent with the precocial timeline of development of the central nervous system in the guinea pig. Dobbing and Sands (1970) reported that most major brain developmental events in the developing guinea pig brain predate myelinogenesis; with appearance of the earliest myelin very close to birth, at day 63 of gestation. This time point represents about 95% of the total gestation length in the guinea pig. However, myelinogenesis started relatively much earlier in the prenatal AGCR at GD120 (80% of the total AGCR gestation).

5.5 Conclusion

In conclusion, this work provides a comprehensive map of the sonographic and morphogenetic developmental features in the indigenous prenatal AGCR. It also chronicles the onset and duration of the development and differentiation of neuronal and non-neuronal cell populations in the developing neocortex of the precocial prenatal AGCR. Collectively, this work deepens our understanding of the embryology and biology of the AGCR. It will promote and boost reproductive and production practices, and conversation of AGCR. It has also enriched our knowledge on the biodiversity and phylogeny of this hystricomorph rodent and its suitability as a research model for neurodevelopmental studies.

5.6 Contribution to Knowledge

1. This work has provided sonographic evaluation of pregnancy in the AGCR with baseline sonographic parameters that would be useful for pregnancy detection and pregnancy estimation in this rodent.
2. It has also generated a comprehensive scale for ontogenetic mapping of AGCR embryos/foetuses coupled with a more reliable predictive age estimation formula that will be useful for staging, ageing and sex estimation in future studies.
3. This study has reported the first proof of evidence of reproductive delay in the AGCR.
4. From this work, the time point of proliferation of pure neural stem cell populations in the prenatal AGCR brain has been established and this would be useful for future neural stem culture studies.
5. This work has provided a detailed profiling of the genesis and peak periods of neurogenesis, neuronal differentiation, gliogenesis and myelinogenesis in the prenatal brain of the AGCR. This is the first comprehensive study on the corticogenesis profile in an indigenous precocial African rodent.

REFERENCES

Addo, P., (2002). Detection of mating, pregnancy and imminent parturition in the grasscutter (*Thryonomys swinderianus*). *Livestock Research for Rural Development, 14*(4), pp.8-13.

Addo, P., Dodoo, A., Adjei, S. and Awumbila B. (2002). Determination of the ovulatory mechanism of the grasscutter (Thryonomys swinderianus). Animal Reproduction Science, 71(1-2), pp.125-137.

Addo, P.G. Awumbila, B., Awotwi, E. and Ankrah, N.A. (2007). Comparative characterization of the estrous cycles of the grasscutter (*Thryonomys swinderianus*) and the guinea pig (*Cavia porcellus*) by the hystricomorph vaginal membrane perforation phenomenon. Livestock Research for Rural Development, 19(5). Retrieved January 9, 2019 from http://www.lrrd.org/lrrd19/5/addo19063.htm

Adebayo, A.O., Akinloye, A.K., Olurode, S.A., Anise, E.O. and Oke, B.O., (2011). The structure of the penis with the associated baculum in the male greater cane rat (*Thryonomys swinderianus*). *Folia Morphologica, 70*(3), pp.197-203.

Adekola, A.G. and Ogunsola, D.S., (2009). Determinants of Productivity Level of Commercial Grasscutter Farming in Oyo State. *Proceedings of the International Conference on Global Food Crisis, Owerri, Nigeria,* pp.15-21.

Adu, E.K. and Yeboah, S., (2000). The efficacy of vaginal plug formation after mating for pregnancy diagnosis and embryonic resorption in utero in the greater cane rat (*Thryonomys swinderianus*, Temminck). *Tropical Animal Health and Production, 32*(1), pp.1-10.

Adu, E.K. and Yeboah, S., (2003). On the use of the perineal stain as an index of sexual maturity and breeding condition in the male greater cane rat (*Thryonomys swinderianus*, Temminck). *Tropical Animal Health and Production, 35*(5), pp.433-439.

Adu, E.K., (1999). Grasscutter Farming: A Manual for Beginners. Institute for scientific and Technological information - Council for scientific and industrial research, Accra, Ghana.

Adu, E.K., Asafu-Adjaye, A., Hagan, B.A. and Nyameasan, J.K., (2017). The grasscutter: an untapped resource of Africa's grasslands. *Livestock Research for Rural Development, 29*(3). Article #47. Retrieved July 12, 2019, from http://www.lrrd29/3/jnya29047.html

Adu, E.K., Wallace, P.A. and Ocloo, T.O. (2002). Efficacy of sex determination in the greater cane rat (*Thryonomys swinderianus*, Temminck). *Tropical Animal Health and Production, 34*(1), pp.27-33

Ajayi, S.S. and Tewe, O.O., (1980). Food preferences and carcass composition of the grasscutter (*Thryonomys swinderianus*) in Captivity. *Africa Journal of Ecology*, *18*(2-3), pp.133-140.

Ajayi, S.S., (1971). Wildlife as a source of protein in Nigeria: Some priorities for development. *The Nigerian Field, 36*, pp.115-127.

Akpan, M.O., Samuel, O.M. and Emikpe, B.O., (2018). Regional skin histomorphology in adult greater cane rats (*Thryonomys swinderianus*): A pilot study. *International Journal of Veterinary Science and Medicine, 6*(2), pp.219-226.

Albert, M. and Huttner, W.B., (2018). Epigenetic and Transcriptional Pre-patterning-An Emerging Theme in Cortical Neurogenesis. *Frontiers in Neuroscience, 12*, pp.359. doi:10.3389/fnins.2018.00359

Alfonso, A., (2017). Neurogenesis as a Factor in the Functional Plasticity of the Nervous System. Chapter 24, In: Conn's Translational Neuroscience, pp.545-552. Edited by: P. MichEL Conn. Academic Press.

Antypa, M., Faux, C., Eichele, G., Parnavelas, J.G. and Andrews, W.D., (2011). Differential gene expression in migratory streams of cortical interneurons. *European Journal of Neuroscience, 34*(10), pp.1584-1594.

Asibey, E.O.A. and Addo, P.G., (2000). The Grasscutter: A Promising Animal for Meat Production. In: African Perspective. Practices and Policies Supporting Sustainable Development. Turnham D. (Ed.). Weaver press, Zimbabwe pp.46.

Asibey, E.O.A., (1974). The Grasscutter (*Thryonomys swinderianus,* Temminck) in Ghana. *Symposia of the Zoological Society of London, 34*, pp.161-170.

Assogbadjo, A.E., Codjia, J.T.C., Sinsin, B., Ekue, M.R.M. and Mensah, G.A., (2005). Importance of rodents as a human food source in Benin. *Belgium Journal of Zoology, 135*, pp.11-15.

Attakumah, M.Y.B., (2013). Breeding grasscutter: sequencing its genome to combat its aggressiveness. Accessed online from http://modernghana.com/news/471539/1/breeding-grasscutter-sequencing. Accessed: 12/12/2015.

AU-IBAR., (2016). (African Union Intra-African Bureau for Animal Resources): Grasscutter (*Thryonomys swinderianus*). http://www.au-ibar.org/2012-10-01-

13-08-42/features/series/know-your-animals-series/grasscutter-thryonomys-swinderianus

Auzel, P. and Wilkie, D., (2000). Wildlife use in northern Congo: hunting in a commercial logging concession. Hunting for sustainability in tropical forests. *Columbia University Press, New York*, pp.413-426.

Barnabe´-Heider, F., Wasylnka, J.A., Fernandes, K.J., Porsche, C., Sendtner, M., Kaplan, D.R. and Miller, F.D., (2005). Evidence that embryonic neurons regulate the onset of cortical gliogenesis via cardiotrophin-1. *Neuron 48,* pp.253-265.

Bear, M.F., Connors, B.W. and Paradiso, M.A., (2001). Neuroscience: Exploring the Brain. Chapter 1: The Structure of the Nervous System. 2nd Edition. Lippincott Williams and Wilkins. Pp.170-188.

Beccaglia, M. and Luvoni, G.C., (2006). Comparison of the accuracy of two ultrasonographic measurements in predicting the parturition date in the bitch. *Journal of Small Animal Practice, 47*(11), pp.670-673.

Behan, M., Steinhacker, K., Jeffrey-Borger, S. and Meredith, M.A., (2002). Chemoarchitecture of GABAergic neurones in the ferret superior colliculus. *Journal of Comparative Neurology, 452*, pp.334-359.

Bernard, R.T.F. and Cumming, G.S., (1997). African bats: Evolution of reproductive patterns and delays. *Quarterly Review of Biology, 72*(3), pp.253-274.

Bhatnagar, M.C. and Bansal, G., (2008). Columbia livia. In: *Chordate,* Krishna Prakashan Media (P) Ltd., India, pp.327-380.

Blanco, G.P., Arias, O.D. and Gobello, C., (2008). Doppler ultrasound in canine pregnancy. *Journal of Ultrasound Medicine, 27*(12), pp.1745-1750.

Bloom, D.E., (2011). 7 Billion and Counting. *Science, 333,* pp.562-569.

Bolla, M.M., Jasmin, J.R., Monteil, R.A. and Loubiere, R., (1991). Embryology of the hair follicle. *Early Human Development, 26*(3), pp.159-166.

Bourrat, F. and Sotelo, C., (1988). Migratory pathways and neuritic differentiation of inferior olivary neurons in the rat embryo; Axonal tracing study using the in vitro slab technique. *Developmental Brain Research, 39*, pp.19-37.

Bowman, C.J., Bowman, N.J., Barlow, K.J., Turner, D.G. and Wallace, P.M., (2003). Effects of in utero exposure to finasteride on androgen-dependent reproductive development in the male rat. *Toxicological sciences, 74*(2), pp.393-406.

Byanet, O., Dzenda, T. and Sulaiman, M.H., (2014). Dimensional sex differences in the cerebellum of the African giant pouched rat (*Cricetomys gambianus* – waterhouse, 1840). *International Journal of Biosciences, 5*, pp.1-10.

Byanet, O., Ojo, S.A. and Onyeanusi, B.I., (2012). Gross anatomical organization of the cerebellum of the grasscutter (*Thryonomys swinderianus*-Temminck, 1827). *Annals of Biological Research, 3*, pp.2755-2762.

Byanet, O., Samuel, O.A., Barth, O.I. and Jonathan, N.A., (2013). Macroscopic organization of the cerebellum of the African giant pouched rat (*Cricetomys gambianus* – Waterhouse, 1840). *Veterinarski Arhiv, 83*, pp.695-707.

Callebaut, M., Nueten, E.V., Passel, H.V., Harrisson, F. and Bortier, H., (2006). Early steps in neural development. *Journal of Morphology, 267*, pp.793-802.

Charles, R.N., Norman, I.S., Robert, J.D. and David, A.R., (2005). The Human Nervous System: Structure and function. 6th Edition, Humana Press, 1-10, pp.219-242.

Charvet, C.J. and Striedter, G.F., (2011). Developmental modes and developmental mechanisms can channel brain evolution. *Frontiers in Neuroanatomy, 5*(4), pp.1-5.

Chen, D., Zhao, M. and Mundy, G.R., (2004). Bone morphogenetic proteins. *Growth Factors, 22*, pp.233-241.

Cirone, J., Sharp, C., Jeffery, G. and Salt, T.E., (2002). Distribution of metabotropic glutamate receptors in the superior colliculus of the adult rat, ferret and cat. *Neuroscience, 109*, pp.779-786.

Clancy, B., Finlay, B.L., Darlington, R.B. and Anand, K.J.S., (2007). Extrapolating brain development from experimental species to humans. *Neurotoxicology, 28*(5), pp.1-15.

Cooper, H.M., Herbin, M. and Nevo, E., (2004). Visual system of a naturally microphthalmic mammal: The blind mole rat. *Journal of Comparative Neurology, 328*, pp.313-350.

CopperKettle, (2006). Corticogenesis in a brain of a mouse. Six cortical layers. https://commons.wikimedia.org/wiki/File:Corticogenesis_in_a_wild-type_mouse_with_captions_in_english_copy.png

Costa, L.G., Vitalone, A. and Giuzetti, M., (2004). Signal transduction mechanisms involved in the antiproliferative effects of ethanol in glial cells. *Toxicology Letter, 149*, pp.67-73.

Dean, A. and Sharpe, R.M., (2013). Clinical review: Anogenital distance or digit length ratio as measures of foetal androgen exposure: relationship to male reproductive development and its disorders. *Journal of Clinical Endocrinology and Metabolism, 98*(6), pp.2230-2238.

Demaerel, P., (2002). Abnormalities of cerebellar foliation and fissuration: classification, neurogenetics and clinicoradiological correlate. *Neuroradiology, 44*, pp.639-646.

Di Salvo, P., Bocci, F. and Polisca, A., (2006). Doppler evaluation of maternal and foetal vessels during normal gestation in the bitch. *Research in Veterinary Sciences, 81*(3), pp.382-388.

Dobbing, J. and Sands, J., (1970). Growth and development of the brain and spinal cord of the guinea pig. *Brain Research, 17*(1), pp.115-123.

Dun, R.B., (1955). Ageing of Merino Foetus. *The Australian Veterinary Journal*, pp.153-154.

Dwyer, N.D., Chen, B., Chou, S.J., Hippenmeyer, S., Nguyen, L. and Ghashghaei, H.T., (2016). Neural Stem Cells to Cerebral Cortex: Emerging Mechanisms Regulating Progenitor Behaviour and Productivity. *The Journal of Neuroscience, 36*(45), pp.11394-11401.

Dyce, K.M., Sack, W.O. and Wensing, C.J.G., (2002). Textbook of veterinary anatomy (3rd edition). Elsevier Science (USA).

Eben, A.B., (2004). Grasscutter: importance, habitat, characteristics, feed and feeding, breeding and diseases. Kumasi, Ghana, Programme organized by Centre for Biodiversity Utilization and Development (CBUD), pp.1-6.

Eisenberg, M.L., Hsieh, M.H., Walters, R.C., Krasnow, R. and Lipshultz, L.I., (2011). The Relationship between Anogenital Distance, Fatherhood, and Fertility in Adult Men. *PloS One, 6*(5), *e18973.* doi:10.1371/journal.pone.0018973

El-Bab, F.M., (2001). Cognitive Event Related Potentials During A Learning Task. PhD Thesis, Department of Clinical Neurological Sciences Faculty of Medicine, University of Southampton, United Kingdom.

Eleccion, A., (2012). Embryology of the brain. www.slideshare.net/anady28/embryology-of-brain-14250142. Accessed on July 22, 2019.

Elshazzly, M. and Caban, O., (2018). Embryology, Central Nervous System. *National Library of Science. In: StatPearls [Internet]. Treasure Island (FL): StatPearls Publishing. Updated Oct 27, 2018. Available from: https://www.ncbi.nlm.nih.gov/books/NBK526024/*

England, G., Yeager, A, and Concannon, P.W., (2003). Ultrasound imaging of the reproductive tract of the bitch. In: Recent Advances in Small Animal Reproduction. *International Veterinary Information Service* (www.ivis.org). Ithaca New York, Document Number A1203.0703.

Ernst, M. and Jenkins, B.J., (2004). Acquiring signalling specificity from the cytokine receptor gp130. *Trends in Genetics, 20*, pp.23-31.

Evans, H.E. and Sack, W.O., (1973). Prenatal Development of Domestic and Laboratory Mammals; growth Curves, External features and Selected References. *Anatomica Histologica Embryologia, 2*, pp.11-45.

Fa, J.E., Juste, J., Burn, R.W. and Broad, G., (2002). Bushmeat consumption of two ethnic groups in Bioko Island, West Africa. *Human Ecology, 30*, pp.397-416.

Ferreira, A.O., Vasconcelos, B.G., Favaron, P.O., Santos, A.C., Leandro, R.M., Pereira, F.T.V., Maria, D.A. and Miglino, M.A., (2018). Bovine central nervous system development. *Pesquisa Veterinaria Brasileria, 38*(1), pp.147-153.

Fietz, S.A. and Huttner, W.B., (2011). Cortical progenitor expansion, self-renewal and neurogenesis-a polarized perspective. *Current Opinion in Neurobiology, 21*(1), pp.23-35.

Fietz, S.A., Keleva, I., Vogt, J., Wilsch-Bräuninger, M., Stenzel, D., Fish, J.L., Corbeil, D., Riehn, A., Distler, W., Nitsch, R. and Huttner, W.B., (2010). OSVZ progenitors of human and ferret neocortex are epithelial-like and expand by integrin signalling. *Nature Neuroscience, 13*(6), pp.690-699.

Finlay, B.L. and Darlington, R.B., (1995). Linked regularities in the development and evolution of mammalian brains. *Science, 268*(5217), pp.1578-1584.

Fletcher, T.F. and Weber, A.F., (2003). Veterinary Development Anatomy. In: http://vanat.cvm.umn.edu/neurLab3/index.html. Accessed on 27th of February, 2019.

Fletcher, T.F., (2013). In: http://vanat.cvm.umn.edu/neurLab3/index.html. Accessed on 27th of February, 2019.

Florio, M. and Huttner, W.B., (2014). Neural progenitors, neurogenesis and the evolution of the neocortex. *Development, 141*(11), pp.2182-2194.

Foley, A.C. and Stern, C.D., (2001). Evolution of vertebrate forebrain development: how many different mechanisms? *Journal of Anatomy, 199*, pp.35-52.

Fortes, E.A., Ferraz, M.S., Bezerra, D.O., Júnior, A.M., Cabral, R.M., Sousa, F., Almeida, H.M., Pessoa, G.T., Menezes, D.J., Guerra, S.P., Sampaio, I.B., Assis Neto, A.C. and Carvalho, M.A., (2013). Prenatal development of the agouti (*Dasyprocta prymnolopha* Wagler, 1831): External features and growth curves. *Animal Reproduction Science, 140*(3-4), pp.195-205. doi: 10.1016/j.anireprosci.2013.06.021.

Gabriele, M.L., Brunso-Bechtold, J.K. and Henkel, C.K., (2000). Plasticity in the development of afferent patterns in the caudal colliculi of the rat after unilateral cochlear ablation. *Journal of Neuroscience,* 20, pp.6939-6949.

Gaspard, N., Bouschet, T., Hourez, R., Dimidschstein, J., Naeije, G., van den Ameele, J., Espuny-Camacho, I., Herpoel, A., Passante, L., Schiffmann, S.N., Gaillard, A., and Vanderhaeghen, P. (2008). An intrinsic mechanism of corticogenesis from embryonic stem cells. *Nature455*, pp.351–357. https://doi.org/10.1371/journal.pone.0020108

Gelpi, E., Budka, H., and Preusser, M. (2013). External granular cell layer bobbling: a distinct histomorphological feature of the developing human cerebellum. *Clinical Neuropathology,32*(1), pp.42-50. doi: 10.5414/NP300518.

GENSAT, (2019). The Gene Expression Nervous System Atlas Project. Rockefeller University (New York. www.gensat.org/atlas/ADULT_ATLAS_08.jpg.

Germain, N., Banda, E. and Grabel, L., (2010). Embryonic Stem Cell Neurogenesis and Neural Specification. *Journal of Cellular Biochemistry, 111*(3), pp.535-542.

Gilbert, S.F. (2000a). Neuronal Specification and Axonal Specificity. In: Developmental Biology. 6th edition. Sunderland (MA): Sinauer Associates. Available from: https://www.ncbi.nlm.nih.gov/books/NBK10108/

Gilbert, S.F. (2000b). Tissue Architecture of the Central Nervous System. In: Developmental Biology. 6th edition. Sunderland (MA): Sinauer Associates. Available from: https://www.ncbi.nlm.nih.gov/books/NBK10047/

Gilbert, S.F. (2010). Developmental biology. Ninth edition. Sinauer Associate, Inc. ISBN 978-0-87893-384-6.

Gilmore, E.C. and Herrup, K., (1997). Cortical development: Layers of complexity. *Current Biology, 7*(4), pp.231-234.

Girard, N., Koob, M. and Brunel, H., (2016). Normal development Chapter 57. In: *Handbook of Clinical Neurology, 136*, pp.1091-1119.

Girman, S.V. and Lund, R.D., (2007). Most superficial sublamina of rat superior colliculus: neuronal response properties and correlates with perceptual figure-ground segregation. *Journal of Neurophysiology, 98*, pp.161-177.

Gonzalez-Soriano, J., Gonzalez-Flores, M.L., Contreras-Rodriguez, J., Rodriguez-Veiga, E. and Martinez-Sainz, P., (2000). Calbindin D28k and parvalbumin immunoreactivity in the rabbit superior colliculus: an anatomical study. *Anatomical Record, 259*, pp.334-346.

Götz, M, and Huttner, W.B., (2005). The cell biology of neurogenesis. *Nature Reviews Molecular Cell Biology, 6*(10), pp.777-788.

Greenwood, P.L., Café, L.M., Hearnshaw, H. and Hennessy, D.W., (2005). Consequences of nutrition and growth retardation early in life for growth and composition of cattle and eating quality of beef. *Recent Advances in Animal Nutrition in Australia, 15*, pp.183-195.

Gutierrez, E. and Zamora, F.M.M., (2004). Ultrasonography study of rabbit pregnancy. Proceedings of 8th World Rabbit Congress, pp.276-280.

Haines, D.E. and Mihailoff, G.A., (2018). The Midbrain, In: Fundamental Neuroscience for Basic and Clinical Applications Fifth Edition. https://doi.org/10.1016/C2014-0-03718-5.

Haines, D.E., (2015). Fundamental Neuroscience for Basic and Clinical Applications (Online Version). Chapter 5: Development of the Nervous System: eds: Evans O.B. 4th Edition. https://clinicalgate.com/development -of-the-nervous-system-3/

Hampe, O., Franke, H., Hipsley, C.A., Kardjilov, N. and Müller, J., (2015). Prenatal Cranial Ossification of the Humpback Whale (*Megaptera novaeangliae*). *Journal of Morphology, 276*(5), pp.564-582.

Hardouin, J., Thys, E., Joiris, V. and Fiedling, D. (2003). Mini-livestock breeding with indigenous species in tropics. *Livestock Research for Rural Development, 15*, Accessed online from http://lrrd.cipav.org.co/lrrd15/4/hard154.htm. Accessed 12/09/2015; 23:37:56 GMT.

Hevner, R.F. and Haydar, T.F., (2012). The convoluted role of basal radial glia in cortical neurogenesis. *Cerebral Cortex, 22*(2), pp.465-468.

Hill, M.A., (2016). Embryology Carnegie Stages. Retrieved from https://embryology.med.unsw.edu.au/embryology/index.php/Carnegie_Stages. Accessed December 22, 2018.

Hill, M.A., (2018). Embryology Paper- Guinea pig development 21 to 35 days. Retrieved from https://embryology.med.unsw.edu.au/embryology/index.php/Paper_-_Guinea_pig_development_2_to_35_days. Accessed December 22, 2018.

Hill, M.A., (2019a). Embryology Carnegie stage table. Retrieved from https://embryology.med.unsw.edu.au/embryology/index.php/Carnegie_Stage_table. Accessed January 6, 2019.

Hill, M.A., (2019b). Embryology Carnegie Stage Comparison. Retrieved from https://embryology.med.unsw.edu.au/embryology/index.php/Carnegie_Stage_comparison. Accessed January 6, 2019.

Hill, M.A., (2019c). Embryology Timeline human development. Retrieved from https://embryology.med.unsw.edu.au/embryology/index.php/Timeline_human_development. Accessed January 9, 2019.

Hoar, R.M., (2005). Resorption in guinea pigs as estimated by counting corpora lutea: The problem of twinning. *Teratology, 2*(3), pp.187-190.

Hof, P.R., Chanis, R. and Marino, L., (2005). Cortical complexity in cetacean brains. *Anatomical Record, 287*, pp.1142-1152.

Hoshiba, Y., Toda, T., Ebisu, H., Wakimoto, M., Yanagi, S. and Kawasaki, H., (2016). Sox11 balances dendritic morphogenesis with neuronal migration in the developing cerebral cortex. *Journal of Neuroscience, 36*(21), pp.5775-5784.

Huttner, W.B. and Brand, M., (1997). Asymmetric division and polarity of neuroepithelial cells. *Current opinion in Neurobiology, 7*(1), pp.29-39.

Ibe, C.S., (2010). Anatomical study of the mesencephalic tectum and myelencephalon in the African giant pouched rat (*Cricetomys gambianus,* Waterhouse-1840). Masters Thesis, Ahmadu Bello University, Zaria.

Ibe, C.S., (2016). Structural and Immunohistochemical Studies of Prenatal and Postnatal Brain Development in the African Grasscutter (*Thryonomys swinderianus* – Temminck, 1827). PhD Thesis, Department of Veterinary Anatomy, Faculty of Veterinary Medicine, Ahmadu Bello University, Zaria, Nigeria.

Ibe, C.S., Onyeanusi, B.I. and Hambolu, J.O., (2014). Functional morphology of the brain of the African giant pouched rat (*Cricetomys gambianus,* Waterhouse, 1840). *Onderstepoort Journal of Veterinary Research, 81*, pp.17. accessed online from http://dx.doi.org/10.4102/ojvr.v8lil.644. Accessed 22/08/2015

Ibe, C.S., Salami, S.O. and Wanmi, N., (2017). Brain size of the African Grasscutter (*Thryonomys swinderianus,* Temminck, 1827) at defined postnatal periods. *Folia Veterinaria, 61*(4), pp.5-11.

Igado, O.O., Adebayo, A.O., Oriji, C.C. and Oke, B.O., (2016). Cranio-facial and ocular morphometrics of the Male Greater Cane Rat (*Thryonomys swinderianus*). *Nigerian Veterinary Journal, 37*(1), pp.54-63.

Inuoye, N. and Oda, S., (1980). Strain-specific variations in the folia pattern of the mouse cerebellum. *Journal of Comparative Neurology, 190*, pp.375-396.

Jacobson, A.G., and Tam, P.P.L., (1982). Cephalic neurulation in the mouse embryo analyzed by SEM and morphometry. The Anatomical Record, 203(3), pp.375-396. https://doi.org/10.1002/ar.1092030308.

Jacobson, S. and Marcus, E.M., (2008). Neuroembryology and congenital malformations. In: Neuroanatomy for the neuroscientist. New York: Springer, pp.43-62.

Jaji, A.Z., Kwari, H.D., Ribadu, A.Y. and Sivachelvan, M.N., (2011). Foetal Age Estimation in One-humped Camel (*Camelus dromedaries*). *Sahel Journal of Veterinary Science, 10*(1), pp.29-35.

Jori, F. and Chardonnet, P., (2001). Cane rat farming in Gabon status and perspective. Proceedings of the 5th International Wildlife Ranching Symposium, March 2001, Pretoria, South Africa, pp.33-51.

Jori, F., Edderai, D. and Houben, P., (2005). Potential of rodents for minilivestock in Africa. In: Paoletti MG, editor. Ecological implications of mini-livestock: rodents, frogs, snails and insects for sustainable development. Enfield, USA. Science Publishers. pp.25-45.

Kandel, E.R. and Squire, L.R., (2000). Neuroscience. Breaking Down Scientific Barriers to the Study of Brain and Mind. *Science, 290*(5494), pp.1113-1120.

Kandel, E.R., Schwartz, J.H., Jessell, T.M., Siegelbaum, S.A. and Hudspeth, A.J., (2012). Principles of neural science, 5th edition. Columbus, Ohio: McGraw-Hill Education.

Kaneko, M., Yamaguchi, K., Eiraku, M., Sato, M., Takata, N., Kiyohara, Y., Mishina, M., Hirase, H., Hashikawa, T., and Kengaku, M. (2011). Remodeling of Monoplanar Purkinje Cell Dendrites during Cerebellar Circuit Formation. *PLoS ONE,6*(5), e20108. doi: 10.1371/journal.pone.0020108.

Kang, Y.S., Park, W.M., Lim, J.K., Kim, S.Y. and Jeon, C.J., (2002). Changes of calretinin, calbindin, D28K and parvalbumin-immunoreactive neurons in the superficial layers of the hamster superior colliculus following monocular enucleation. *Neuroscience Letter, 13*, pp.104-108.

Kawamura, K., Murase, S. and Yuasa, S., (1990). Development of the rodent cerebellum and synaptic re-formation of donor climbing terminals on spines of the host Purkinje dendrites after chemical differentiation. *Journal of Experimental Biology, 153*, pp.289-303.

Kessaris, N., Pringle, N., and Richardson, W. D. (2008). Specification of CNS glia from neural stem cells in the embryonic neuroepithelium. *Philosophical transactions of the Royal Society of London. Series B, Biological sciences*, *363*(1489), pp71–85. https://doi.org/10.1098/rstb.2006.2013

Kim, C.H., Park, H.W., Kim, K. and Yoon, J.H., (2004). Early development of the nose in human embryos: a stereomicroscopic and histologic analysis. *Laryngoscope*, *114*(10), pp.1791-1800.

Kim, Y., Travis, A.J. and Meyers-Wallen, V.N., (2007). Parturition prediction and timing of canine pregnancy. *Theriogenology, 68*(8), pp.1177-1182.

Kornack, D.R. and Rakic, P., (1998). Changes in cell-cycle kinetics during the development and evolution of primate neocortex. *Proceedings of the National Academy of Sciences of the United States of America, 95*(3), pp.1242-1246.

Kramer, L.A. and Greek, R., (2018). Human Stakeholders and the Use of Animals in Drug Development. *Business and Society Review, 123*(1), pp.3-58.

Krauzlis, R.J., (2004). Activity of rostral superior colliculus neurons during passive and active viewing of motion. *Journal of Neurophysiology, 92*, pp.949-958.

Krubitzer, L. and Kaas, J., (2005). The evolution of the neocortex in mammals: How is phenotypic diversity generated? *Current Opinion in Neurobiology, 15*(4), pp.444-453.

Kurkin, S., Akao, T., Fukushima, J., Shichinohe, N., Kaneko, C.R., Belton, T. and Fukushima, K., (2014). No-go neurons in the cerebellar oculomotor *vermis* and caudal fastigial nuclei: planning tracking eye movements. *Experimental Brain Research, 232*, pp.191-210.

Kustritz, M.V., (2005). Pregnancy diagnosis and abnormalities of pregnancy in the dog. *Theriogenology, 64*(3), pp.755-765.

Kutzler, M.A., Yeager, A.E., Mohammed, H.O. and Meyer-Wallen, V.N., (2003). Accuracy of canine parturition date prediction using foetal measurements obtained by ultrasonography. *Theriogenology, 60*(7), pp.1309-1317.

Laing, J.A., (1979). Fertility and Infertility in Domestic Animals, 3rd (Ed) Bailliere and Tindall, pp.262.

Landis, D.M.D. and Reese, T.S., (1977). Structure of the Purkinje cell membrane in staggerer and weaver mutant mice. *Journal of Comparative Neurology, 171*, pp.247-260.

Lanzetti, A., Berta, A. and Ekdale, E.G., (2018). Prenatal Development of the Humpback Whale: Growth Rate, Tooth Loss and Skull Shape Changes in an Evolutionary Framework. *Anatomy Record.* https://doi.org/10.002/ar.23990.

Larsell, O., (1952). The morphogenesis and adult pattern of the lobules and fissures of the cerebellum of the white rat. *Journal of Comparative Neurology, 97*, pp.281-356.

Llinas, R.R., Walton, K.D. and Lang, E.J., (2004). Cerebellum. In: Shepherd, G.M. (Ed.). the Synaptic Organization of the Brain. Oxford University Press, New York, pp.271-310.

Loftus, W.C., Malmierca, M.S., Deborah, C., Bishop, D.C. and Olive, D.L., (2008). The cytoarchitecture of the caudal colliculus revisited: a common organization of the lateral cortex in rat and cat. *Neuroscience, 154*, pp.196-205.

Luvoni, G.C. and Grioni, A., (2000). Determination of gestational age in medium and small size bitches using ultrasonographic foetal measurements. *Journal of Small Animal Practice, 41*(7), pp.292-294.

Lyne, A.G. and Hollis, D.E., (1972). The structure and development of the epidermis in sheep foetuses. *Journal of Ultrastructure Research, 38*(5-6), pp.444-458.

Ma, S., Kwon, H.J. and Huang, Z., (2011). Radial glia regulates Cajal-Retzius cell positioning in the early embryonic cerebral cortex. *Development Biology, 351*(1), pp.25-34.

Macleod, D.J., Sharpe, R.M., Welsh, M., Fisken, M., Scott, H.M., Hutchison, G.R., Drake, A.J. and van den Driesche, S., (2010). Androgen action in the masculinization programming window and development of male reproductive organs. *International journal of Andrology, 33*(2), pp.279-287.

McGeady, T.A., Quinn, P.J., Fitzpatrick, E.S. and Ryan, M.T., (2006). Veterinary Embryology. Chapter 13 Nervous system. Blackwell Publishing Ltd. pp.377.

McGuire, B. and Bernis, W.E., (2008). Parental care. In Wolff, J.O. and Sherman, P.W. rodent Societies. An Ecological Perspective. University of Chicago press, pp.231-235.

McIntosh, G.H., Baghurst, K.I., Potter, B.J. and Hetzel, B.S., (2008). Foetal brain development in the sheep. *Neuropathology and Applied Neurobiology, 5*(2), pp.103-114.

Mensah-Brown, E.P.K. and Garey, L.J., (2006). The superior colliculus of the camel: a neuronal-specific nuclear protein (NeuN) and neuropeptide study. *Journal of Anatomy, 208*, pp.239-250.

Meyer, G., (2007). Genetic Control of Neuronal Migrations in Human Cortical Development (Advances in Anatomy, Embryology and Cell Biology). Beck, F.F., Melbourne, F.C., Madrid, M.F., Freiburg, D.E.H., Jackson, H.W.K., Frankfurt, E.M., Enschede, R.P., München, Y.S., Kyoto, T.H.S., Würzburg, K. and Zilles, D. (Eds). New York, NY Springer.

Millen, S., (2003). Dogfish Brain. Accessed online from *http://www.zoology.ubc.com.* Accessed: 09/09/2012.

Miller, F.D. and Gauthier, A.S., (2007). Timing is everything: making neurons versus glia in the developing cortex. *Neuron, 54*(3), pp.357-369.

Monk, C.S., Webb, S.J. and Nelson, C.A., (2001). Prenatal neurobiological development: molecular mechanisms and anatomical change. *Developmental Neuropsychology, 19*, pp.211-236.

Montiel, J.F., Vasistha, N.A., Garcia-Moreno, F. and Molnár, Z., (2016). From sauropsids to mammals and back: New approaches to comparative cortical development. *Journalof Comparative Neurology, 524*(3), pp.630-645. doi:10.1002/cne.23871

Muralidhar, S., Wang, Y., and Markram, H. (2014). Synaptic and cellular organization of layer 1 of the developing rat somatosensory cortex. *Frontiers in Neuroanatomy, 7*: pp.52. doi: 10.3389/fnana.2013.00052

Mustapha, O.A., Aderounmu, O.A., Olude, M.A., Okandeji, M.E., Akinloye, A.K., Oke, B.O. and Olopade, J.O., (2015). Anatomical Studies on the Spinal Cord of the AGCR (*Thryonomys swinderianus,* Temminck) 1: Gross Morphometry. *Nigerian Veterinary Journal, 36*(2), pp.1192-1202. http://journals.nvj.com.ng/index.php/nvj/article/view/23

Mustapha, O.A., Taiwo, S., Olude, A., Aderounmu, O.A., Okandeji, M.E., Akinloye, A.K., Olopade, J.O. and Oke, B.O., (2017). Anatomical Studies on the Spinal Cord of the Greater Cane Rat (*Thryonomys swinderianus,* Temminck) II: Histomorphology and Spinal Tracings. *Nigerian Veterinary Journal, 38*(2), pp.129-139.

Nacher, J., Palop, J.J., Ramirez, C., Molowny, A. and Lopez-Garcia, C., (2000). Early Histological Maturation in the Hippocampus of the Guinea Pig. *Brain Behaviour and Evolution, 56*(1), pp.38-44.

Nadarajah, B., (2003). Radial glia and somal translocation of radial neurons in the developing cerebral cortex. *Glia, 43*(1), pp.33-36.

Nagayama, S., Homma, R. and Imamura, F., (2014). Neuronal organization of olfactory bulb circuits. *Frontiers in Neural Circuits* 8:98. doi:10.3389/fncir.2014.00098.

National Research Council (1991). Microlivestock: Little Known Small Animals with a Promising Economic Future. National Academy Press, Washington, DC. pp.233-240.

Noctor, S.C., Flint, A.C., Weissman, T.A., Dammerman, R.S. and Kriegstein, A.R., (2001). Neurons derived from radial glial cells establish radial units in neocortex. *Nature, 409*(6821), pp.714-720.

Noctor, S.C., Martinez-Cerdeño, V., Ivic, L. and Kriegstein, A.R., (2004). Cortical neurons arise in symmetric and asymmetric division zones and migrate through specific phases. *Nature Neuroscience, 7*(2), pp.136-144.

Nomina Anatomica Vetreinaria (2017). International Committee on Veterinary Gross Anatomical Nomenclature. 6th Edition. Hannover Columbia. pp. 1-178

Notebaert, H., (2018). Evaluation of cognitive training in a rat model for traumatic brain injury with advanced diffusion scanning and tractometry. Master's dissertation, Department of Electronics and Information Systems, Faculty of Engineering and Architecture. Ghent University.

Nzalak, J.O., Ayo, J.O., Neils, J.S., Okpara, J.O., Onyeanusi, B.I., Ghaji, A. and Ojo, S.A. (2005). Morphometric studies of the cerebellum and forebrain of the African giant rat (*Cricetomys gambianus,* Waterhouse). *Tropical Veterinarian. 23*(3&4), pp.87-92.

Nzalak, J.O., Byanet O., Salami, S.O., Umosen, A.D., Maidawa, S.M., Ali, M.N. and Imam, J., (2008). Comparative morphometric studies of the cerebellum and forebrain of the African giant rat (AGR) (*Cricetomys gambianus*-Waterhouse) and that of grasscutter (*Thryonomys swinderianus*). *Journal of Animal and Veterinary Advances, 7*, pp.1090-1092.

O'Leary, D.D.M., Chou, S.J. and Sahara, S., (2007). Area Patterning of the Mammalian Cortex. *Neuron, 56*(2), pp.252-269.

O'Leary, D.D.M., Stocker, A.M. and Zembrzycki, A., (2013). Area Patterning of the Mammalian Cortex. *Patterning and Cell Type Specification in the Developing CNS and PNS,* pp.61-85.

O'Rahilly, R. and Müller, F., (1987). Developmental stages in human embryos. Carnegie Institution of Washington, pp.637.

O'Rahilly, R. and Müller, F., (2002). The two sites of fusion of the neural folds and the two neuropores in the human embryo. *Teratology, 65*, pp.162-170.

Ohuma, E.O., Papageorghiou, A.T., Villar, J. and Altman, D.G., (2013). Estimation of gestational age in early pregnancy from crown-rump length when gestational age range is truncated: the case study of the intergrowth-21st Project. *BMC Medical Research Methodology, 13*(1), pp.151.

Okorafor, K.A., Okete, J.A., Eleng, I.E. and Odaibo, A.B., (2013). Seasonal variations in the mean body weight, length and capture rate of cane rats (*Thryonomys swinderianus*) in Ibadan, Oyo State, Nigeria. *European Journal of Experimental Biology, 3*(3), pp.301-306.

Olude, M.A., Mustapha, O.A., Sonubi, A.C., Ogunbunmi, T.K., Falade, E.T., Adebayo, O.A. and Akinloye, A.K., (2014). Morphometric analysis of the skull of the Greater cane rat (*Thryonomys swinderianus,* Temminck). *Nigeria Veterinary Journal, 35*(3), pp.1026-1037.

Olukole, S.G., Oyeyemi, M.O. and Oke, B.O., (2014). Semen Characteristics and Spermiogram of the African Greater Cane Rat (*Thryonomys swinderianus*, Temminck). *Slovak Journal of Animal Science, 47*(3), pp.125-131.

Onadeko, S.A. and Amubode, F.O., (2002). Reproductive indices and performance of captive reared grasscutters (*Thryonomys swinderianus*, Temminck). *Nigerian Journal of Animal Production, 29*(1), pp.142-149.

Onwuama, K.T., Ojo, S.A., Hambolu, J.O., Dzenda, T., Zakari, F.O. and Salami, S.O., (2018). Macro-anatomical and morphometric studies of the hindlimb of grasscutter (*Thryonomys swinderianus*, Temminck-1827). *Anatomia Histologia Embryologia, 47*(1), pp.21-27.

Onwuama, K.T., Ojo, S.A., Hambolu, J.O., Salami, O.S. and Dzenda, T. (2014). Gross-anatomical and morphometric studies of the Grasscutter (*Thryonomys swinderianus*), axial skeleton. *Standard Scientific Research and Essays, 2*, pp.406-417.

Opara, M.N., (2010). The Grasscutter I: A Livestock of Tomorrow. *Research Journal of Forestry, 4*(3), pp.119-135.

Orr, T.J. and Zuk, M., (2014). Reproductive delays in mammals: an unexplored avenue for post-copulatory sexual selection. *Biological Reviews, 89*(4), pp.889-912.

Orr, T.J., (2012). Delayed implantation in the Carnivora: causes and consequences. PhD Thesis. University of California, Riverside, USA.

Osuagwuh, A.I.A. and Aire, T.A., (1986). Studies on the estimation of the developmental age of the caprine foetus: External measurements and appearance. *Tropical Veterinarian, 4*, pp.39-51.

Owusu, B.A., Adu, E.K., Awotwi, E.K. and Awumbila, B., (2010). Embryonic resorption, litter size and sex ratio in the grasscutter, *Thryonomys swinderianus, Animal Reproduction Science, 118*(2-4), pp.366-371.

Palay, S.I.. and Chan-Palay, V. (1974). Cerebellar Cortex: Cytology and Organization. Springer-Verlag, New York, pp.1-348.

Pansky, B., (1982). Review of Medical Embryology, Nervous System.

Paridaen, J.T., and Huttner, W.B., (2014). Neurogenesis during development of the vertebrate central nervous system. EMBO reports, 15(4), pp.351-364. Doi:10.1002/embr.201438447

Perrin, S., (2014). Preclinical research: make mouse studies work: *Nature 507*, pp.423-425. 10:1038/507423a

Pointing, J. and Teinaz, Y., (2004). Halal meat and food crime in the United Kingdom. In: *International Halal Food seminar,* Islamic University College of Malaysia, Accessed online from https://warmwell.com/hayunes.htm. Accessed: 04/04/2014.

Purves, D., Augustine, G.J., Fitzpatrick, D., Katz, L.C., LaMantia, A.S., McNamara, J.O. and Williams, S.M., (2001). Circuits within the Cerebellum. In: *Neuroscience,* 2nd edition, Sunderland (MA): Sinauer Associates. Accessed online from http://.ncbi.nlm.nih.gov/books/NBK10865/. Accessed: 23/06/2012; 09:05:32 GMT.

Qian, X., Shen, Q., Goderie, S.K., He, W., Capela, A., David, A.A. and Temple, S., (2000). Timing of CNS cell generation: a programmed sequence of neuron and glial cell production from isolated murine cortical stem cells. *Neuron, 28*(1), pp.69-80.

Rahimi-Balaei, M., Bergen, H., Kong, J., and Marzban, H. (2018). Neuronal Migration During Development of the Cerebellum. *Frontiers in cellular neuroscience*, *12*, pp.484. https://doi.org/10.3389/fncel.2018.00484

Rakic, P., (1995). A small step for the cell, a giant leap for mankind: a hypothesis of neocortical expansion during evolution. *Trends in Neuroscience, 18*(9), pp.383-388.

Rakic, P., (2009). Evolution of the neocortex: a perspective from developmental biology. *Nature Reviews Neuroscience, 10*(10), pp.724-735.

Randall, J.D., Burggren, W.W., French, K. and Eckert, R., (2002). Eckert Animal Physiology: Mechanisms and Adaptations. Freeman and Co., pp.102.

Rash, B.G. and Grove, E.A., (2006). Area and layer patterning in the developing cerebral cortex. *Current Opinion in Neurobiology, 16*(1), pp.25-34.

Roeling, K., Goeritz, F. and Hildebrandt, T.B., (2010). Ultrasonographic characterization of prenatal development in European brown hares (Lepus europaeus PALLAS, 1778): an evolutionary approach. *Reproduction, Fertility and Development* 22, pp.448-458. www.publish.csiro.au/journals/rfd.

Roeling, K., Menzies, B.R., Hildebrandt, T.B. and Boeritz, F., (2011). The concept of superfetation: a critical review on a 'myth' in mammalian reproduction. *Biological Reviews, 86*(1), pp.77-95.

Ruberte, J., Navarro, M., Carretero, A., Köing, H.E. and Puelles, L. (2017). The Nervous System (Chapter 13). In: Morphological Mouse Phenotyping: Anatomy, Histology and Imaging. Eds: Jesús Ruberte, Ana Carretero, Marc Navarro. Academic Press. Pages 377-474. https://doi.org/10.1016/B978-0-12-812972-250013-1.

Sacramento, T.I., Sinabaragui, O.S., Aizoun F., Farougou, S., Mensah, G.A. and Ategbo, J., (2013). Determination of grasscutter age (*Thryonomys swinderianus* Temminck, 1827) from anogenital distance. *Journal of Applied Biosciences, 62*, pp.4637-4643.

Sadler, T.W., (2005). Embryology of Neural Tube Development. *American Journal of Medical Genetics Part C, 135*(1), pp.2-8.

Saitsu, H., Yamada, S., Uwabe, C., Ishibashi, M. and Shiota, K., (2004). Development of the posterior neural tube in human embryos. *Anatomy and Embryology, 209*(2), pp.107-117.

Sanchez-Villagra, M.R. and Sultan, F., (2002). The Cerebellum at Birth in Therian Mammals with Special Reference to Rodents. *Brain, Behaviour and Evolution, 59*(3), pp.101-113.

Sauerland, C., Menzies, B.R., Glatzle, M., Seeger, J., Renfree, M.B. and Fietz, S.A., (2016). The Basal Radial Glia Occurs in Marsupials and Underlies the Evolution of an Expanded Neocortex in Therian Mammals. *Cerebral Cortex, 28*(1), pp. 145-157.

Scheiber, I.B.R., Weiß, B.M., Kingma, S.A. and Komdeur, J., (2017). The importance of the altricial- precocial spectrum for social complexity in mammals and birds- a review. *Frontiers in Zoology 14*(3), pp.1-20.

Schindelin, J., Arganda-Carreras, I., Frise, E., Kaynig, V., Longair, M., Pietzsch, T. and Cardona, A., (2012). Fiji: an open-source platform for biological-image analysis. *Nature Methods, 9*(7), pp.676-682.

Schulz, E.B., Thamke, H. and Rehmer, H. (1972). Qualitative and Quantitative cytoarchitectural studies on the variability of the olfactory bulb of the adult Wistar rat (*Rattus norvegicus*). *Journal of Brain Research, 19*, pp.211-221.

Shehu, S.A., Ojo, S.A., Hambolu, J.O., Ibrahim, N.D.G. and Hena, S.A., (2012). External Features (Development Horizons) in Developing Camel Foetus as a Guide to age Estimation. *Journal of Veterinary Advances, 2*(4), pp.178-183.

Shen, Q., Wang, Y., Dimos, J.T., Fasano, C.A., Phoenix, T.N., Lemischka, I.R., Ivanova, N.B., Stifani, S., Morrisey, E.E. and Temple, s., (2006). The timing of cortical neurogenesis is encoded within lineages of individual progenitor cells. *Nature Neuroscience, 9*(6), pp.743-751.

Shiota, K., (2008). Embryology of the Human Brain. *Donald School Journal of Ultrasound in Obstetrics and Gynaecology,* 2(3), pp.1-8.

Silva, F.M.O., Alcantara, D., Carvalho, R.C., Favaron, P.O., Dos-Santus, A.C., Viana, D.C. and Miglino, M.A., (2016). Development of the central nervous system in guinea pig (*Cavia porcellus,* Rodentia, Caviidae). *Pesquisa Veterinaria Brasileria, 36*(8), pp.753-760.

Sinowatz, F., (2010). Development of the central and peripheral nervous system. In: Hyttel P., Sinowatz F. and Vejlsted M. (Eds), Essential of Domestic Animal Embryology. Elsevier, China.

Sivachelan, M.N., Ali, M.G. and Chibuzo, G.A., (1996). Foetal age estimation in sheep and goats. *Small Ruminant Research, 19*(1), pp.69-76.

Skinner, J.D. and Chimimba, C.T., (2005). The Mammals of the Southern African Subregion. Third edition. Cambridge University Press, Cambridge, UK. Pp.93-96.

Smeyne, R.J., and Goldowitz, D. (1989). Development and Death of External Granular Layer Cells in the Weaver Mouse Cerebellum: A Quantitative Study. *The Journal of Neuroscience, 9*(5), pp1608-1620

Sousa, F.C., Alves, F.R., Fortes, E.A.M., Ferraz, M.S., Machado, J.A.A., de Menezes, D.J. and de Carvalho, M.A., (2012). Pregnancy in Hystricomorpha: Gestational age and embryonic-foetal development of Agouti (*Dasyprocta prymnolopha,* Wagler, 1831) estimated by ultrasonography. *Theriogenology,78*(6), pp.1278-1285.

Spruston, N., (2008). Pyramidal neurons: dendritic structure and synaptic integration. *Nature Reviews Neuroscience, 9*(3), pp.206-221.

Stein, J.F. and Glickstein, M., (1992). Role of the cerebellum in visual guidance of movement. *Physiological Reviews, 72*(4), pp.967-1017.

Štěrba, O., (1995). Staging and Ageing of Mammalian Embryos and Foetuses. *Acta Veterinaria Brno, 64*(1), pp.83-89.

Štěrba, O., Kilma, M. and Schildger, B., (2000). Embryology of dolphins. Staging and ageing of embryos and foetuses of some cetaceans. *Advances in Anatomy, Embryology and Cell Biology, 157*(3-10), pp.1-133.

Sterling, G., (2008). The development of the nose. In: The Anatomy of the Human Embryo: A Scanning Electron-Microscopic Atlas. Basel. Karger. 146-165. DOI:10.1159/000159956.

Stiles, J. and Jernigan, T.L., (2010). The Basics of Brain Development. *Neurophysiology Review, 20*(4), pp.327-348.

Suckow, M.A., Weisbroth, S.H. and Franklin, C.L., (2006). The Laboratory Rat. Elsevier Academic Press, Oxford UK, pp.130-439.

Sudarov, A. and Joyner, A.L., (2007). Cerebellum morphogenesis: the foliation pattern is orchestrated by multi-cellular anchoring centres. *Neural Development, 2*, pp.26-46.

Sultan, F. and Braitenberg, V., (1993). Shapes and sizes of different mammalian cerebella. A study in quantitative comparative neuroanatomy. *Journal of Hirnforsch, 34*, pp.79-92.

Sumitra, M., Manikanda, P., Rao, K.V.K., Nayeem, M., Manohar, B.M. and Puvanakrishnan, R., (2004). Cardiorespiratory effects of diazepam-ketamine, xylazine-ketamine and thiopentone anaesthesia in male Wistar rats – A comparative analysis. *Life Science, 75*(15), pp.1887-1896.

Super, H., del Rio, J.A., Martinez, A., Perez-Sust, P. and Soriano, E., (2000). Disruption of neuronal migration and radial glia in the developing cerebral cortex following ablation of Cajal-Retzius cells. *Cerebral Cortex, 10*(6), pp.602-613. doi:10.1093/cercor/10.6.602

Sur, M. and Rubenstein, J.L., (2005). Patterning and plasticity of the cerebral cortex. *Science, 310*(5749), pp.805-810.

Tawfik, H.A., Abdulhafez, M.H., Fouad, Y.A. and Dutton, J.J., (2016). Embryologic and Foetal Development of the Human Eyelid. *Ophthalmic Plastic and Reconstructive Surgery, 32*(6), pp.407-414.

Telford, S., Wang, S. and Redgrave, P., (1996). Analysis of nociceptive neurons in the rat superior colliculus using c-fos immunohistochemistry. *Journal of Comparative Neurology, 375*, pp.601-617.

Thomas, F. and Alvin, F., (2013). Veterinary Developmental Anatomy (Veterinary Embryology). pp.59-62.

Thomson, C. and Hann, C., (2012). Neuroembryology. In: Edwards, R. and Leng, H. (Eds.). Veterinary Neuroanatomy, A Clinical Approach. Elsevier Ltd., London, pp.22-27.

Toma, K. and Hanashima, C., (2015). Switching modes in corticogenesis: mechanisms of neuronal subtype transitions and integration in the cerebral cortex. *Frontiers in Neuroscience, 9*, pp.274.

Toma, K., Kumamoto, T. and Hanashima, C., (2014). The Timing of Upper-Layer Neurogenesis is conferred by Sequential Derepression and Negative Feedback from Deep-Layer Neurons. *Journal of Neuroscience, 34*(39), pp.13259-13257.

Tortora, G.J. and Derrickson, B., (2016). Principle of Anatomy and Physiology (15th edition).

Van der Merwe, M., (2000). Tooth succession in the greater cane rat *Thryonomys Swinderianus* (Temminck, 1827). *Journal of Zoology, 251*(4), pp.541-545.

Van Essen, D.C. and Glasser, M.F., (2018). Parcellating Cerebral Cortex: How Invasive Animal Studies Inform Non-invasive Mapmaking in Humans. *Neuron, 99*(4), pp.640-663.

Van Zyl, A., Rambau, R.V. and van der Merwe, M., (2005). Aspects of the anatomy and histology alimentary canal of the greater cane rat, *Thryonomys swinderianus* with reference to feeding physiology. *African Zoology, 40*(1), pp.25-36.

Vogt, A., McElwee, K.J. and Blume-peytavi, U., (2008). Biology of the Hair follicle. In: Hair Growth and Disorders, pp.1-9. Springer-Verlag New York Inc.

Wadiche, J.I. and Jahr, C.E. (2001). Multivesicular release at climbing fibre-Purkinje cell synapses. *Neurone, 32*, pp.301-313.

Watakabe, A., (2009). Comparative molecular neuroanatomy of mammalian neocortex: What can gene expression tell us about areas and layers? *Development, Growth and Differentiation, 51*(3), pp.343-354.

Waziri, M.A., Sivachelvan, N.M., Mustapha, A.R. and Ribadu, A.Y., (2012). Time-related and sequential developmental horizons of Sahel goat foetuses. *Sokoto Journal of Veterinary Sciences, 10*(2), pp.32-39.

Witter, K., Pavlikova, H., Matulova, P. and Misek, I., (2005). Relationship between Vestibular Lamina, Dental Lamina, and the Developing Oral Vestibule in the Upper Jaw of the Field Vole (*Microtus agrestis*, Rodentia). *Journal of Morphology, 265*(3), pp.264-270.

Wodarz, A. and Huttner, W.B., (2003). Asymmetric cell division during neurogenesis in Drosophila and vertebrates. *Mechanisms of Development, 120*(11), pp.1297-1309.

Wurst, W. and Bally-Cuif, L., (2001). Neural plate patterning: upstream and downstream of the isthmic organizer. *Natural Review of Neuroscience, 2*, pp.99-108.

Young, K.M., Bartlett, P.F. and Coulson, E.J., (2006). Neural progenitor number is regulated by nuclear factor-kBp65 and p50 subunit-dependent proliferation rather than cell survival. *Journal of Neuroscience Research, 83*, pp.39-49.